The Effects of Designed Scaffold Architecture and Biodegradable Material on Chondrogenesis *in vitro* and *in vivo*

By

Gayoung Claire Jeong

A dissertation submitted in partial fulfillment
of the requirements for the degree of
Doctor of Philosophy
(Biomedical Engineering)
in The University of Michigan
2010

Doctoral Committee:

Professor Scott. J. Hollister, Chair
Professor Paul H. Krebsbach
Associate Professor Blake J. Roessler
Assistant Professor Asheesh Bedi

2010

To my parents, who encouraged and inspired me to dream big and take on challenges with their everlasting love and support.

ACKNOWLEDGEMENTS

Reflecting on all my precious memories from my graduate school, I still cannot believe that I finally have reached this far and I am writing these acknowledgements right now. I had several ups and downs but it has been certainly a challenging yet wonderful and unforgettable journey with much of learning that I could not have earned otherwise: piles of non-stop snowing in the winter, countless visits to slaughterhouse for pig's knees, BBQ party at the lab, the time with my nine-letter words-'scaffolds', the friendship with machines like T66, MTS, and microCT, fun TERMIS conferences with our awesome labmates, a sweet coffee break with Chanho and Hee-suk, and hours of paper writing including this dissertation. Of course, I could not have made all these precious memories and completed this journey without the help, advice, inspiration, encouragement, support, love, and prayer of people who have been my side.

First, I would like to thank my advisor, Dr. Scott Hollister, for offering me both guidance and freedom to explore and learn through my research at my pace. I truly appreciate your time, support, insight, and advice (especially in research, writing, and career development). I could not have come this far without your mentorship. I'd like to thank my other committee members, Asheesh Bedi, Paul Krebsbach, and Blake Roessler, for insightful questions and constructive suggestions on this work.

I also want to express thanks to all of our formal and current Scaffold Tissue Engineering Group members: Alisha Diggs, Annie Mitsak, Carolyn Slopsema, Chanho Park, Chia-Ying Lin, Colleen Flanagan, Darice Wong, Eiji Saito, Elly Liao, Erin Moffitt, Frank Winterroth, Greg Bratkovich, Heesuk Kang, Huina Zhang, Jessica Kemppainen, Sarah Mantilla, and Shelley Brown. A special thanks to Huina, for being a mentor, friend, and dim-sum partner, for teaching me how to do assays and analyze my obscure data, and for sharing your ideas and fun moments! Carolyn, you were a huge part of my final year of research, helping with tons of knee harvests, scaffolds fabrication, and compression tests. I appreciate your diligence, effort, and reliable research assistance. I also extend my gratitude to Chris Strayhorn and Cynthia Zuccaro for their time and efforts preparing my unfriendly histological samples, to Dr. Mohamed El-Sayed for advice and refreshing jokes as a qualifying exam committee member, and to the crew at Northwest Market for providing knees with happy smiles. Thank you to the supportive and helpful BME staff, especially Maria Steele, for all her fast and accurate administrative work behind during my graduate studies, and Tonya Brown, for taking care of my urgent supply orders.

I would like to thank two of my soulmates, Jaeyoun Roh who has been my friend, my sister, my counselor, and my *private* driver in Washington, D.C., and Jeehee Park who has been my friend and supporter regardless of our long distance between us from Korea to the States, for continuous prayer, support, encouragements, and sharing joyful moments and memories whenever I visited D.C or Korea. Thanks to my family in the Gospel: my adopted parents and family in D.C., Dr. Seong Jin Kim, Mr. Sung kuk Kim, Mrs. Jung Sook Kim, Dong-Hyun, Ka-Hyun, Dae-Chul, and Hyung-Seung. I could not

have survived through my down time during graduate studies without all of your love, support, and prayer. Pastors Dae Suk Seo and Sang Bum Kim: no one could fathom how much your endless prayer and spiritual advices helped me to learn and grow through the past ten years.

Lastly, I express my sincere thanks to my family for their love, support, positive expectations, and encouragement over the past five years: mom and dad, both grandmas, 'big father' uncle and aunts, and cousins. Particularly mom and dad, how could I express all of my gratitude and love in this writing! You are my first and last superstars and fans. Finally, thanks to my Lord and Savior, Jesus Christ, without whom I could not live a day.

TABLE OF CONTENTS

LIST OF FIGURES

FIGURE

LIST OF TABLES

TABLES

LIST OF APPENDICES

APPENDIX

ABSTRACT

Poly (1, 8-octanediol-co-citric acid) (POC) is a synthetic biodegradable biocompatible elastomer that can be processed by solid freeform fabrication into 3D scaffolds for cartilage tissue engineering. We investigated the effect of designed porosity on the mechanical properties, permeability, and degradation profiles of the POC scaffolds. Increased porosity was associated with increased degradation rate, increased permeability, and decreased mechanical stiffness that also became less nonlinear.

One goal of this work was to examine the effects of pore shape and permeability of two different POC scaffold designs on matrix production, mRNA gene expression, and differentiation of chondrocytes in both *in vitro* and *in vivo* models and the consequent mechanical property changes of the scaffold/tissue constructs. We also examined the effects of collagen I gel concentration on chondrogenesis as a cell carrier and found that a lower collagen gel concentration provides a favorable microenvironment for chondrocytes. With regards to scaffold design, low permeability with a spherical pore shape better enhanced the chondrogenic performance of chondrocytes in terms of matrix production, cell phenotype, and mRNA gene expression *in vitro* and *in vivo* compared to the highly permeable scaffold with a cubical pore shape. There were higher mRNA expressions for cartilage specific proteins and matrix degradation proteins in the high permeable design *in vivo*, resulting in overall less sGAG retained in the high permeable scaffold compared with the low permeable scaffold.

Another goal of this work was to determine material effects on cartilage regeneration for scaffolds with the same controlled architecture. Three dimensional polycaprolactone (PCL), poly (glycerol sebacate) (PGS), and poly (1, 8 octanediol-co-citrate) (POC) scaffolds of the same design were physically characterized and tissue regeneration was compared to find which material would be most optimal for cartilage regeneration *in vitro*. POC provided the best support for cartilage regeneration while PGS was seen as the least favorable material based on mRNA expressions. PCL still provided microenvironments suitable for chondrocytes to be active, yet it seemed to cause de-differentiation of chondrocytes inside the scaffold while growing cartilage outside the scaffold.

Scaffold architectures and materials characterization and analysis in this work will provide design guidance for scaffolds to meet the mechanical and biological parameters needed for cartilage regeneration.

CHAPTER 1

INTRODUCTION

1.1 Problem Statement

Over the past several decades, much has been learned about articular cartilage and its notoriously poor physiological capacity to restore itself. Despite many scientists and clinicians' efforts to find cures for cartilage damage, no technique has been completely successful in achieving normal regenerative articular cartilage to date. Osteoarthritis (OA), or degenerative joint disease, is the most prevalent joint disease in the United States, affecting approximately 60% of individuals over 70 years of age. Not only is OA the most common cause of disability in the elderly but it also costs $65 billion in the United States annually with an increasingly affected population and rising costs. This is not limited to the United States alone; in fact, musculoskeletal impairments are the most common cause of physical disability and reduced quality of life worldwide [1,2].

1.2 Causes of Articular Cartilage Damage

The poor self-repair and regenerative capability of articular cartilage stems from its avasculature nature and absence of lymphatic vessels and nerves. For its main function of load support and distribution, transport of fluid and solutes through the extracellular matrix (ECM) plays a critical role in providing necessary nutrients like oxygen and glucose for cells to maintain viability. In general, aging leads to poor nutrient supply to

and inadequate removal of waste products from articular cartilage. This triggers inefficient regulation of matrix degradation and synthesis, which are known to be the primary causes of the onset and progression of tissue degeneration that lead to osteoarthritis. Obesity, abnormal joint trauma or rotations due to sports or accidents are secondary causes of osteoarthritis with anticipation that these will steadily increase[3-6].

1.3 Current Treatments

Spontaneous repair of cartilage takes place only when the damage reaches the subchondral bone and mesenchymal stem cells are released from bone marrow. There are a number of treatments utilizing this repair capacity from bone marrow: drilling, abrasion arthroplasty, and microfracture. However these methods are applicable only for small lesions and tend to form fibrocartilage-like tissues rather than the desired hyaline-like tissues and eventually undergo progressive degeneration. Another technique developed by orthopedic surgeons, osteochondral transplantation (mosaicplasty), resurfaces the damaged cartilage but is also limited by the size of the injured area and donor-site morbidity [5,7-10].

Finally, a treatment option inspired by tissue engineering techniques called autologous chondrocyte implantation (ACI) has been introduced and it has been applied successfully for more than a decade. This technique, however, is still limited by a number of factors including the necessity of two surgeries (one to obtain cells, the second to re-implant cells) and the wide arthrotomy incision often required. In addition, the outcomes

after ACI repair were not better than microfracture despite the much greater cost of ACI[10-12].

An improved version of the ACI technique retains cells within matrices instead of using a periosteal flap, which involves additional tissue-engineering-based strategies and has been applied as a clinical treatment. For instance, membranes formed out of type I or/and III collagens are clinically available for autologous chondrocyte implantation such as matrix-induced autologous chondrocyte implantation (MACI® (Verigen, Germany), Chondro-gide® (Geistlich Biomaterials, Switzerland), and Atelocollagen® (Koken Co. Ltd, Japan). A hyaluronic-acid-based matrix called HYAFF-11®(Hyalograft® C, Fidia Advanced Biopolymers, Italy), fibrin glue based treatments (Tissucol®, DeNovo NT graft), and implantation of minced cartilage in combination with copolymers of polyglycolic acid (Bio-Seed-® C (BioTissue Technologies, Germany)) and polycaprolactone (cartilage autograft implantation system) are currently available treatments showing promising clinical outcomes [12,13].

To date, ACI and MACI are prime examples of clinical tissue engineering treatments for articular cartilage defects that incorporate the well-known tissue engineering triad: cells, biomaterials, and growth factors, in order to repair and regenerate tissues. Among various cell sources that have been contemplated for cartilage tissue engineering, chondrocytes from articular cartilage have been considered the most logical cells of choice. However, they still have major disadvantages such as their difficult expansion in monolayer culture and the rare donor tissue availability [14]. Multipotent mesenchymal stromal cells or mesenchymal stem cells (MSCs) such as bone marrow

stromal cells and pre-adipocytes [15-19] have been considered an attractive source of cells for cartilage engineering. These cells overcome the disadvantages of chondrocytes because of their relative ease of availability and their high capacity of *in vitro* expansion. Implantation of MSCs often requires the proper use of growth and differentiation factors which will effectively induce specific differentiation pathways and the maintenance of the chondrocyte phenotype. Hence, wide ranges of growth factors have been actively explored for enhancing chondrogenesis including transforming growth factor beta (TGF-β), the bone morphogenetic protein (BMP) family, the fibroblastic growth factor (FGF) family, and the insulin-like growth factor (IGF) family [20-25]. Sole or combined effects of various growth factors have been studied with multiple cell types and culture conditions. Together with the other two components of the tissue engineering triad, various aspects of scaffolds have been explored for further advances in tissue engineered cartilage. Not only does the scaffold play a role as cell carrier, but it can also provide a proper microenvironment for cell maintenance/differentiation and/or as a tool for controlled release of growth factors. The scaffold should also provide biomimetic mechanical integrity and proper mass transport properties to enhance the quality of tissue engineered cartilage.

Potentials of Scaffold Tissue Engineering Strategies

Although the currently available treatment options mentioned above, especially ACI and MACI, are showing some positive clinical outcomes, there is a need and desire to develop more robust treatment for cartilage damage using scaffolds and cells [26]. ACI and MACI typically do not provide sufficient mechanical support and cell retention at the

defect site, a limitation that could be addressed with improved biomaterial scaffolds. A scaffold can play a significant role by not only offering mechanical integrity withstanding loads in the body but also providing an adequate mechanical environment to cells. Chondrocytes are known to favor a three-dimensional (3D) environments for their differentiation, and mechanical stimulation has been shown to be directly related to the maintenance of the chondrocytic phenotype and extracellular matrix formation, which are directly related to the mechanical environments [27,28]. Not only could the scaffold help to retain cells and deliver biofactors, but it could also provide proper mechanical and mass transport properties that are similar to native cartilage, thus enhancing cartilage repair and regeneration.

1.4 Aims of this Thesis

The work in this thesis will examine two aspects of scaffolds via physical/mechanical and biochemical assessments: (1) scaffold architectural effects using poly (1, 8 octanediol-co-citrate) (POC) *in vitro* and *in vivo* and (2) scaffold material effects on chondrogenesis *in vitro* using chondrocytes for cartilage tissue regeneration. These two specific aspects are derived from the global hypothesis of scaffold tissue engineering: a combination of a biocompatible and biodegradable polymer scaffold with mechanical and mass transport properties in the range of normal articular cartilage that delivers chondrogenically favorable factors enhance cartilage matrix production and will provide an alternative method for repairing cartilage injuries. For the scaffold architectural effects, we investigate the scaffold permeability and pore shape effects on chondrogenesis *in vitro* and *in vivo* using primary chondrocytes and POC as the scaffold

material. For scaffold material effects, we first examine if architectural effects are consistent across scaffold materials and if not, what material would be most favorable for chondrogenesis among three biocompatible materials that we have selected based on their different mechanical, physical, and biochemical properties. The more detailed rationale of the three material selections will follow in chapters 3 and 8.

The two main criteria for successful cartilage scaffolds are (1) mechanical integrity that mimics the target effective stiffness of native cartilage and provides a sufficiently supportive frame for cell retention and growth into desired tissues, and (2) optimally designed mass transport properties that induce regenerated cartilage tissue quality that mimics native cartilage in terms of cell phenotype, genotype, and matrix production. Several biomaterials have been used and developed in order to create optimal scaffolds for soft tissues including cartilage and are reviewed in depth in chapter 3. In this thesis, polycaprolactone (PCL), poly (glycerol-co-sebacate) (PGS), and poly (1, 8 octanediol-co-citrate) (POC) are the three biomaterials that are explored and compared to each other as 3D scaffold materials. Among the three materials, the main focus is on evaluating the feasibility and potential of POC as a cartilage scaffold material. POC is relatively new in the field of tissue engineering and has not been explored in depth for cartilage engineering using controlled 3D architectures made with solid freeform fabrication. As an additional investigation, a study comparing two dimensional (2D) discs of four materials (three materials mentioned above and RGD modified PCL (PCL-RGD)) was conducted to support the data obtained for the three selected scaffold materials (shown in chapter 7) and to further explain the observations obtained in the scaffold material comparison study.

1.5 Dissertation Overview

Chapter 2 reviews the structural and biochemical aspects of articular cartilage that we aim to regenerate and specifies the targeted metrics for native articular cartilage in terms of compressive, tensile and permeability properties. Chapter 3 describes and thoroughly reviews currently available biomaterials for cartilage applications and how they could provide mechanical support to damaged cartilage regions. In particular, mechanical properties of three materials—PCL, PGS, and POC—are explored in depth and the rationales for choosing these three materials for cartilage scaffolds are provided. Chapter 3 will also have a comprehensive review on scaffold design factors for cartilage tissue engineering that are related to mass transport properties. These include pore size, porosity, pore shape, pore interconnectivity, permeability, and other relevant factors. Chapter 4 characterizes and explains the mechanical, permeability, and degradation properties of solid freeform fabricated POC scaffolds of several designs and how we optimized our design for cartilage regeneration. Chapter 5 & 6 introduce and compare the performance of two optimized designs (selected from chapter 4) to examine the coupled effects of scaffold pore shape and permeability on chondrogenesis *in vitro* and *in vivo*. Chapter 7 explores and compares scaffold architectural effects vs. scaffold material effects on chondrogenesis *in vitro* using the most optimal design (selected from Chapter 5 & 6) for three different materials (PCL, PGS, and POC). Here, the important scaffold design considerations and the selected scaffold material for cartilage tissue engineering are revealed. Chapter 8 describes a follow up experiment to chapter 7 to further investigate material affects, specifically hydrophilicity, on chondrogenesis using two-dimensional discs with the three different materials (PCL, PGS, & POC) and one

additional material (PCL-RGD) in order to clarify any cell-material interactions that may further explain the results obtained from Chapter 7. This part is rooted from the results illustrated in chapter 7 and is more of a supplementary study. In Chapter 9, the conclusions and future directions of this work are presented. The simple flow chart of the experimental study design presented in this thesis is shown below (Figure 1.1).

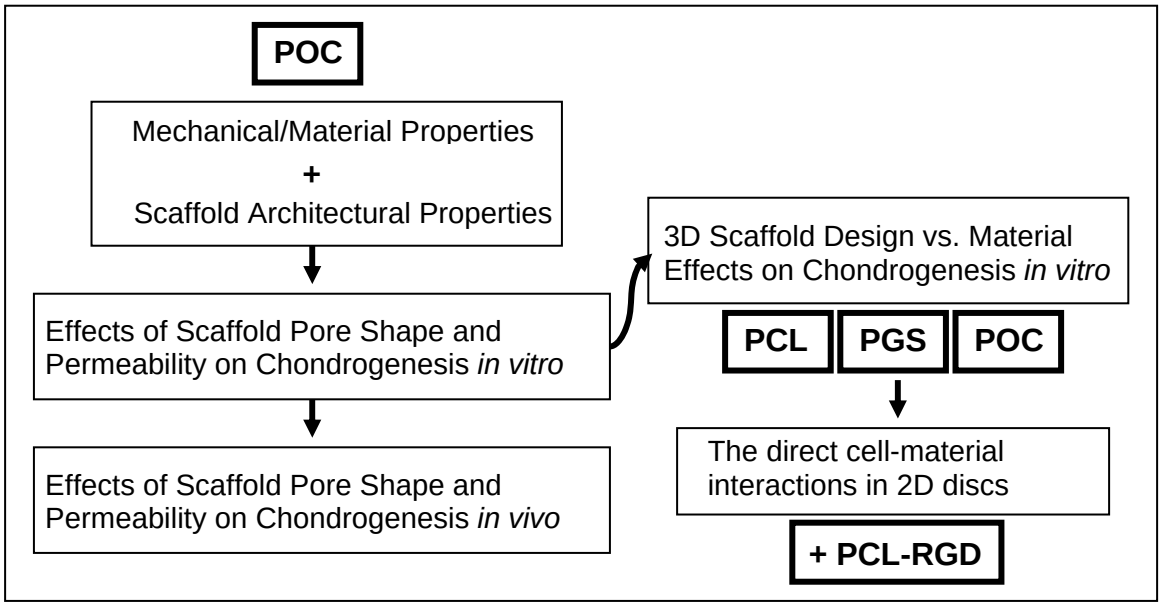

Figure 1.1 This flow chart illustrates the overview of this thesis.

References

1. Lawrence, R.C., Helmick, C.G., Arnett, F.C., Deyo, R.A., Felson, D.T., Giannini, E.H., Heyse, S.P., Hirsch, R., Hochberg, M.C., Hunder, G.G., Liang, M.H., Pillemer, S.R., Steen, V.D., and Wolfe, F. Estimates of the prevalence of arthritis and selected musculoskeletal disorders in the United States. Arthritis and Rheumatism 41, 778, 1998.

2. Center for Disease Control and Prevention (CDC). Prevalence and impact of arthritis by race and ethnicity - United States, 1989-1991. MMWR Morb Mortal Wkly Rep 45, 373-8, 1996.

3. Grimshaw, M.J., and Mason, R.M. Bovine articular chondrocyte function in vitro depends upon oxygen tension. Osteoarthritis and cartilage / OARS, Osteoarthritis Research Society 8, 386, 2000.

4. Horner, H.A., and Urban, J.P. 2001 Volvo Award Winner in Basic Science Studies: Effect of nutrient supply on the viability of cells from the nucleus pulposus of the intervertebral disc. Spine 26, 2543, 2001.

5. Mow, V.C., Ratcliffe, A., and Poole, A.R. Cartilage and diarthrodial joints as paradigms for hierarchical materials and structures. Biomaterials 13, 67, 1992.

6. Hunziker, E.B. The elusive path to cartilage regeneration. Adv Mater , 2009, 21, 3419-3424.

7. Insall, J. The Pridie debridement operation for osteoarthritis of the knee. Clinical orthopaedics and related research (101), 61, 1974.

8. Johnson, L.L. Arthroscopic abrasion arthroplasty historical and pathologic perspective: present status. Arthroscopy: The Journal of Arthroscopic & Related Surgery : Official Publication of the Arthroscopy Association of North America and the International Arthroscopy Association 2, 54, 1986.

9. Johnson, L.L. Arthroscopic abrasion arthroplasty: a review. Clinical orthopaedics and related research (391 Suppl), S306, 2001.

10. Lutzner, J., Kasten, P., Gunther, K.P., and Kirschner, S. Surgical options for patients with osteoarthritis of the knee. Nature reviews.Rheumatology 5, 309, 2009.

11. Kessler, M.W., Ackerman, G., Dines, J.S., and Grande, D. Emerging technologies and fourth generation issues in cartilage repair. Sports medicine and arthroscopy review 16, 246, 2008.

12. Ahmed, T.A., and Hincke, M.T. Strategies for Articular Cartilage Lesion Repair and Functional Restoration. Tissue engineering.Part B, Reviews, 2010.

13. Brittberg, M. Cell Carriers as the Next Generation of Cell Therapy for Cartilage Repair: A Review of the Matrix-Induced Autologous Chondrocyte Implantation Procedure. The American Journal of Sports Medicine, 2009.

14. Brittberg, M., Lindahl, A., Nilsson, A., Ohlsson, C., Isaksson, O., and Peterson, L. Treatment of deep cartilage defects in the knee with autologous chondrocyte transplantation. The New England journal of medicine 331, 889, 1994.

15. Wei, Y., Hu, H., Wang, H., Wu, Y., Deng, L., and Qi, J. Cartilage regeneration of adipose-derived stem cells in a hybrid scaffold from fibrin-modified PLGA. Cell transplantation 18, 159, 2009.

16. Jung, Y., Kim, S.H., Kim, Y.H., and Kim, S.H. The effects of dynamic and three-dimensional environments on chondrogenic differentiation of bone marrow stromal cells. Biomedical materials (Bristol, England) 4, 55009, 2009.

17. Jakobsen, R.B., Shahdadfar, A., Reinholt, F.P., and Brinchmann, J.E. Chondrogenesis in a hyaluronic acid scaffold: comparison between chondrocytes and MSC from bone marrow and adipose tissue. Knee surgery, sports traumatology, arthroscopy : official journal of the ESSKA , 2009.

18. Diekman, B.O., Rowland, C.R., Caplan, A.I., Lennon, D., and Guilak, F. Chondrogenesis of adult stem cells from adipose tissue and bone marrow: Induction by growth factors and cartilage derived matrix. Tissue engineering.Part A , 2009.

19. Kemppainen, J.M., and Hollister, S.J. Differential effects of designed scaffold permeability on chondrogenesis by chondrocytes and bone marrow stromal cells. Biomaterials 31, 279, 2010.

20. Grimaud, E., Heymann, D., and Redini, F. Recent advances in TGF-beta effects on chondrocyte metabolism. Potential therapeutic roles of TGF-beta in cartilage disorders. Cytokine & growth factor reviews 13, 241, 2002.

21. Sekiya, I., Larson, B.L., Vuoristo, J.T., Reger, R.L., and Prockop, D.J. Comparison of effect of BMP-2, -4, and -6 on in vitro cartilage formation of human adult stem cells from bone marrow stroma. Cell and tissue research 320, 269, 2005.

22. Kuo, A.C., Rodrigo, J.J., Reddi, A.H., Curtiss, S., Grotkopp, E., and Chiu, M. Microfracture and bone morphogenetic protein 7 (BMP-7) synergistically stimulate articular cartilage repair. Osteoarthritis and cartilage / OARS, Osteoarthritis Research Society 14, 1126, 2006.

23. Dailey, L., Ambrosetti, D., Mansukhani, A., and Basilico, C. Mechanisms underlying differential responses to FGF signaling. Cytokine & growth factor reviews 16, 233, 2005.

24. Schmidt, M.B., Chen, E.H., and Lynch, S.E. A review of the effects of insulin-like growth factor and platelet derived growth factor on in vivo cartilage healing and repair. Osteoarthritis and cartilage / OARS, Osteoarthritis Research Society 14, 403, 2006.

25. Ellman, M.B., An, H.S., Muddasani, P., and Im, H.J. Biological impact of the fibroblast growth factor family on articular cartilage and intervertebral disc homeostasis. Gene 420, 82, 2008.

26. Ochi, M., Uchio, Y., Kawasaki, K., Wakitani, S., and Iwasa, J. Transplantation of cartilage-like tissue made by tissue engineering in the treatment of cartilage defects of the knee. The Journal of bone and joint surgery.British volume 84, 571, 2002.

27. Bonaventure, J., Kadhom, N., Cohen-Solal, L., Ng, K.H., Bourguignon, J., Lasselin, C., and Freisinger, P. Reexpression of cartilage-specific genes by dedifferentiated human articular chondrocytes cultured in alginate beads. Experimental cell research 212, 97, 1994.

28. Grodzinsky, A.J., Levenston, M.E., Jin, M., and Frank, E.H. Cartilage tissue remodeling in response to mechanical forces. Annual Review of Biomedical Engineering 2, 691, 2000.

CHAPTER 2

ARTICULAR CARTILAGE

Articular cartilage is a highly specialized tissue that reduces joint friction at the extremities of long bones, and is a unique and complex organ due to its isolation from the body with avasculature, and absence of lymphatic vessel and nerves. It is hyaline cartilage which mainly consists of water (75%), a limited number of chondrocytes, and a rich extracellular matrix (ECM) that is composed of a network of collagens (20%), in particular, type II collagen, which gives the tissue its shape, strength, and functionality, and proteoglycans (5%), which give resistance to mechanical loading [1,2]. In addition, the synovial fluid around it allows frictionless movements between articulating surfaces and provides nutrient supply to articular cartilage [3]. These components form the intricate macromolecular structure of this tissue and work in harmony remarkably to absorb everyday forces and to serve as a bearing material for movable joints such as the hip, knee or shoulder [4].

In spite of relatively simple components, articular cartilage is extremely challenging tissue to repair and regenerate with our native self-repair mechanisms and/or modern remedies. It has a very poor intrinsic healing capacity because it lacks blood vessels and lymphatic vessels isolated from systemic regulation and chondrocytes are surrounded by a dense ECM, thus the usual wound healing mechanism through cell

infiltration or cell migration is not likely to occur when cartilage damage takes place[2]. Furthermore, the complexity in cartilage tissue repair and regeneration relies on its unique zonal structures. Cartilage is divided into four zones from the articular surface to the subchondral bone: superficial, middle, deep and calcified cartilage (Figure 2.1) and each zone is different in extracellular macromolecular composition, chondrocyte morphology, collagen fiber composition and arrangement, hydrophilic proteoglycan accumulation and its consequent variation in functionality.

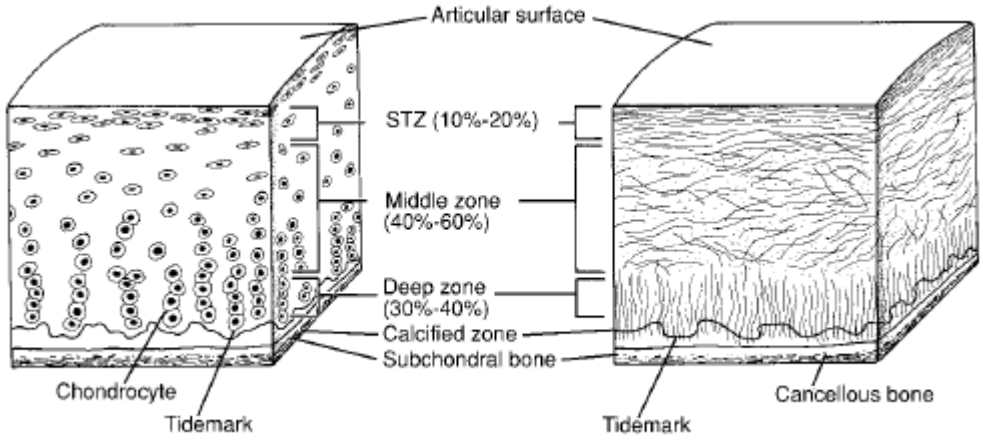

Figure 2.1: A schematic diagram of chondrocyte organization in the three main zones of the uncalcified cartilage (STZ = superficial tangential zone), the tidemark, calcified zone, and the subchondral bone (right) and sagittal cross-sectional diagram of collagen fiber architecture shows the three salient zones of articular cartilage (left) [5].

The superficial zone is exposed to the synovial fluid of the intra-articular space and contains elongated fibroblast-like cells with the highest and lowest quantities of collagen and aggrecan, respectively. The middle zone comprising 40-60% of articular cartilage thickness is occupied by randomly distributed spherical chondrocytes with the randomly oriented collagen fibrils that are thicker but less dense than the superficial zone,

and the richest aggrecan contents. The deep zone contains resident oblong cells with large collagen fibril bundles and significantly lower aggrecan contents [5-7].

All this delicate and complex organization of articular cartilage requires a variety of qualitative and quantitative assessments to evaluate tissue engineered cartilage, including histological, immunohistological, biochemical, mechanical, and molecular genetic measures. Hence, with the brief survey of the development of articular cartilage as an introduction, we will review and detail the biochemical and molecular genetic measures we used in this study highlighting molecules responsible for formation and degradation of ECM constituents. Also, mechanical properties of native articular cartilage will be reviewed, which we will strive to target and match our engineered scaffold/tissue constructs' mechanical properties with.

For engineered cartilage grown within scaffolds *in vitro and in vivo*, we quantify matrix production by seeded chondrocytes and measure the cellular expression of genes that relate to chondrogenic differentiation, ossification, and matrix degradation. More specifically, we measure the amount of sulfated-glycosaminoglycans (sGAGs) formed and contained by chondrocytes seeded scaffolds and compare the sGAG contents with the cellular mRNA expression of collagens (Type 1, 2, and 10), aggrecan, and matrix metalloproteinase (MMPs - 3 & 13). The significance and relevance of each component in native tissue will be detailed in this chapter. Then, other relevant roles of biophysical and mechanical stimuli present in cartilage which affect chondrogenesis will be briefly reviewed as well.

2.1 Articular Cartilage Development

The formation and development of the cartilage proceeds via an analogous series of events but they can be summarized into two main steps: condensation and differentiation of skeletal progenitor cells which have potentials to form a skeletal cell and tissue type in embryos and in adults. First, undifferentiated prechondrogenic mesenchymal cells migrate to the sites of the prospective skeletal elements and subsequently assemble into compact cellular condensations mediated by a combination of precartilage matrix and cell adhesion molecules [8]. Once this cellular condensation reaches a critical size, the aggregated mesencymal cells enable crucial cell-cell interactions and signaling events that trigger overt chondrocyte differentiation: changing from an elongated fibroblastic-like shape to the spherical morphology of hyaline chondrocytes and synthesizing cartilage-specific ECM molecules such as collagen types 2, 4, and 6 and the highly-sulfated proteoglycan aggrecan [9]. From this stage, there are only two possible developmental paths hyaline chondrocytes can take: (1) further differentiation into hypertrophic chondrocytes expressing collagen type 10 and forming the growth plate or (2) remaining hyaline chondrocytes responsible for organization and maintenance of the ECM [10]. In this study, we focus on how scaffold pore shape and permeability and materials may affect chondrogenic differentiation of chondrocytes measuring the mRNA expressions of collagen 2 and 10 due to their relevance in this developmental stage.

2.2 Articular Cartilage Extracellular Matrix Molecules

Matrix Glycosaminoglycans

Two major constituents of the cartilage ECM are proteoglycans and collagens. The two most abundant proteoglycans in the cartilage matrix are aggrecan and decorin. Aggrecan is a glycosaminoglycan-containing molecule with three globular (G1, G2 and G3) domains and the G1 domain binds to hyaluronan chains with the aid of a link protein. It is a large proteoglycan consisting of a 200kDa core protein to which keratin sulfate, chondroitin sulfate, and hyaluronic acid GAG side-chains are attached. The sulfated GAG side-chains attached to the aggrecan core protein are highly negatively charged and capable of attracting osmotically active cations and their associated water, which confers upon cartilage the ability to withstand compressive force [9]. For this reason, the two sulfated GAGs are commonly measured through biochemical assays as an indication of production and accumulation of extracellular cartilaginous matrix.

As aggrecan is the main proteoglycan found in cartilage, it is also a typical biomarker for differentiated chondrocytes. During chondrogenesis, aggrecan messenger-RNA (mRNA) begins to accumulate immediately before cellular condensation and continues to be expressed throughout the differentiation process [11]. Here, mRNA expression of aggrecan normalized to GAPDH was used to quantify the extent of chondrogenesis when comparing scaffold designs and materials along with sGAG quantification. Even though not measured in this study, decorin is a member of the small leucine-rich proteoglycan (SLRP) family and it has one GAG side-chain attached to its core protein. Decorin is able to bind collagen types 1, 2, and 6 and has been shown to

regulate fibrillar diameter of collagens 2 and 6. Overall, decorin as one of the SLRP family helps to maintain the integrity of cartilage tissue and its metabolism [6,12,13].

Cartilage Collagens

Collagen type 2 is the major collagen type found in both embryonic and adult cartilages accounting for 90-95% of the overall collage content and it is categorized as a fibril-forming or interstitial collagen [14]. Collagen type 2 is responsible for the tensile properties of cartilage tissue [6]and collagen type 2 based hydrogels have been shown to maintain the typical rounded chondrocyte phenotype significantly better than collagen type 1 based hydrogels with highest GAG production per cell seeded in hydrogels and enhanced mRNA expression of collagen type 2 and aggrecan [15-17]. Also, a significant increase in the type 2 collagen mRNA takes place coincidentally with the condensation in chondrogenesis and a continuous increase in the type 2 collagen mRNA expression has been found with progressive accumulation of ECM. Due to these reasons, collagen type 2 alone is used as a positive biomarker for chondrocyte differentiation. However, when Type 2 collagen is destroyed, it is replaced with a type I collagen fibro-cartilage that does not have the same functional properties as type II collagen. The ratio of collagen 2 gene expression to collagen 1 gene expression, recently known as the "differentiation index", attains a higher value with a more chondrocytic genotype, and a lower value with a more fibroblastic gene expression [18,19]

Collagen type 1 is categorized as a fibril-forming or interstitial collagen and is mostly associated with bone and partly with fibrocartilage. It is generally accepted as a

biomarker for chondrocyte de-differentiation and is known to cause chondrocytic rounded morphology to change to be fibroblastic-like. However, collagen type 1 gels are a popular scaffold in which to seed chondroprogenitor or chondrocytic cells to generate cartilage constructs *in vitro* and *in vivo* with successful outcomes of producing cartilage [15,16,20].

Collagen type 10 is specific to cartilage and is developmentally regulated. It is synthesized by terminally differentiating chondrocytes such as hypertrophic chondrocytes and it is known to facilitate the process of calcification through metrical organization changes. Type 10 collagen gene expressions have been detected in chondrocytes present in osteoarthritis (OA) tissue, particularly in areas where the endochondral ossification and bone formation appear to be initiated. Hence, type 10 collagen is a reliable marker for terminally differentiated or hypertrophic chondrocytes in engineered articular cartilage and it is used as a negative marker for chondrogenesis [21].

Matrix metalloproteinase (MMPs)

Matrix metalloproteinase (MMPs) along with a disintegrin and metalloproteinase with thrombospondin motifs (ADAMTS) are capable of degrading aggrecan and only MMPs are known to be capable of degrading fibrillar collagens including type 2 collagen which is extremely resistant to most proteinases. Among MMP members, MMP-13 and MMP-3 play critical roles in cartilage extracellular matrix degradation. MMP-13, known as the collagenase, is a product of the chondrocytes that reside in the cartilage and MMP-3, known as stromelysins, is elevated in arthritis, which degrades non-collagen matrix components of the joints. In addition to collagen, MMP-13 also degrades the

proteoglycan molecule, aggrecan, giving it a dual role in matrix destruction [22-24]. The mRNA expressions of MMP-13 and MMP-3 were measured in this study to have a more comprehensive view on matrix production (sGAG quantification) along with mRNA expressions representing matrix formation (i.e. collagen 2 and aggrecan) as the overall sGAG amount per scaffold would be an outcome of matrix formation and matrix degradation.

All these quantitative measures of these genes expressed in engineered cartilage tissue are compared within each study of tissue/scaffold constructs in this work rather than to gene expression levels normally found in native healthy cartilage due to the wide variance in the gene expression levels reported. Since the goal in this work is not to exactly match the gene expression levels with native cartilage tissue, it is more accurate to compare expression levels within scaffold designs or materials to compare and determine the best choice for chondrogenesis.

2.3 Roles of three-dimensional environment and biophysical and mechanical stimuli

Chondrocytes are infamous for monolayer cell culture expansion as isolated chondrocytes will lose their differentiated phenotype in two-dimensional (2D) culture whereas chondrocytes proliferate and differentiate happily within a complex three-dimensional (3D) environment [25]. The de-differentiation process usually causes cell phenotype changes from rounded chondrocytic to fibroblast-like with an increased expression of type I collagen, which is easy to find in 2D culture. However, it has been shown to be reversible when cells are cultured back in a 3D environment, confirming that

the 3D environment is a crucial condition that has a significant role in supporting and restoring the chondrocytic phenotype and chondrogenesis [26,27].

Chondrocytes receive oxygen and nutrients via a passive diffusion from the synovial fluid hence articular chondrocytes are not metabolically active and experience low oxygen tension. Hypoxia conditions not only help to maintain the chondrocytic phenotype but also have been shown to increase the synthesis of ECM proteins in cultured chondrocytes *in vitro* [27,28]. In addition, hypoxia has also recently been suggested to inhibit the expression of type 10 collagen during the chondrogenesis of epiphyseal chondrocytes, assuring that hypoxia is probably a required condition for cartilage engineering along with 3D environments [29].

Cartilage is well-known for its weight bearing and under physiological conditions it is subjected to various mechanical stimuli such as hydrostatic, compressive, and tensile pressure and shear strain. The mechanical stimuli are considered to be an essential factor influencing the chondrogenic differentiation and the maintenance of cartilage integrity as mechanical stimuli also affect gene expressions that are relevant to ECM molecules and degradation proteins mentioned above [30,31]. Bioreactors are commonly used in cartilage tissue engineering to accommodate such conditions.

Aging affects the properties of healthy cartilage by altering the content, composition, and structural organization of collagen and proteoglycan [32]. The matrix functions to maintain the homeostasis of the cellular environment and the structure of cartilage. When the degradation of the extracellular matrix (ECM) exceeds its synthesis, a net decrease in the amount of cartilage matrix and a subsequent elevation in the

proteolytic enzymes' activities eventually lead to the destruction of articular cartilage as shown in diseases such as osteoarthritis (OA) and rheumatoid arthritis (RA). The main enzymes responsible for degradation of aggrecan and collagens in cartilage, the matrix metalloproteinases (MMPs), are overexpressed in cartilage of patients with RA and OA [33]. This disruption in cartilage homeostasis causes not only an imbalance in biochemical composition of cartilage but also its mechanical instability. Hence it is crucial to regenerate an engineered cartilage with well-balanced biochemical compositions and proper material/mechanical properties similar to native cartilage. The permeability and mechanical properties of native cartilage are discussed more in detail in chapter 3, which are also the targeted properties for our tissue/scaffold constructs in this work. The biochemical assessments of chondrogenesis to examine the matrix formation and chondrocyte phenotype shift during differentiation or de-differentiation/ossification inside each scaffold design are presented in chapter 5-8 for *in vitro* and *in vivo* studies.

References

1. Ateshian, G.A. Artificial cartilage: weaving in three dimensions. Nature materials 6, 89, 2007.

2. Ochi, M., Adachi, N., Nobuto, H., Yanada, S., Ito, Y., and Agung, M. Articular cartilage repair using tissue engineering technique--novel approach with minimally invasive procedure. Artificial Organs 28, 28, 2004.

3. Schmidt, T.A., and Sah, R.L. Effect of synovial fluid on boundary lubrication of articular cartilage. Osteoarthritis and cartilage / OARS, Osteoarthritis Research Society 15, 35, 2007.

4. Poole, A.R., Kojima, T., Yasuda, T., Mwale, F., Kobayashi, M., and Laverty, S. Composition and structure of articular cartilage: a template for tissue repair. Clinical orthopaedics and related research (391 Suppl), S26, 2001.

5. Buckwalter, J.A., Mow, V.C., and Ratcliffe, A. Restoration of Injured or Degenerated Articular Cartilage. The Journal of the American Academy of Orthopaedic Surgeons 2, 192, 1994.

6. Poole, A.R. Cartilage in health and disease. In: Koopman, W.J. and Moreland, L.W., eds. Arthritis and Allied Conditions: A Textbook of Rheumatology CH 15. Philadelphia: Lippincott Williams & Wilkins, 2005, pp. 223-269.

7. Tuan, R.S., and Chen, F.H. Cartilage. In: Battler, A. and Leor, J., eds. Stem Cell and Gene-Based Therapy: Frontiers in Regenerative Medicine. London: Springer, 2006, pp. 179-193.

8. DeLise, A.M., Fischer, L., and Tuan, R.S. Cellular interactions and signaling in cartilage development. Osteoarthritis and cartilage / OARS, Osteoarthritis Research Society 8, 309, 2000.

9. Bobick, B.E., Chen, F.H., Le, A.M., and Tuan, R.S. Regulation of the chondrogenic phenotype in culture. Birth defects research.Part C, Embryo today: reviews 87, 351, 2009.

10. Beier, F. Cell-cycle control and the cartilage growth plate. Journal of cellular physiology 202, 1, 2005.

11. Kosher, R.A., Gay, S.W., Kamanitz, J.R., Kulyk, W.M., Rodgers, B.J., Sai, S., Tanaka, T., and Tanzer, M.L. Cartilage proteoglycan core protein gene expression during limb cartilage differentiation. Developmental biology 118, 112, 1986.

12. Roughley, P.J. The structure and function of cartilage proteoglycans. European cells & materials 12, 92, 2006.

13. Danielson, K.G., Baribault, H., Holmes, D.F., Graham, H., Kadler, K.E., and Iozzo, R.V. Targeted disruption of decorin leads to abnormal collagen fibril morphology and skin fragility. The Journal of cell biology 136, 729, 1997.

14. Bruckner, P., and van der Rest, M. Structure and function of cartilage collagens. Microscopy research and technique 28, 378, 1994.

15. Bosnakovski, D., Mizuno, M., Kim, G., Takagi, S., Okumura, M., and Fujinaga, T. Chondrogenic differentiation of bovine bone marrow mesenchymal stem cells (MSCs) in different hydrogels: influence of collagen type II extracellular matrix on MSC chondrogenesis. Biotechnology and bioengineering 93, 1152, 2006.

16. Nehrer, S., Breinan, H.A., Ramappa, A., Shortkroff, S., Young, G., Minas, T., Sledge, C.B., Yannas, I.V., and Spector, M. Canine chondrocytes seeded in type I and type II collagen implants investigated in vitro. Journal of Biomedical Materials Research 38, 95, 1997.

17. Nehrer, S., Breinan, H.A., Ramappa, A., Young, G., Shortkroff, S., Louie, L.K., Sledge, C.B., Yannas, I.V., and Spector, M. Matrix collagen type and pore size influence behaviour of seeded canine chondrocytes. Biomaterials 18, 769, 1997.

18. Kosher, R.A., Kulyk, W.M., and Gay, S.W. Collagen gene expression during limb cartilage differentiation. The Journal of cell biology 102, 1151, 1986.

19. Martin, I., Jakob, M., Schafer, D., Dick, W., Spagnoli, G., and Heberer, M. Quantitative analysis of gene expression in human articular cartilage from normal and osteoarthritic joints. Osteoarthritis and cartilage / OARS, Osteoarthritis Research Society 9, 112, 2001.

20. Wakitani, S., Goto, T., Young, R.G., Mansour, J.M., Goldberg, V.M., and Caplan, A.I. Repair of large full-thickness articular cartilage defects with allograft articular chondrocytes embedded in a collagen gel. Tissue engineering 4, 429, 1998.

21. Shen, G. The role of type X collagen in facilitating and regulating endochondral ossification of articular cartilage. Orthodontics & craniofacial research 8, 11, 2005.

22. Burrage, P.S., Mix, K.S., and Brinckerhoff, C.E. Matrix metalloproteinases: role in arthritis. Frontiers in bioscience: a journal and virtual library 11, 529, 2006.

23. Malemud, C.J. Matrix metalloproteinases: role in skeletal development and growth plate disorders. Frontiers in bioscience: a journal and virtual library 11, 1702, 2006.

24. Cawston, T.E., and Wilson, A.J. Understanding the role of tissue degrading enzymes and their inhibitors in development and disease. Best practice & research.Clinical rheumatology 20, 983, 2006.

25. Darling, E.M., and Athanasiou, K.A. Rapid phenotypic changes in passaged articular chondrocyte subpopulations. Journal of orthopaedic research: official publication of the Orthopaedic Research Society 23, 425, 2005.

26. Malda, J., van Blitterswijk, C.A., Grojec, M., Martens, D.E., Tramper, J., and Riesle, J. Expansion of bovine chondrocytes on microcarriers enhances redifferentiation. Tissue engineering 9, 939, 2003.

27. Domm, C., Schunke, M., Christesen, K., and Kurz, B. Redifferentiation of dedifferentiated bovine articular chondrocytes in alginate culture under low oxygen tension. Osteoarthritis and cartilage / OARS, Osteoarthritis Research Society 10, 13, 2002.

28. Lafont, J.E., Talma, S., and Murphy, C.L. Hypoxia-inducible factor 2alpha is essential for hypoxic induction of the human articular chondrocyte phenotype. Arthritis and Rheumatism 56, 3297, 2007.

29. Robins, J.C., Akeno, N., Mukherjee, A., Dalal, R.R., Aronow, B.J., Koopman, P., and Clemens, T.L. Hypoxia induces chondrocyte-specific gene expression in mesenchymal cells in association with transcriptional activation of Sox9. Bone 37, 313, 2005.

30. Zuscik, M.J., Hilton, M.J., Zhang, X., Chen, D., and O'Keefe, R.J. Regulation of chondrogenesis and chondrocyte differentiation by stress. The Journal of clinical investigation 118, 429, 2008.

31. Grodzinsky, A.J., Levenston, M.E., Jin, M., and Frank, E.H. Cartilage tissue remodeling in response to mechanical forces. Annual Review of Biomedical Engineering 2, 691, 2000.

32. Goldring, M.B., and Marcu, K.B. Cartilage homeostasis in health and rheumatic diseases. Arthritis research & therapy **11**, 224, 2009.

33. Nagase, H., and Kashiwagi, M. Aggrecanases and cartilage matrix degradation. Arthritis research & therapy **5**, 94, 2003.

CHAPTER 3

INFLUENCE OF POLYMERIC SCAFFOLD DESIGN AND MATERIAL ON CARTILAGE TISSUE ENGINEERING

There have been numerous natural and synthetic materials used for cartilage tissue engineering scaffolds. These scaffolds have been fabricated using a number of techniques and researchers are still investigating new synthetic materials to support cartilage regeneration. The ideal scaffold should be biocompatible (no inflammatory response), non-cytotoxic, capable of supporting cell attachment and proliferation, and biodegradable serving as a temporary support for the cells yet allowing eventual replacement by at the implanted sites. Also, it should be permeable and well-interconnected for cells to be distributed and grown evenly throughout the scaffold and to allow nutrient diffusion throughout for cellular proliferation and extracellular matrix formation. In addition to appropriate effective mass transport properties, scaffolds should possess effective mechanical properties to provide protect seeded and host cells from joint loading until desired tissues are grown to provide sufficient mechanical support. Furthermore, scaffold materials should be readily available and able to be processed into a variety of shapes and sizes with relatively low cost[1,2]. To fulfill these requirements, many researchers have hypothesized that scaffolds should have mechanical and transport properties similar or close to native cartilage tissue. This would allow the scaffold to support cartilage regeneration by providing appropriate local mass transport, mechanical

and biochemical microenvironments to stimulate chondrogenic differentiation and cartilage matrix production by seeded and/or host cells.

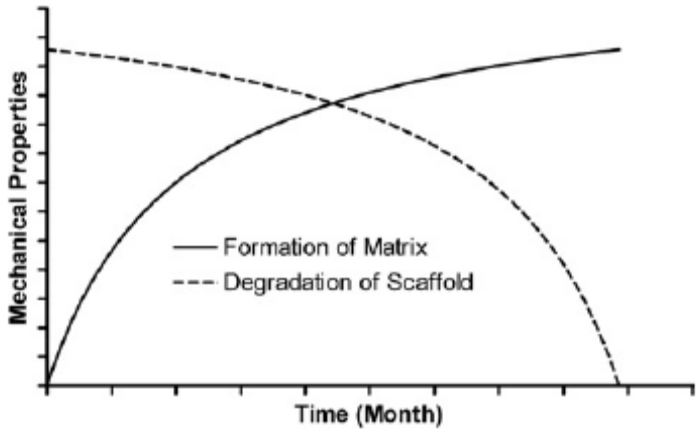

Figure 3.1 A schematic diagram displaying the optimum model of mechanical properties of scaffold with gradual mass loss of a scaffold and new tissue development (figure taken from Raghunath et al.) [3].

The optimal scaffold/tissue response for a biodegradable scaffold that this work aims to achieve is shown schematically in Figure 3.1. The scaffold initially carries mechanical forces resulting from joint loading. However as the scaffold starts to degrade and tissue in-growth takes place, the cells seeded within the scaffold and/or host cells migrating into the scaffold gradually making cartilage matrix and neotissues. The newly formed cartilage tissues experience physiological loading that further enhances cartilage matrix production. Eventually the scaffold completely degrades and gets reabsorbed by the body and the regenerated tissue alone bears the joint loads [3].

Cartilage regeneration using seeded biologics thus significantly depends on the initial scaffold mechanical, mass transport and biocompatibility properties, and on how these properties change during scaffold degradation and cartilaginous matrix production. There are thus two critical questions regarding scaffolds. First, what is the best material

for a cartilage tissue engineering scaffold? Second, what are the mechanical and mass transport properties a scaffold should possess to carry joint forces and provide an appropriate microenvironment for cartilage tissue regeneration initially and during degradation? An appropriate starting point for defining scaffold properties is the mechanical and mass transport properties of native articular cartilage.

3.1 Mechanical Properties of Native Articular Cartilage

Articular cartilage is a complex tissue which consists of chondrocytes and an extracellular matrix (ECM) that is mainly composed of a network of collagens and proteoglycans. The ECM serves to support and distribute applied loads. The ECM achieves this load bearing through its composition as a multiphasic material with anisotropic, inhomogeneous, nonlinear and viscoelastic properties [4]. Its distinct mechanical properties not only serve its crucial function as a load-supporting and low-friction bearing surface, but also give matrix proper signals and biomechanical stimuli for maintaining a proper balance between development and degradation [5].

A long postulated design goal for any cartilage tissue engineering scaffold is to replicate native articular cartilage mechanical and mass transport properties. Generally, mass transport is characterized by effective permeability, as effective permeability is known to play a significant role not only in cartilage nutrition, but also in its mechanical response as characterized using biphasic theory [6]. Mechanical properties are typically characterized by linear aggregate modulus (if biphasic theory is used to model cartilage) or nonlinear elastic strain energy functions. Articular cartilage has also been represented

by straight nonlinear elasticity theory [12]. A summary of native articular cartilage properties is presented in Table 3.1

Matching native articular cartilage properties, however, especially permeability raises a significant conundrum. The extremely low articular cartilage effective permeability is likely due to two factors. First, proteoglycans in the articular cartilage matrix bind water through negative electrostatic charges. This in itself restricts fluid flow in and out of the cartilage matrix, effectively reducing cartilage effective permeability. Second, pores in cartilage matrix are on the nanometer or single micron scale which further reduces fluid movement in the matrix. With current fabrication methods, it is difficult to achieve low effective permeability on the scale of articular cartilage, simply because pore sizes in synthetic scaffolds are likely to be on the order of hundreds of microns, not single microns or hundreds of nanometers. It is unclear, even, whether producing scaffolds with effective permeability in the measured range of cartilage (10^{-14} to 10^{-15} m^4/Ns) is even advantageous for cartilage tissue engineering. One limitation is that creating the pore sizes to reach this permeability level would make it extremely difficult to seed chondrocytes or progenitor cells within the scaffold, as these cells have a typical diameter of 10-40μm (10-12μm smaller, 30-40μm larger cells) [7]. Although our group has shown that lower permeability is generally beneficial for chondrogenesis using primary chondrocytes [8,9] it is unclear what the lower floor is for permeability that would benefit chondrogenesis by primary chondrocytes. Malda's [10] results showing less cartilage matrix production in sponge scaffold architecture with significant tortuosity and thus lower permeability when compared with scaffolds having designed regular interconnected porosity and higher permeability suggests there may be a lower floor on

effective permeability that promotes enhanced chondrogenesis even with primary chondrocytes. Furthermore, Kemppainen and Hollister [8] demonstrated conclusively that chondrogenesis with chondrogenically pulsed bone marrow stromal cells (BMSC) is significantly enhanced with higher permeability, since BMSC likely have higher metabolic activity.

A second difficulty in determining effective mass transport and mechanical property design targets that enhance chondrogenesis is simply the plethora of possible design targets. As Table 3.1 demonstrates, cartilage exhibits a tremendous variation in compressive and tensile mechanical properties such that it may not be feasible with available synthetic materials and computational design techniques to match all the reported properties. Therefore, this work will focus on how well synthetic polymer scaffolds match two basic articular cartilage effective properties, namely hydraulic permeability, and compressive Young's modulus.

Table 3.1 Biomechanical properties of human native articular cartilage [4]

Tensile Properties	Human Articular cartilage
Ultimate tensile stress	15-35 MPa
Ultimate tensile strain	10-40%
Tensile modulus (10% strain)	5-25.5 MPa
Poisson's ratio	0.9-2.2
Equilibrium relaxation modulus	6.5-45 MPa
Compressive properties	
Aggregate modulus	0.1-2.0 MPa
Hydraulic permeability	0.5-5.0 x $10^{-15}m^4N^{-1}s^{-1}$
Young's modulus	0.4-0.8 MPa
Shear properties	
Equilibrium shear modulus	0.05-0.25 MPa
Complex shear modulus	0.2-2.0 MPa
Loss angle	~10°

3.2 Scaffold Materials and Stiffness for Cartilage Engineering

The two main material types which have been successfully applied in developing cartilage scaffolds are (1) natural polymers such as agarose, alginate, hyaluronic acid, gelatin, fibrin glue, collagen derivatives and acellular cartilage matrix, and (2) synthetic polymers, based on polyhydroxyacids (i.e. polylactic acid (PLA), polyglycolic acid (PGA and their co-polymers), and polycaprolactone (PCL)), and other several bioelastomers (i.e. poly(glycerol sebacate) (PGS), poly (1, 8 Octanediol-co-citrate) (POC), polyurethanes) [3,11]. Even though there are many advantageous properties of natural polymers reported for cartilage engineering, natural polymers also present significant limitations for cartilage tissue engineering and eventual clinical application. First of all, it is difficult to reproducibly control the architecture and thus effective mechanical and mass transport properties when manufacturing natural polymers. Thus, if we determine that controlled effective permeability and compressive modulus are indeed important for enhancing chondrogenesis, it will be difficult to achieve reproducible results with natural materials. Second, the mechanical properties and strength of natural polymers actually falls significantly below that of natural articular cartilage [3].

. Third, the ability to mass produce natural polymer scaffolds with controlled effective properties is also limited. Thus, in this work, we will focus on reviewing synthetic polymer scaffolds for cartilage regeneration. There are numerous synthetic materials that possess promising compressive modulus values that fall within or close to the ranges of native cartilage tissue (Table 3.1: 0.1-2.0 MPa for aggregate modulus, 0.4-0.8 MPa for compressive young's modulus). Table 3.2 shows a list of example materials that have been fabricated into 3D scaffolds with architectures for cartilage engineering.

These synthetic materials readily manufactured in a variety of designs and dimensions, while presenting a range of hydrophilicity and other cell-material interaction characteristics.

Table 3.2 Review of compressive modulus, pore diameter and dimension values for synthetic materials used for cartilage engineering

Scaffold Materials/Cells*	Dimensions (mm) /Shape	Porosity/Pore Diameter(μm)	Young's Modulus (MPa)
PCL/CH	3(D)x1-2(H)/ 3D cylinder	70 ± 2 %, 200μm	0.26-0.57[12]
PCL/agarose-fibrin gel/CH	3D woven	70-74%, 390x320x104μm	0.005-0.1[4]
PCL/CH or MSC or None	8(D)x2(H)/ 3D nanofibers	-	0.2-1.5 (depending on cell types)[13]
PLCL	2mm(H)/sponges	71-86%, 300-500μm	0.002-0.006[14]
PLLA/CS-PLLA	7(D) x 3(H)mm /cylinder	85-%, 50-250μm	1.44-3.35 (depending on CS%)[15]
PLLA/CH	7(D) x 3(H)mm /cylinder	85-%, 50-250μm	2.305[15]
PLGA sponge/collagen mesh	200μm-1.5mm(H) /thin-sandwich	120-μm	7.24-13.16[16]
PGS	6.45(D)x3(H)mm /cylinder	48.1 ± 4.24 %, 1004 ± 0.04μm	0.57 ± 0.24[17]
POC	6.35(D)x3.5(H)mm /cylinder	32-62%, 890μm	0.29-0.78 [9,18]
polyurethane	8(D)x4(H)mm /cylindrical sponges	85%, 200-400μm	0.023-0.050[19]

*CH - chondrocytes, MSC - mesenchymal stem cells
PLCL – poly(L-lactide-co-epsilon-caprolactone,
CS-PLLA - chondroitan sulfate-PLLA
PLGA – poly(lactic-glycolic acid)

As synthetic materials offer the potential for designed control of scaffold properties, solid freeform fabrication (SFF) is an ideal choice for scaffold fabrication using synthetic polymers. SFF provides the capability for translating the computational design of controlled effective properties into a realizable physical scaffold embodying those properties. Furthermore, SFF also allows relatively precise fabrication, accurate reproducibility of the design, and the ability to regulate scaffold pore size, pore shape, interconnectivity, porosity, and entire scaffold dimension. This advantage of SFF in

control over scaffold design and manufacture compared to conventional methods (i.e. solvent casting/salt leaching, freeze-drying, electrospinning etc.), provides benefits not only for cartilage but also for many other tissues and clinical applications. Table 3.3 shows elastic properties of selected scaffolds manufactured by the SFF technique, demonstrating that SFF techniques enable a broader range of architectures with wider porosity ranges and lower variation in resultant effective properties than conventional methods.

Table 3.3 Elastic properties of selected scaffolds fabricated by SFF [20].

SFF Fabrication Method	**Material**	**Porosity (%)**	**Tangent Modulus at 10% strain (MPa) = ABe^{BE}**	**Variation (%)**
Fused Deposition Molding	PCL	48-77	4-77	4-12
Nozzle Deposition	PLGA/PLLA/TCP	74-81	17-23	5-17
Nozzle Deposition	HA	41	1110-1240	7-23
Nozzle Deposition	PEOT/PBT	29-91	0.2-13.7	3-19
3D Printing	PLLA	0	187-601	0.7-11
Selective Laser Sintering	PCL	37-55	54-65	4-5
Inverse SFF	HA	40	1400	28
Inverse SFF	Col1	-	0.1-1	-
Inverse SFF	POC	30/50/70	0.35-1.05	14-53

Since SFF may provide a reproducible and scalable manufacturing technique that can satisfy current Good Manufacturing Practices (cGMP) requirements in addition to scalable commercialization demands, we will focus on reviewing scaffold materials for cartilage tissue engineering that either have been or have the potential for SFF based manufacturing. We first focus on synthetic material characteristics and their possible impact on cartilage tissue engineering followed by a review of design factors that may impact cartilage tissue engineering. In this work, we exploit SFF methods to fabricate scaffolds from three synthetic polymers in order to reach our goal of matching the

mechanical properties of 3D designed scaffolds to target compressive properties of native cartilage. The three biomaterials used in this work are poly (1, 8 Octanediol-co-Citrate) (POC), polycaprolactone (PCL), and poly (glycerol sebacate) (PGS). POC and PGS are relatively new materials developed in the field of tissue engineering and PCL is a widely used in various designs for cartilage application. The main focus of this work will be to test the feasibility of POC mechanically and biochemically *in vitro* and *in vivo* as a cartilage scaffold material with 3D controlled design solid-freeform scaffolds. Then, the performance of POC as a scaffold will be compared to that of PGS and PCL *in vitro* with the same 3D scaffold design to see which material is more suitable for cartilage regeneration and to check if either scaffold material or design factor is more influential or not in chondrogenesis. In order to access the feasibility of POC as cartilage scaffold material, we also look at the effects of physical parameters—coupled effects of scaffold pore shape and permeability on chondrogenesis, which precise and almost identical scaffolds with controlled design permeability are reproduced via SFF. The rationale for selection of the three candidate materials was based on their mechanical stiffness, hydrophilicity, and potential use in the field of cartilage engineering. We wanted to choose a biocompatible material which can be fabricated via solid freeform fabrication method with a higher stiffness than any other two materials with slow or no degradation over short periods and PCL is a perfect fit for such requirement. Whereas, we wanted to choose two other materials which are relatively similar in their mechanical performance but different in some other physical properties such as hydrophilicity, permeability, and degradation etc. POC and PGS are perfect candidates to fulfill our interests since both of

them are relatively new materials in this field and they have similar mechanical stiffness (much less than PCL), but differ in material permeability.

Poly (1, 8 Octanediol-co-Citrate) (POC)

Poly (1, 8 Octanediol-co-Citrate) (POC) is a family of poly (diol citrates) recently developed by Yang et al. [21] POC is an elastomeric, biodegradable, hydrophilic "cell-friendly" material. Furthermore, it has the following advantages: non-toxic monomers, a relatively simple synthesis without addition of catalysts or crosslinking reagents, cost-effective scale-up, controllable mechanical and biodegradation properties and easy processing, and inherent surface affinity for various cell types including chondrocytes [22], human aortic endothelial cells[23], and cardiomyocytes[24]. POC is synthesized by first creating a pre-polymer via reacting the polyfunctional monomer citric acid with the difunctional monomer 1, 8-octanediol, then it can further post-polymerized to create a polyester network with a controllable number of crosslinks to tailor the elasticity and biodegradability of the resulting material (Figure 3.2).

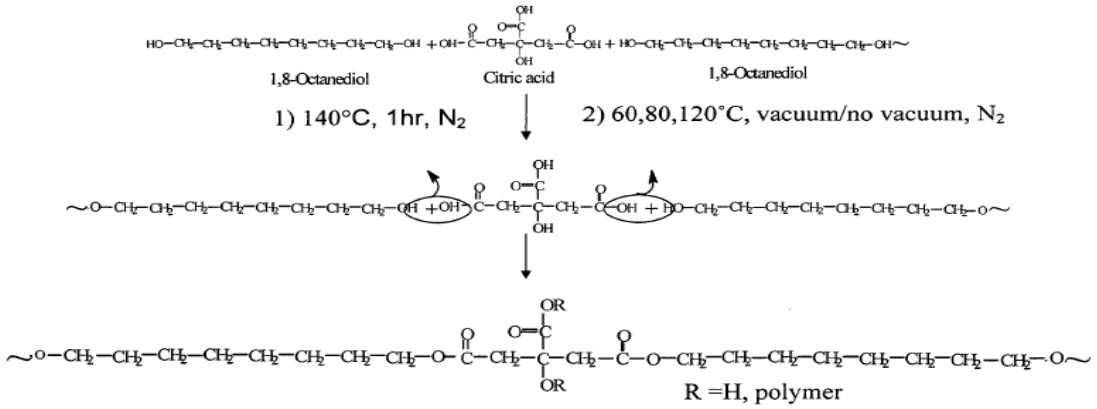

Figure 3.2: Polycondensation of 1, 8 octanediol and citric acid to produce pre-polymer for POC [25]

POC is degraded by hydrolysis of its ester linkages in physiological conditions and its byproducts, citric acid and 1, 8-octanediol, are excreted by the body. Citric acid is a non-toxic metabolic product of Krebs cycle in the body and 1, 8-octanediol enables ester bonds to form with citric acid and is water-soluble with no reported toxicity. These monomers ensure a beneficial property of the degradation process leaving no insoluble or toxic complexes in the body. One of the unique properties of POC is that its mechanical and degradation properties can be tailored easily by changing curing temperature and reaction time, the molar ratio of monomers, and the presence and the level of vacuum when curing [21,25]. In general, harsher curing conditions such as high temperature, longer reaction time, and high vacuum increase the mechanical strength and decrease the overall degradation rate. The tensile strength was as high as 6.1 MPa and the Young's moduli ranged from 0.92 to 16.4 MPa with the maximum elongation at break at 265% of initial length. The complete degradation time of POC in PBS at 37°C is reported to be about 6 months yet the degradation rate may get accelerated *in vivo* due to enzymatic, cellular effects and friction due to movements.[21] In this thesis, the 1:1 molar ratio between monomers was used when creating the pre-polymer and post-polymerize the pre-polymer with one curing condition (100°C for 1 day of curing followed by 3 days of curing with high vacuum) in order to reduce variation in manufacturing. The overall mechanical properties of scaffolds were varied through different scaffold designs to match native cartilage. The Chapter 4 presents the more detailed mechanical characterization of solids and scaffolds with various designs for the specific curing conditions.

In fact, Kang et al. [22] reported a study using POC as a scaffold material for cartilage engineering. The scaffolds used by Kang et al were fabricated through a salt-

leaching method. They demonstrated that chondrocytes attached well and grew cartilage within POC scaffolds. The current thesis work was the first study to demonstrate the ability to fabricate POC scaffolds through SFF methods in order to create regularly interconnected and controlled pore. In order to create such controlled scaffold architectures by SFF methods, a two step mold fabrication was involved. First, since as POC must be cured at temperatures greater than the melting temperature of ProtoBuild wax molds used in SFF methods, an intermediate hydroxyapatite (HA) mold (inverse of the wax mold) must be made using the wax mold then cast into the pre- poly (1, 8 Octanediol-co-Citrate) (pPOC). Second, the POC is cured within the HA mold followed by removal of the HA mold to obtain the final POC scaffold. A schematic of fabrication steps is shown in Figure 3.3.

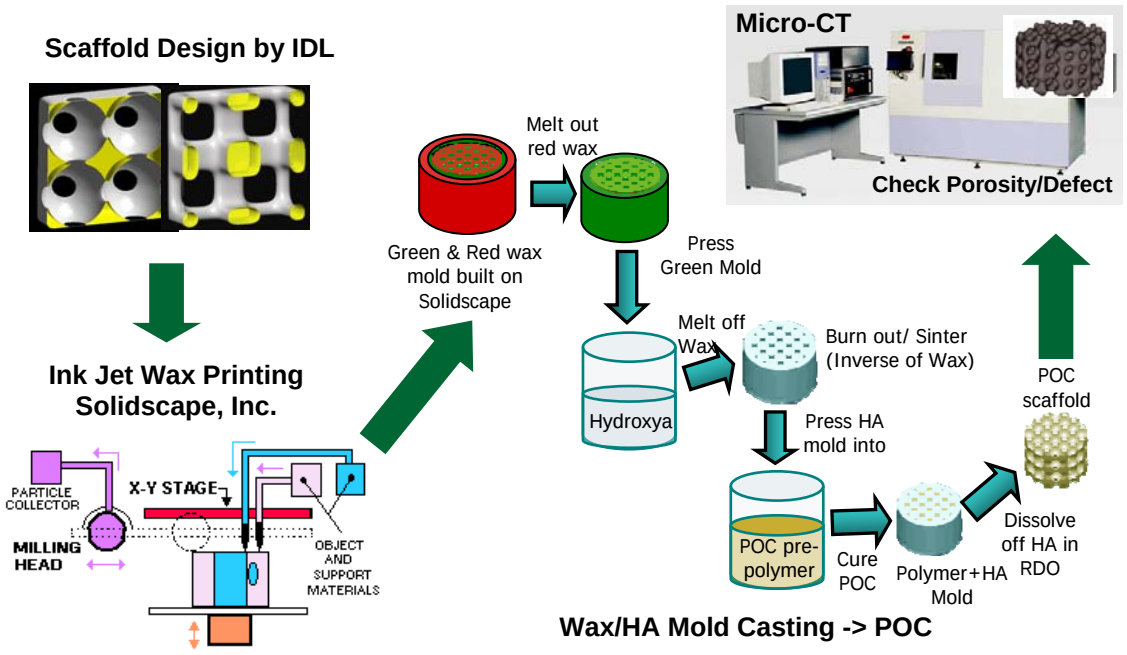

Figure 3.3: A schematic of designing, fabrication, and porosity analysis of 3D POC scaffolds: with 3D scaffold designs by IDL, first wax molds are built in Solidscape, which then are cast into HA creating a secondary inverse mold. POC prepolymer/HA constructs are cured and a resulting 3D POC scaffold is analyzed by micro-CT for its porosities and defects. [18,26]

To date since 2004, POC has been most actively used in heart[24] and vascular[23,27,28] tissue engineering, with composite materials of POC with HA[29], chitosan[30] or PLA[30] being used for orthopedic applications. Also, the degradation properties make POC a good candidate for drug delivery reservoirs [31] broadening its potential application areas in tissue engineering.

Poly (ε-caprolactone) (PCL)

PCL, the stiffest material out of three materials used in this work, is probably one of the most widely used polymers in the field of tissue engineering as it is FDA approved, non-toxic, and readily available with relatively low cost. Unlike POC and PGS (thermoset), PCL is a biodegradable thermoplastic semi-crystalline polyester which is synthesized via ring opening polymerization of ε-caprolactone (Figure 3.4).[12]

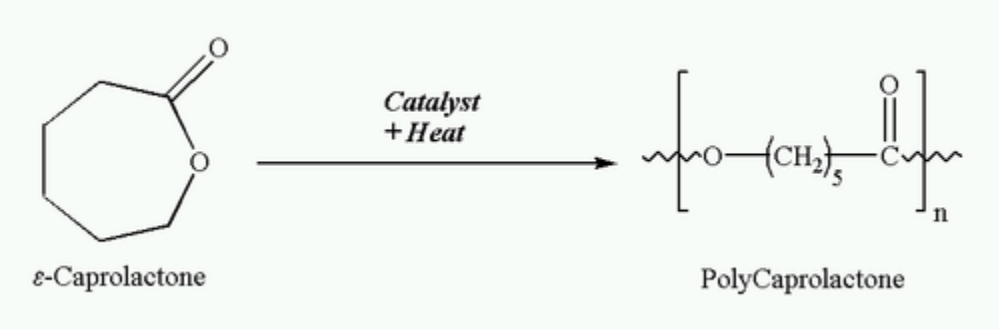

Figure 3.4 Ring opening polymerization of ε-caprolactone to polycaprolactone

Even though it is degraded by hydrolysis like POC and PGS, it degrades much slower than other biodegradable polymers via hydrolysis of its ester linkages in physiological conditions. Because of the rather slow degradation properties of PCL, it is also a good candidate for long-term *in vitro* and *in vivo* applications as the scaffolds will maintain their architectural integrity and strengths during tissue growth [32]. PCL is used

not only for a scaffold material, but also as drug delivery devices, adhesion barriers, sutures, and staples.

PCL has biocompatibility with a variety of cell types for skeletal tissue engineering including adipose stem cells[33], bone marrow stromal cells[8,34], chondrocytes[8,12], fibroblasts[35-38], osteoblasts[39] in skeletal tissue engineering. In particular, several studies [8,12,40-42] have shown that PCL scaffolds provide suitable microenvironments for cell infiltration, differentiation, re-differentiation and proliferation of seeded chondrocytes. These studies have demonstrated gene expression and formation of cartilaginous tissues such as type II collagen expression and matrix formation (i.e. rich proteoglycan contents) both *in vitro* and *in vivo*. However, PCL is relatively hydrophobic compared to biodegradable elastomers, which is considered as a disadvantage for tissue engineering as it may lead to poor cell attachment. To improve cell attachment, PCL has been modified to increase hydrophilicity using surface hydrolysis with the use of acid or alkaline solution[43], adsorption of cell-adhesive proteins (i.e. collagen and fibronectin)[43] or Arg-Gly-Asp (RGD) peptides[34,44]. These modifications improve PCL hydrophilicity and hence cell attachment, increasing its applicability for many tissue engineering applications. Another advantage of PCL is that scaffolds can be fabricated using many methods including porogen leaching and solvent casting, SFF techniques, photopolymerization, selective laser sintering, bioextrusion, salt leaching and melt casting. In this work, we used the SFF method of melt-casting in order to create accurately designed and controlled 3D PCL scaffolds (Figure 3.5); unlike POC and PGS, we use the ProtoBuild Wax mold directly to cast into the melted PCL powders instead of using the intermediate HA mold (Figure 3.3)

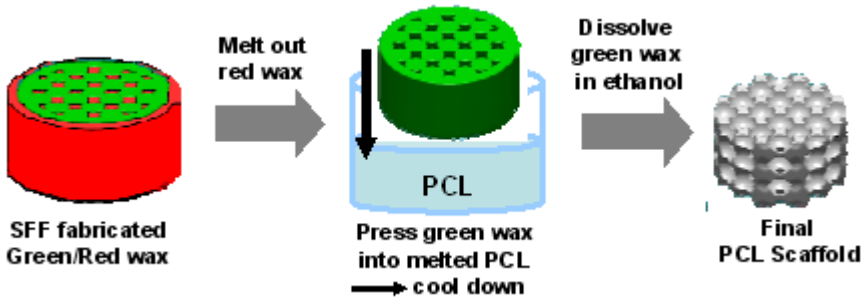

Figure 3.5: Direct PCL scaffold fabrication from a SFF fabricated wax mold without use of an intermediate HA mold (modified from a work by Kemppainen [26])

.

Poly (glycerol sebacate) (PGS)

Poly (glycerol sebacate) (PGS) is another recently developed biodegradable elastomer that has potential application in soft tissue engineering like cartilage. There are many similarities between POC and PGS; PGS is also synthesized via a polycondensation reaction of two monomers. Glycerol is the basic building block of lipids and sebacic acid is the natural metabolic intermediate in fatty acid oxidation thus the degradation byproducts of PGS are presumably non-toxic. It shares the same advantages as POC including a simple and relatively cheap synthesis process, adjustable mechanical and degradation properties, excellent biocompatibility, and rubber-like behavior. In fact, it has been more widely used than POC so far in various applications for cartilage, [17] arterial constructs, [45] heart, [46,47] and as a drug carrier [48].

PGS is synthesized exactly the same way as POC. First, the pre-polymer of PGS (pPGS) is made at high temperatures with monomers (glycerols and sebacic acids). Then a thermoset PGS is fabricated through a polycondensation reaction of pPGS with desired temperatures (mostly 120~150°C) and duration shown in Figure 3.6. Again, the molar ratios of monomers and curing conditions such as temperature, reaction time, and vacuum levels determine the mechanical and degradation properties of PGS, which makes PGS as

a good candidate for scaffold materials in soft tissue engineering. According to Wang et al.[49], PGS showed a Young's modulus of 0.282 ± 0.025 MPa, a tensile strain of at least 267 ± 59.4% and a tensile strength of at least 0.5 MPa.

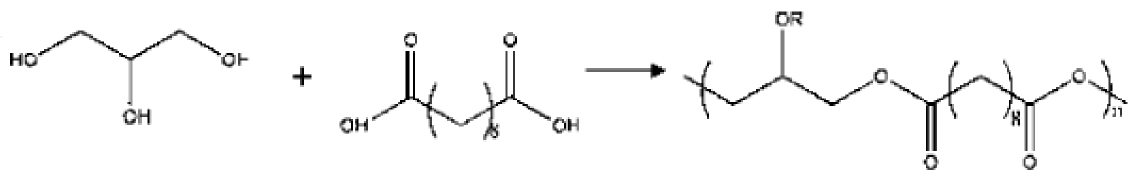

Figure 3.6 Polycondensation reaction of glycerol and sebacic acid to make PGS.[49]

The degradation profiles can be easily controlled by molar ratios and crosslinking density, which is highly related with the post-polymerization conditions. The mechanical properties represented by compressive modulus decreased linearly and in parallel with the degradation rates of PGS suggesting that the mechanism of PGS degradation is surface erosion [50]. PGS has shown to degrade much faster than PCL does such that PGS has lost 17% of its original mass after 2 months, [49,50] which is similar to POC (even though the degradation profiles of POC and PGS all depend on its curing conditions.). In this work, we fabricated PGS scaffolds via SFF methods with one curing condition such that mechanical properties were within the ranges of native cartilage in order to compare the performance of PGS scaffolds in chondrogenesis compared to POC and PCL scaffolds. Details of the fabrication steps are the same as shown for POC in Figure 3.3.

There has not been much study done with PGS scaffolds for cartilage application. From our previous work [17], Kemppainen et al. demonstrated the feasibility of creating PGS scaffolds via SFF methods and grew cartilage on PGS scaffolds for 2 weeks *in vitro* with seeded chondrocytes as proof of concept. In this work, PGS scaffolds were

compared to other two material scaffolds (POC and PCL) in terms of permeability with and without tissues, mechanical and physical properties, and cellular activities for chondrogenesis (details in Chapter 7 & 8).

3.3 Factors involved in Scaffold Design for Cartilage Tissue Engineering

The optimal properties of a cartilage tissue engineering scaffold should be defined as those properties that enhance cartilaginous tissue formation *in vitro* or/and *in vivo*. Besides a careful selection of suitable scaffold material which will determine the basic material stiffness ranges and approximate degradation profiles for a specific application, ensuring required scaffold mass transport properties is another critical issues (Figure 3.7). Unlike native cells and tissues in the body, nutrient supply through blood is not available for most of tissue engineered constructs either *in vitro* or during the immediate post-implantation *in vivo,* hence the ability of a scaffold to enable the adequate supply of nutrients to resident cells and effective removal of wastes is a key to the success of any scaffold-based tissue engineering.

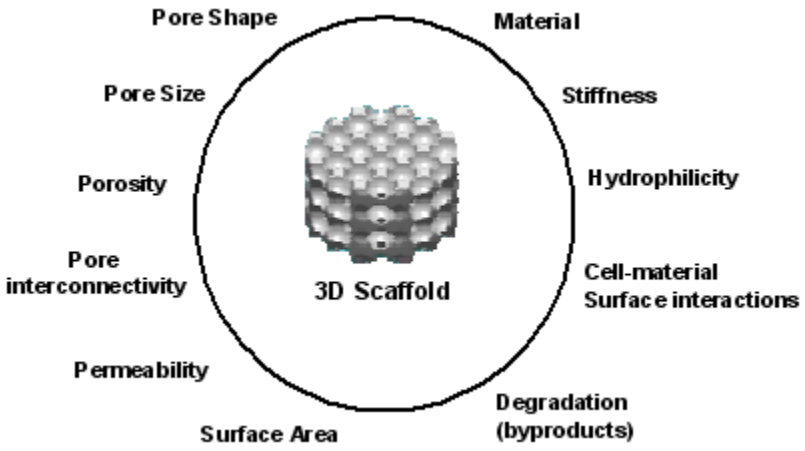

Figure 3.7: The factors need to be considered for 3D scaffolds in tissue engineering.

Mass transport is related to oxygen and nutrient delivery, waste removal, protein transport and cell migration, which in turn are governed by scaffold architectural properties; the pore size, geometry (shape), orientation, interconnectivity, porosity, diffusivity and permeability. Furthermore, surface chemistry of pores and surface area directly influence the extent and nature of nutrient/wastes exchanges and tissue in-growth [51]. All these scaffold architectural properties are closely linked. Effective diffusivity and permeability are physical properties that can be computed and measures, and thus incorporate in a quantitative manner architectural parameters like pore shape, pore size, interconnectivity and orientation [52]. Also, these design parameters are often bounded by fabrication methods so even the optimized design produced by computational models may not be realized due to limitations of actual scaffold fabrication.

Permeability

Permeability of the scaffold or tissue/scaffold construct in cartilage engineering is important as it controls the migration of cells into the scaffolds as well as the diffusion of nutrients and removal of wastes. Since permeability is probably the best representative measure accounting for all the scaffold architectural factors[51], the effects of permeability have been studied in various biological materials such as bone [53], tumor tissue[54], cartilage[55] and tissue/scaffold constructs [8,9,56]. Coupled with mechanical loading, scaffold permeability affects the magnitude of pressure and fluid shear stresses within the construct or tissue, which in turn work as potential stimuli for cellular differentiation or functional adaptation. Also, construct permeability has been shown to affect the

degradation rate of biodegradable scaffolds as it determines the exchange rate of degradation byproducts between cells/tissues and scaffolds [57-59].

Native tissue permeability can be a good starting point for defining scaffold mass transport design targets and this parameter is closely linked with metabolic activity of tissues. For instance, cartilage is much less metabolically active than other tissues and it is much less permeable than any other tissues such as bone or highly vascularized tissues [20]. Low permeability affects oxygen diffusion to cells and regenerated tissues. Partial oxygen pressure (PO_2) is a factor that can clearly affect chondrocytic differentiation in that lower PO_2 favors chondrogenic matrix production and maintenance of chondrocyte phenotype [8,60]. In contrast, a higher PO_2 favors bone matrix formation and bone matrix related gene expressions by osteoblasts and bone marrow stromal cells [61,62]. These results prove that a specific tissue may require a specific or favorable permeability range. Therefore, permeability should be a main design parameter for tissue/scaffold constructs.

Pore size

Pore size is one of key players in defining scaffold permeability. It has been reported that optimal pore size is of 5μm for neovascularization, 5-15μm for fibroblastic ingrowth, approximately 20μm for the ingrowth of hepatocytes, 20-125μm for regeneration of adult mammalian skin, 40-100μm for osteoid ingrowth, 100-350 μm for regeneration for bone, and greater than 500 μm for fibrovascular tissues [63-65]. However, it is critical to note that determination of these "optimal" pore sizes has been performed with scaffolds that have widely varying pore structures, which is why the use of

permeability as a design factor that accounts for pore tortuosity should be presented in addition to pore size.

It's been shown that the scaffold pores for cartilage need to be large enough to allow cells to migrate into the structure (~20μm), but small enough to establish a sufficiently high specific surface area (~120 μm)[56,66] hence pore size affects an individual cell's response in terms of cell adhesion, attachment and proliferation [56,66,67]. However, it has also been reported that pore size did not affect the formation of cartilaginous tissue with chondrocytes *in vitro*, but rather influenced the cellularity of the tissue, the quality of the tissue (i.e. the amount of collagen accumulation per cell in the composition of the neo-cartilaginous tissue) [68] and the maintenance of chondrocytic phenotype [69]. Al-Munajjed et al.[59] also suggested that the pore size plays a significant role as it influences permeability, porosity, and the mechanical properties of scaffolds thereby having an effect on chondrogenesis, rather than having a direct influence on chondrogenesis. However many of these pore sizes were including micro (diameter < 100μm) and macro (diameter > 100μm) pores and determined using random pore geometries, hence do not define or represent optimum pore sizes accurately. Rather, they define the broad range of pore sizes in which a certain tissue type formation with specific cells was applied, still leaving no definite guidelines for the optimal pore size for a specific tissue type.

Pore geometry – pore interconnectivity and pore shape

Another important design consideration affecting scaffold permeability is pore geometry. Pore geometries can be divided into pore interconnectivity and a unit pore shape. A scaffold should provide an open porous interconnected structure allowing for

smooth cell penetration and evenly distributed nutrient/waste exchanges throughout the entire scaffold dimension Quite often viable tissue formation is found only in the peripheral regions of scaffolds whereas the interior fails to support viable tissue due to lack of adequate nutrient and oxygen supply. In order to minimize mass transport limitations and pore occlusions, it is essential that a scaffold possess a high degree of interconnectivity in conjunction with a suitable pore size, which has been confirmed in bone formation, osteoconduction, and cartilage matrix formation [10,70-73]. Unfortunately, many conventional scaffold fabrication methods such as porogen leaching and solvent casting do not provide a controlled scaffold pore network, with pore geometry being difficult to control in fabrication. Hence pore shape has not been widely studied in scaffold tissue engineering. However, it has been recently suggested that a spherical pore shape enhances chondrogenesis in SFF fabricated scaffolds [8,74] and both the change from cubical to spherical pore shapes with more homogeneous pore structure may be responsible for the higher rupture stress and the tensile moduli [59], yet all these studies were limited as other mass transport properties such as permeability were never characterized experimentally but rather postulated. Hence, we examine the pore shape and consequent permeability effects on chondrogenesis characterizing and controlling other scaffold design factors in this work to elucidate the effect of scaffold pore shape.

Porosity

Besides pore size and pore geometry, porosity is highly connected with permeability. Porosity and permeability often control the cell migration into and out of the 3-D construct as well as nutrient and waste transport. Although it is usually true that

an increase in porosity leads to an increase in permeability, this only happens when the pores are highly interconnected. Again, this is why permeability should be treated as a single parameter for transport properties as it encompasses a combination of other scaffold parameters mentioned in this chapter. Several studies have emphasized the need for sufficiently high porosity and high surface area-to-volume ratio in scaffold design for ensuring uniform cell delivery and tissue in-growth [63,75,76], however extremely high porosity (i.e. over 80%) would compromise the mechanical integrity of the scaffold with possible faster degradation rate due to initial lower mass, which still poses a conflict between optimizing the porosity and maximizing mechanical properties. Porosity and permeability can also have a significant impact on the degradation characteristics of biodegradable scaffolds. For instance, low porosity and permeability of scaffold may accelerate scaffold degradation exhibiting a decrease in mass, molecular weight, and mechanical properties due to the inhibition of autocatalytic degradation with better diffusion or waste removal [57]. For cartilage, chondrocytes have shown to prefer lower porosity and permeability as it mimics native cartilage environment and possible forcing cell aggregation *in vitro* whereas BMSCs prefer higher porosity and permeability even for cartilage regeneration [8].

Other related factors

There are several other additional factors that are not scaffold mass transport design factors yet could significantly influence cartilage regeneration including surface area, overall mechanical stiffness, and hydrophilicity of scaffold surface. A large surface area favors cell attachment and growth and a large pore volume is required to

accommodate and deliver cell nutrients and cell waste products. Hence some researchers advocated the use of the surface area to volume ratio [63,77] explaining the effects of pore geometry on chondrogenesis in that an increase in the surface area: volume ratio due to pore geometry may increase cellular attachment and growth and increases the amount of extracellular matrix deposition in the scaffold pore space. Again, total scaffold surface area is highly linked with pore geometry and porosity and the ideal design for cartilage would need a high surface area with highly interconnected pore geometry and low permeability.

Mechanical properties of the scaffold or tissue/scaffold construct are another factor that is closely influenced by architectural factors and likely plays a significant role in chondrogenesis. It is predicted that increasing the stiffness of the scaffold increases the amount of cartilage formation and reduce the amount of fibrous tissue formation in the defect but with a limited threshold stiffness value close to native cartilage [78]. Besides, surface modification and hydrophilicity due to scaffold material composition has been proposed as an important influential factor on chondrogenesis [34,44,73,79]. Surface modification increasing hydrophilicity may enhance cellular infiltration into the inner spaces of scaffolds, rendering more uniform cell distribution, adhesion, and proliferation than hydrophobic ones [34,79].

Due to the complex interaction of this multitude of scaffold design parameters, the ability to vary a limited number of design parameters while holding the remaining design parameters constant is of paramount importance when testing scaffold design hypotheses. Creating scaffolds that enhance tissue regeneration can only be achieved if we can test scaffold design hypotheses to determine if a range of a proposed scaffold

design variable enhances tissue regeneration or, indeed, influences tissue regeneration at all. Given this prerogative, the goal in this thesis was to test the relative influence of scaffold pore shape, effective permeability and material on cartilage tissue regeneration *in vitro* and in an *in vivo* sub-cutaneous mouse model, while fixing other scaffold variables.

References

1. Safran, M.R., Kim, H., and Zaffagnini, S. The use of scaffolds in the management of articular cartilage injury. The Journal of the American Academy of Orthopaedic Surgeons 16, 306, 2008.

2. Buckley, C.T., and O'Kelly, K.U. Regular scaffold fabrication techniques for investigations in tissue engineering. In: Prendergast, P.J. and McHugh, P.E., eds. Topics in Bio-Mechanical Engineering. Dublin, Ireland: Trinity Center for Bioengineering & National Center for Biomedical Engineering Science, 2004, pp. 147-166.

3. Raghunath, J., Rollo, J., Sales, K.M., Butler, P.E., and Seifalian, A.M. Biomaterials and scaffold design: key to tissue-engineering cartilage. Biotechnology and applied biochemistry 46, 73, 2007.

4. Moutos, F.T., Freed, L.E., and Guilak, F. A biomimetic three-dimensional woven composite scaffold for functional tissue engineering of cartilage. Nature materials 6, 162, 2007.

5. Vinatier, C., Guicheux, J., Daculsi, G., Layrolle, P., and Weiss, P. Cartilage and bone tissue engineering using hydrogels. Bio-medical materials and engineering 16, S107, 2006.

6. Ateshian, G.A., Warden, W.H., Kim, J.J., Grelsamer, R.P., and Mow, V.C. Finite deformation biphasic material properties of bovine articular cartilage from confined compression experiments. Journal of Biomechanics 30, 1157, 1997.

7. Stockwell, R.A. Chondrocyte structure. In: Anonymous Biology of Cartilage Cells (Biological Structure and Function Books). : Cambridge university press, 1979, pp. 24-27.

8. Kemppainen, J.M., and Hollister, S.J. Differential effects of designed scaffold permeability on chondrogenesis by chondrocytes and bone marrow stromal cells. Biomaterials 31, 279, 2010.

9. Jeong, C.G., and Hollister, S.J. A comparison of the influence of material on *in vitro* cartilage tissue engineering with PCL, PGS, and POC 3D scaffold architecture seeded with chondrocytes. Biomaterials , 2010 Mar 8.

10. Malda, J., Woodfield, T.B., van der Vloodt, F., Wilson, C., Martens, D.E., Tramper, J., van Blitterswijk, C.A., and Riesle, J. The effect of PEGT/PBT scaffold architecture on the composition of tissue engineered cartilage. Biomaterials 26, 63, 2005.

11. Shi, R., Chen, D., Liu, Q., Wu, Y., Xu, X., Zhang, L., and Tian, W. Recent advances in synthetic bioelastomers. International journal of molecular sciences 10, 4223, 2009.

12. Martinez-Diaz, S., Garcia-Giralt, N., Lebourg, M., Gomez-Tejedor, J.A., Vila, G., Caceres, E., Benito, P., Monleon Pradas, M., Nogues, X., Gomez Ribelles, J.L., and Monllau, J.C. In Vivo Evaluation of 3-Dimensional Polycaprolactone Scaffolds for Cartilage Repair in Rabbits. The American Journal of Sports Medicine, 2010.

13. Li, W.J., Chiang, H., Kuo, T.F., Lee, H.S., Jiang, C.C., and Tuan, R.S. Evaluation of articular cartilage repair using biodegradable nanofibrous scaffolds in a swine model: a pilot study. Journal of tissue engineering and regenerative medicine 3, 1, 2009.

14. Xie, J., Ihara, M., Jung, Y., Kwon, I.K., Kim, S.H., Kim, Y.H., and Matsuda, T. Mechano-active scaffold design based on microporous poly(L-lactide-co-epsilon-caprolactone) for articular cartilage tissue engineering: dependence of porosity on compression force-applied mechanical behaviors. Tissue engineering 12, 449, 2006.

15. Lee, C.T., Huang, C.P., and Lee, Y.D. Biomimetic porous scaffolds made from poly(L-lactide)-g-chondroitin sulfate blend with poly(L-lactide) for cartilage tissue engineering. Biomacromolecules 7, 2200, 2006.

16. Dai, W., Kawazoe, N., Lin, X., Dong, J., and Chen, G. The influence of structural design of PLGA/collagen hybrid scaffolds in cartilage tissue engineering. Biomaterials 31, 2141, 2010.

17. Kemppainen, J.M., and Hollister, S.J. Tailoring the mechanical properties of 3D-Designed Poly(glycerol Sebacate) scaffolds for cartilage applications. J Biomed Mater Res A , 2010 Jan 20.

18. Jeong, C.G., and Hollister, S.J. Mechanical, Permeability, and Degradation Properties of 3D Designed Poly(1,8 Octanediol-co-Citrate)(POC) Scaffolds for Soft Tissue Engineering. Journal of Biomedical Materials Research: Part B , 2010 Jan 20.

19. Grad, S., Kupcsik, L., Gorna, K., Gogolewski, S., and Alini, M. The use of biodegradable polyurethane scaffolds for cartilage tissue engineering: potential and limitations. Biomaterials 24, 5163, 2003.

20. Hollister, S.J. Scaffold design and manufacturing: from concept to clinic. Adv Mater, 2009, 21, 3330-3342.

21. Yang, J., Webb, A.R., and Ameer, G.A. Novel Citric Acid-Based Biodegradable Elastomers for Tissue Engineering. Advanced Materials 16, 511-16, 2004.

22. Kang, Y., Yang, J., Khan, S., Anissian, L., and Ameer, G.A. A new biodegradable polyester elastomer for cartilage tissue engineering. Wiley Periodicals, Inc. published online (www.interscience.wiley.com), 2006.

23. Motlagh, D., Allen, J., Hoshi, R., Yang, J., Lui, K., and Ameer, G. Hemocompatibility evaluation of poly(diol citrate) in vitro for vascular tissue engineering. Journal of biomedical materials research.Part A 82, 907, 2007.

24. Hidalgo-Bastida, L.A., Barry, J.J., Everitt, N.M., Rose, F.R., Buttery, L.D., Hall, I.P., Claycomb, W.C., and Shakesheff, K.M. Cell adhesion and mechanical properties of a flexible scaffold for cardiac tissue engineering. Acta biomaterialia 3, 457, 2007.

25. Yang, J., Webb, A.R., Pickerill, S.J., Hageman, G., and Ameer, G.A. Synthesis and evaluation of poly(diol citrate) biodegradable elastomers. Biomaterials 27, 1889, 2006.

26. Kemppainen, J.M. Mechanically stable solid freeform fabricated scaffolds with permeability optimized for cartilage tissue engineering. (Unpublished, Ph.D. thesis). University of Michigan, Ann Arbor, MI, U.S.A. 2008.

27. Kibbe, M.R., Martinez, J., Popowich, D.A., Kapadia, M.R., Ahanchi, S.S., Aalami, O.O., Jiang, Q., Webb, A.R., Yang, J., Carroll, T., and Ameer, G.A. Citric acid-based elastomers provide a biocompatible interface for vascular grafts. Journal of biomedical materials research.Part A , 2009.

28. Yang, J., Motlagh, D., Webb, A.R., and Ameer, G.A. Novel biphasic elastomeric scaffold for small-diameter blood vessel tissue engineering. Tissue engineering 11, 1876, 2005.

29. Qiu, H., Yang, J., Kodali, P., Koh, J., and Ameer, G.A. A citric acid-based hydroxyapatite composite for orthopedic implants. Biomaterials 27, 5845, 2006.
30. Ameer, G., and Webb, A.R. Biodegradable nanocomposites with enhanced mechanical properties for soft tissue. , 2006.

31. Hoshi, R.A., Behl, S., and Ameer, G.A. Nanoporous biodegradable elastomers. Adv Mater 21, 188-192, 2009.

32. Lam, C.X., Hutmacher, D.W., Schantz, J.T., Woodruff, M.A., and Teoh, S.H. Evaluation of polycaprolactone scaffold degradation for 6 months in vitro and in vivo. Journal of biomedical materials research.Part A 90, 906, 2009.

33. Im, G.I., and Lee, J.H. Repair of osteochondral defects with adipose stem cells and a dual growth factor-releasing scaffold in rabbits. Journal of biomedical materials research.Part B, Applied biomaterials 92, 552, 2010.

34. Zhang, H., Lin, C.Y., and Hollister, S.J. The interaction between bone marrow stromal cells and RGD-modified three-dimensional porous polycaprolactone scaffolds. Biomaterials 25, 4063-9, 2009 Sep;30.

35. Lowery, J.L., Datta, N., and Rutledge, G.C. Effect of fiber diameter, pore size and seeding method on growth of human dermal fibroblasts in electrospun poly(epsilon-caprolactone) fibrous mats. Biomaterials 31, 491, 2010.

36. Roosa, S.M., Kemppainen, J.M., Moffitt, E.N., Krebsbach, P.H., and Hollister, S.J. The pore size of polycaprolactone scaffolds has limited influence on bone regeneration in an in vivo model. Journal of biomedical materials research.Part A 92, 359, 2010.

37. Oh, S.H., Park, I.K., Kim, J.M., and Lee, J.H. In vitro and in vivo characteristics of PCL scaffolds with pore size gradient fabricated by a centrifugation method. Biomaterials 28, 1664, 2007.

38. Williams, J.M., Adewunmi, A., Schek, R.M., Flanagan, C.L., Krebsbach, P.H., Feinberg, S.E., Hollister, S.J., and Das, S. Bone tissue engineering using polycaprolactone scaffolds fabricated via selective laser sintering. Biomaterials 26, 4817, 2005.

39. Mavis, B., Demirtas, T.T., Gumusderelioglu, M., Gunduz, G., and Colak, U. Synthesis, characterization and osteoblastic activity of polycaprolactone nanofibers coated with biomimetic calcium phosphate. Acta biomaterialia 5, 3098, 2009.
40. Thorvaldsson, A., Stenhamre, H., Gatenholm, P., and Walkenstrom, P. Electrospinning of highly porous scaffolds for cartilage regeneration. Biomacromolecules 9, 1044, 2008.

41. Garcia-Giralt, N., Izquierdo, R., Nogues, X., Perez-Olmedilla, M., Benito, P., Gomez-Ribelles, J.L., Checa, M.A., Suay, J., Caceres, E., and Monllau, J.C. A porous PCL scaffold promotes the human chondrocytes redifferentiation and hyaline-specific extracellular matrix protein synthesis. Journal of biomedical materials research.Part A 85, 1082, 2008.

42. Izquierdo, R., Garcia-Giralt, N., Rodriguez, M.T., Caceres, E., Garcia, S.J., Gomez Ribelles, J.L., Monleon, M., Monllau, J.C., and Suay, J. Biodegradable PCL scaffolds with an interconnected spherical pore network for tissue engineering. Journal of biomedical materials research.Part A 85, 25, 2008.

43. Cheng, Z., and Teoh, S.H. Surface modification of ultra thin poly (epsilon-caprolactone) films using acrylic acid and collagen. Biomaterials 25, 1991, 2004.

44. Zhang, H., and Hollister, S. Comparison of bone marrow stromal cell behaviors on poly(caprolactone) with or without surface modification: studies on cell adhesion, survival and proliferation. Journal of biomaterials science.Polymer edition 20, 1975, 2009.

45. Crapo, P.M., and Wang, Y. Physiologic compliance in engineered small-diameter arterial constructs based on an elastomeric substrate. Biomaterials 31, 1626, 2010.

46. Kenar, H., Kose, G.T., and Hasirci, V. Design of a 3D aligned myocardial tissue construct from biodegradable polyesters. Journal of materials science.Materials in medicine 21, 989, 2010.

47. Crapo, P.M., and Wang, Y. Small intestinal submucosa gel as a potential scaffolding material for cardiac tissue engineering. Acta biomaterialia , 2009.

48. Sun, Z.J., Chen, C., Sun, M.Z., Ai, C.H., Lu, X.L., Zheng, Y.F., Yang, B.F., and Dong, D.L. The application of poly (glycerol-sebacate) as biodegradable drug carrier. Biomaterials 30, 5209, 2009.

49. Wang, Y., Ameer, G.A., Sheppard, B.J., and Langer, R. A tough biodegradable elastomer. Nature biotechnology 20, 602, 2002.

50. Wang, Y., Kim, Y.M., and Langer, R. In vivo degradation characteristics of poly(glycerol sebacate). Journal of biomedical materials research.Part A 66, 192, 2003.

51. Karande, T.S., Ong, J.L., and Agrawal, C.M. Diffusion in musculoskeletal tissue engineering scaffolds: design issues related to porosity, permeability, architecture, and nutrient mixing. Annals of Biomedical Engineering 32, 1728, 2004.

52. Li, S.H., de Wijn, J.R., Layrolle, P., and de Groot, K. Accurate geometric characterization of macroporous scaffold of tissue engineering. Bioceramics 240–2, 541–545, 2003.

53. Knothe Tate, M.L., and Knothe, U. An ex vivo model to study transport processes and fluid flow in loaded bone. Journal of Biomechanics 33, 247, 2000.

54. Netti, P.A., Berk, D.A., Swartz, M.A., Grodzinsky, A.J., and Jain, R.K. Role of extracellular matrix assembly in interstitial transport in solid tumors. Cancer research 60, 2497, 2000.

55. Mansour, J.M. Biomechanics of Cartilage. In: Anonymous : Lippincott Williams and Wilkins, 2003, pp. CH 5: 68-77.

56. O'Brien, F.J., Harley, B.A., Waller, M.A., Yannas, I.V., Gibson, L.J., and Prendergast, P.J. The effect of pore size on permeability and cell attachment in collagen scaffolds for tissue engineering. Technology and health care : official journal of the European Society for Engineering and Medicine 15, 3, 2007.

57. Agrawal, C.M., McKinney, J.S., Lanctot, D., and Athanasiou, K.A. Effects of fluid flow on the in vitro degradation kinetics of biodegradable scaffolds for tissue engineering. Biomaterials 21, 2443, 2000.

58. Owan, I., Burr, D.B., Turner, C.H., Qiu, J., Tu, Y., Onyia, J.E., and Duncan, R.L. Mechanotransduction in bone: osteoblasts are more responsive to fluid forces than mechanical strain. The American Journal of Physiology 273, C810, 1997.

59. Al-Munajjed, A.A., Hien, M., Kujat, R., Gleeson, J.P., and Hammer, J. Influence of pore size on tensile strength, permeability and porosity of hyaluronan-collagen scaffolds. Journal of materials science.Materials in medicine 19, 2859, 2008.

60. Malda, J., van Blitterswijk, C.A., van Geffen, M., Martens, D.E., Tramper, J., and Riesle, J. Low oxygen tension stimulates the redifferentiation of dedifferentiated adult human nasal chondrocytes. Osteoarthritis and cartilage / OARS, Osteoarthritis Research Society 12, 306, 2004.

61. Utting, J.C., Robins, S.P., Brandao-Burch, A., Orriss, I.R., Behar, J., and Arnett, T.R. Hypoxia inhibits the growth, differentiation and bone-forming capacity of rat osteoblasts. Experimental cell research 312, 1693, 2006.

62. D'Ippolito, G., Diabira, S., Howard, G.A., Roos, B.A., and Schiller, P.C. Low oxygen tension inhibits osteogenic differentiation and enhances stemness of human MIAMI cells. Bone 39, 513, 2006.

63. Yang, S., Leong, K.F., Du, Z., and Chua, C.K. The design of scaffolds for use in tissue engineering. Part I. Traditional factors. Tissue engineering 7, 679, 2001.

64. Whang, K., Healy, K.E., Elenz, D.R., Nam, E.K., Tsai, D.C., Thomas, C.H., Nuber, G.W., Glorieux, F.H., Travers, R., and Sprague, S.M. Engineering bone regeneration with bioabsorbable scaffolds with novel microarchitecture. Tissue engineering 5, 35, 1999.

65. Wake, M.C., Patrick, C.W.,Jr, and Mikos, A.G. Pore morphology effects on the fibrovascular tissue growth in porous polymer substrates. Cell transplantation 3, 339, 1994.

66. O'Brien, F.J., Harley, B.A., Yannas, I.V., and Gibson, L.J. The effect of pore size on cell adhesion in collagen-GAG scaffolds. Biomaterials 26, 433, 2005.

67. Lee, S.J., Lee, Y.M., Han, C.W., Lee, H.B., and Khang, G. Response of human chondrocytes on polymer surfaces with different micropore sizes for tissue-engineered cartilage. J Applied polymer Science 92, 2784-2790, 2004.

68. Bhardwaj, T., Pilliar, R.M., Grynpas, M.D., and Kandel, R.A. Effect of material geometry on cartilagenous tissue formation in vitro. Journal of Biomedical Materials Research 57, 190, 2001.

69. Nehrer, S., Breinan, H.A., Ramappa, A., Young, G., Shortkroff, S., Louie, L.K., Sledge, C.B., Yannas, I.V., and Spector, M. Matrix collagen type and pore size influence behaviour of seeded canine chondrocytes. Biomaterials 18, 769, 1997.

70. Ishaug-Riley, S.L., Crane-Kruger, G.M., Yaszemski, M.J., and Mikos, A.G. Three-dimensional culture of rat calvarial osteoblasts in porous biodegradable polymers. Biomaterials 19, 1405, 1998.

71. Chang, B.S., Lee, C.K., Hong, K.S., Youn, H.J., Ryu, H.S., Chung, S.S., and Park, K.W. Osteoconduction at porous hydroxyapatite with various pore configurations. Biomaterials 21, 1291, 2000.

72. Leong, K.F., Cheah, C.M., and Chua, C.K. Solid freeform fabrication of three-dimensional scaffolds for engineering replacement tissues and organs. Biomaterials 24, 2363, 2003.

73. Miot, S., Woodfield, T., Daniels, A.U., Suetterlin, R., Peterschmitt, I., Heberer, M., van Blitterswijk, C.A., Riesle, J., and Martin, I. Effects of scaffold composition and architecture on human nasal chondrocyte redifferentiation and cartilaginous matrix deposition. Biomaterials 26, 2479, 2005.

74. Liao, E.E. Enhancement of chondrogenesis by directing cellular condensation through chondroinductive microenvironments and designed solid freeform fabricated scaffolds. (Unpublished, Ph.D. thesis). University of Michigan, Ann Arbor, MI, U.S.A., 2007.

75. Kim, B.S., and Mooney, D.J. Development of biocompatible synthetic extracellular matrices for tissue engineering. Trends in biotechnology 16, 224, 1998.

76. Mooney, D.J., Mazzoni, C.L., Breuer, C., McNamara, K., Hern, D., Vacanti, J.P., and Langer, R. Stabilized polyglycolic acid fibre-based tubes for tissue engineering. Biomaterials 17, 115, 1996.

77. Liao, E., Yaszemski, M., Krebsbach, P., and Hollister, S. Tissue-engineered cartilage constructs using composite hyaluronic acid/collagen I hydrogels and designed poly(propylene fumarate) scaffolds. Tissue engineering 13, 537, 2007.

78. Kelly, D.J., and Prendergast, P.J. Prediction of the optimal mechanical properties for a scaffold used in osteochondral defect repair. Tissue engineering 12, 2509, 2006.

79. Ju, Y.M., Park, K., Son, J.S., Kim, J.J., Rhie, J.W., and Han, D.K. Beneficial effect of hydrophilized porous polymer scaffolds in tissue-engineered cartilage formation. Journal of biomedical materials research.Part B, Applied biomaterials 85, 252, 2008.

CHAPTER 4

MECHANICAL, PERMEABILITY, AND DEGRADATION PROPERTIES OF 3D POC SCAFFOLDS

4.1. INTRODUCTION

Tissue engineering requires the use of three dimensional scaffolds as a template on which cells differentiate, proliferate, and grow new tissues. Optimal scaffolds should be biocompatible, biodegradable, permeable, reproducible, non-cytotoxic, and capable of serving as a temporary support for the cells with elastic properties similar to native tissue which will allow eventual replacement by tissue matrix[1]. The choice of scaffold material and architecture will determine the effective scaffold mechanical and mass transport properties that can significantly influence tissue regeneration. Particularly for cartilage regeneration, many researchers have tried to develop novel materials which are elastomeric yet mechanically tough. Recently, novel elastomeric materials such as poly(1,8-octanediol-co-citrate) (POC) [2-5], poly(glycerol sebacate) (PGS) [6-11], and polycaprolactone fumarate (PCLF) [12]have been developed and shown to have potential for soft tissue applications. Among them, POC has been shown to be a good candidate for cartilage tissue engineering [13]due to its biocompatibility, biodegradability, and compressive properties. Cartilage applications require 3D designed porous architecture with well characterized mechanical and mass transport properties. Even though Kang et al. [13]has shown that POC has potential as a base material for cartilage, the influence of

designed POC scaffold porosity on mechanical, mass transport and degradation properties has not been elucidated.

Scaffold architecture, mechanical, and degradation properties are intimately coupled. Scaffold pore architecture in addition to base POC material properties are the two determinants of effective POC scaffold mechanical properties. Furthermore, since POC is mainly degraded by hydrolysis of its ester linkages [2, 3], scaffold architecture significantly affects scaffold degradation by directing fluid diffusion. To characterize the coupling of architecture and materials with mechanical, mass transport and degradation properties, we fabricated 3-dimensional (3D) scaffolds with varying porosities, characterizing the resulting mechanical, permeability, and degradation properties of different designs. Scaffold architecture is defined to include pore shape, pore size, and pore interconnectivity. In order to solely examine the effects of porosity on scaffold property changes in this work, pore shape and pore size were kept constant.

4.2 MATERIALS AND METHODS

Synthesis of pre-Poly (1, 8 Octanediol-co-Citrate) (POC)

All chemicals were purchased from Sigma-Aldrich (Milwaukee, WI). Poly(1,8 Octanediol-*co*-Citrate) pre-polymer (pPOC) was synthesized following protocols described by Yang J et al. [2, 3, 5] with some curing process modifications. Briefly, equimolar amounts of citric acid and 1,8-octanediol were added to a 500 ml three-neck round bottom flask fitted with an inlet and outlet adapter. The mixture was melted at 160–165 °C for 15-20 min under a flow of nitrogen gas while stirring. The temperature of

the system was subsequently lowered to 140 °C for 45 min with constant stirring to create a pre-polymer.

Scaffold Design & Fabrication

Previously developed image-based design processes and software were used to design 3D POC scaffold architectures [5, 14-16]. Porous POC scaffolds (6.35mm Diameter, 4.0mm Height, 900μm interconnected cylindrical (C) or spherical pores (S), porosity = C32%, C44%, S50%, C62 %) were designed using custom IDL programs (RSI, Boulder, CO). For description purposes, the scaffold with a cubical pore design and 32% porosity is labeled as C32 (similar labeling for other cubical pore porosities, i.e. C44 = 44% cubical pore porosity), and the scaffold with a spherical pore design and 50% porosity is labeled S50. The details of POC solid and scaffold fabrications were previously reported by Kim et al. (2008). [5] In brief, wax molds with 3D-image based design architecture were built by a Solidscape Patternmaster^{TM} machine and inversely solid freeform fabricated hydroxyapatite (HA) molds were prepared before curing pPOC into architecture scaffolds [17]. Wax molds that embody the designed 3D architecture are fabricated first. However, as the wax molds melt POC curing temperatures, secondary HA molds were created from the wax molds as the HA easily withstands the pPOC curing temperatures that reach over 100^{o}C. pPOC was poured into the wells of a Teflon mold and HA molds were embedded within the pPOC. The pPOC/HA/Teflon mold unit was post-polymerized at 100°C for 1 day followed by curing at 100°C for 3 days more with vacuum (-20in.Hg). The HA mold was removed using a decalcifying reagent (RDO, APEX Engineering Products Corp, Plainfield, IL) followed by incubation in water (Milli-Q water purification system, Billerica, Mass, USA) for 24 hr to obtain the final porous POC scaffolds (Figure 4.1).

Figure 3.3 in chapter 3 summarizes the complete procedure from design through fabrication and evaluation.

Mechanical Tests

For scaffold unconfined compression tests, seven porous scaffolds from each design were tested in compression (Alliance RT/30 electromechanical test frame, 50N load cell with 0.5% error range, MTS Systems Corp., MN) and TestWorks4 software (MTS Systems Corp., MN) was used to collect data during compression testing. MATLAB (The MathWorks Inc., MA) software was used to fit a nonlinear elasticity model, $T = A[e^{BE} - 1]$, where T is the 1st Piola-Kirchoff stress, E is the large strain, and A and B are constants fit to data.. Specifically, the sum of least square error between the model stress and experimental stress was minimized using the LSQNONLIN minimization program in the MATLAB optimization toolbox. Tangent moduli were calculated at 1, 10, 30, and 50% strain from fit data [18]. All residuals between model and experimental stress were below 1%. The compressive Young's modulus of 62% porous scaffolds (N =4, 0.1M NaOH degradation samples) was determined from the initial slope of the stress–strain data (10-20% strain range) obtained from compression tests at a crosshead speed of 2 mm/min. The initial height of each scaffold was measured with an electronic caliper.

To determine if POC exhibited viscoelastic properties, confined compression tests were performed. The same compression test frame as for the unconfined test was used except that the sample was confined by acrylic confined chamber similar to the one described in [19-23]with a constant chamber temperature of 37°C. A 6.35mm diameter porous metal indenter was used for compression instead of a regular fixed metal platen.

Ten solid cylinders (6.35mm in diameter, 4.0mm in height) with the same curing conditions as other scaffolds were tested and the resulting data was fit to the nonlinear elastic model.

Tensile mechanical tests were conducted according to ASTM D412a on the same test frame equipped with 500N load cell. Briefly, the dumbbell-shaped sample (33x6x2.0 mm,) was pulled at a rate of 2 mm/sec. Assuming POC to be incompressible, the tensile tests were fit to a Neohookean nonlinear elastic model (Holzapfel, G. Nonlinear Solid Mechanics, Wiley; 1st edition) [24] of the form:

$$W\left(\lambda_1,\lambda_2,\lambda_3\right)=\frac{\mu_1}{2}\left(\lambda_1^2+\lambda_2^2+\lambda_3^2\right)$$

Where W is the strain energy function, λ_i are principal stretch ratios, and μ_1 is a model constant determined by fitting the model to experimental data. The Neohookean model was fit to experimental data by first deriving the 1st Piola-Kirchoff model stress. The least square error between the model stress and 1st Piola-Kirchoff experimental stress was minimized using the MATLAB unconstrained minimization function FMINUNC. The Baker-Ericksen inequality (required for physical stability of the model constants) was calculated for each fit and found to be satisfied.

Porosity and Permeability Measurements

Seven scaffolds from each porosity were scanned in air using a MS-130 high resolution μCT scanner (GE Medical Systems, Toronto, CAN) at 19 μm voxel resolution, at 75 kV and 75 mA. The porosity of each specimen was calculated by defining a region of interest that encompassed the entire scaffold and an appropriate threshold level was applied to delineate the solid POC material using GEMS Microview software (GE

Medical Systems, Toronto, CAN). All porosity scanning was performed before mechanical tests to avoid any artifacts due to compression. Also, any possible residuals of HA were checked by μCT images by applying a threshold level of HA. The intensity threshold of POC is -510 and that of HA is 2000-2500 at grayscale values of Micro-CT images viewed by GEHC MicroView. By applying different threshold values, any HA residual within the POC scaffold can be determined.

Scaffold permeability (N=7, each design) with and without composite Hyaluronic Acid (HyA)/collagen I (Col I) gel was measured using a previously built flow chamber [25]. Permeability was calculated as average mass flow from Bernoulli's equation (with a frictional loss correctional term) [23] with Darcy's Law used to calculate permeability. Permeability of scaffolds with hydrogels was measured to mimic cell loading conditions *in vitro* or *in vivo*.

Chondrocytes were seeded into 3D scaffolds by first suspending the cells in media with composite HyA/Col I gels and then pushing the gel into the 3D scaffolds [26]. The gelation procedure is as follows: 625μL of Col I (stock concentration: 8.37mg/mL diluted to 6mg/ml with filtered sterile 0.02N Acetic Acid; BD Bioscience Discovery Labs, San Jose) with 62.5 μL HyA (stock concentration: 3 mg/mL in 1.5M sodium chloride (NaCl), molecular weight 2.4~3 million Da; Hyalogic LLC, Edwardsville, KS) were well-mixed. The pH of the HyA/Col I suspension was increased with the addition of 9μL of 0.5N sodium hydroxide with 220 mg/mL sodium bicarbonate to initiate gelation. As soon as 0.5N sodium hydroxide is added to HyA/Col I gel mixture, gel contents were evenly re-suspended. Hydrogel mixtures were then dripped down onto pre-prepared sterile POC scaffolds until POC scaffolds were fully soaked and filled with gels up to the top surface.

This was followed by incubation at 37°C for at least 30 min to solidify gels further. The gel mixture volumes used for each design varied depending on porosity of each design. Roughly, 90µl, 110µl, 120 µl and 150µl of gel mixtures were used for 32, 44, 50 and 62% porous scaffolds respectively. The permeabilities are presented as mean ± standard deviation.

In-Vitro Scaffold Degradation

Four solid cylinders and four porous scaffolds (6.35mm in diameter, 4.0-4.3mm thickness) for each design (except S50) were placed in a tube containing 10ml phosphate buffer saline (PBS- pH 7.4) for 3 weeks. Additionally, nine porous scaffolds for each design were degraded by 0.1M NaOH for 9, 24, 33hr at 37°C to rapidly obtain relative degradation rates among samples. After incubation, samples were washed with water and oven-dried at 50°C for 24 hours. Mass loss was calculated by comparing the initial mass (W_0) with the mass measured at a given time point (Wt), as shown in the following equation: Mass loss = $[(W_0 - W_t)/ W_0]*100\%$. The results are presented as means ± standard deviation. For NaOH degradation, four 62% porous scaffolds were mechanically tested before and after degradation [2, 3, 5].

In Vitro Cell Culture & Histology

Porcine chondrocytes (pChon) were isolated and seeded onto scaffolds following the methods previously published [26]with some modifications. In short, cells were re-suspended at a density of $3.5x10^6$ cells/mL in 600µL of composite HyA/Col I with ~60µL of culture medium. Collagen gels are used as a cell carrier for POC scaffolds to provide better cell distribution within scaffold pores. 5% hyaluronic acids were added to provide a favorable environment for chondrocyte differentiation/proliferation based on our

previous work[26]. The remaining steps were the same as previously described (See *Porosity and Permeability Measurements* section). Scaffolds seeded with pChon were cultured with chondrogenic medium (basal medium (DMEM, 10% fetal bovine serum (FBS), 1% P/S, Gibco) supplemented with 50 mg/mL 2-phospho-L-ascorbic acid (Sigma)), 0.4mM proline (Sigma), 5 mg/mL insulin (Gibco), and 0.1mM non-essential amino acids (Gibco)). Chondrocytes were cultured for 3 weeks under gentle agitation on an orbital shaker and the media was changed every other day. All polymer samples were sterilized by incubation in 70% ethanol for 30 min followed by UV light exposure for another 15 min each side before plating cells. After sterilization, all scaffolds were briefly rinsed with PBS followed by soaking in basal medium to neutralize. Cell culture was maintained in a water-jacket incubator equilibrated with 5% CO2 at 37°C for 4 weeks. For histology, constructs were fixed in 10% buffered formalin overnight, dehydrated with a series of graded ethanol, and embedded in paraffin. Tissue sections were stained with safranin-O (saf-O), to assess cell distribution, morphology, and sGAG staining as a measure for cartilage application. Three slides (4 sections/slide) were obtained from the center of each scaffold (top to bottom and left to right).

Statistical Analysis

Data are expressed as mean ± standard deviation. The statistical significance among different porosities was calculated using linear regressions and one way ANOVA with post-hoc comparison (Tukey). Data were taken to be significant when a *P*-value of 0.05 or less was obtained.

4.3. RESULTS

Scaffold Fabrication and Mechanical Tests

Figure 4.1 shows the digital pictures (A) and micro-CT images (top (B) and side views(C)) for successfully fabricated four different 3D scaffold designs. The porosity of each scaffold was quantified using micro-computed tomography (microCT) images. The micro-CT calculations revealed that the porosities of scaffolds (32.7 ± 2.27, 44.0 ± 1.92, 50.0 ± 1.62, 62.3 ± 2.36%) were slightly less than that of the design files (26, 45, 52, 66%, respectively) except the 32% design, yet each scaffold maintained its pore diameters (902 ± 6 μm) relative to designed pore sizes (900μm).

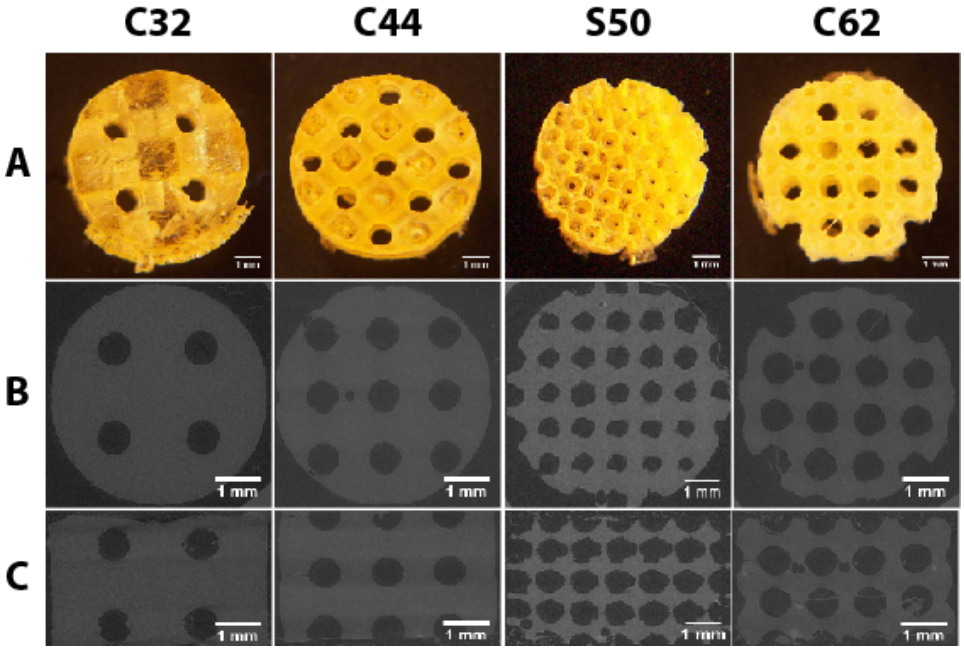

Figure 4.1: The digital images (A) and microCT images of top (B) and side (C) view for successfully fabricated 3D-designed POC scaffolds. The letter 'C' indicates cylindrical pore shape and 'S' indicates spherical pore shape. The following number represents the porosity of each scaffold design.

Figure 4.2 (a) shows that unconfined compressive tests of POC solid and scaffolds produced stress–strain curves characteristic of elastomeric materials. As

porosity of scaffolds increased, tangent moduli decreased. Solid and 32% porous scaffolds exhibited non-linear behavior with increased strain level while 44, 50 and 62% porous scaffolds were more linear, which suggests that there is a possible threshold porosity which determines the behavior of nonlinearity. Figure 4.2 (b) is an example of nonlinear model fit for a 44% porous scaffold.

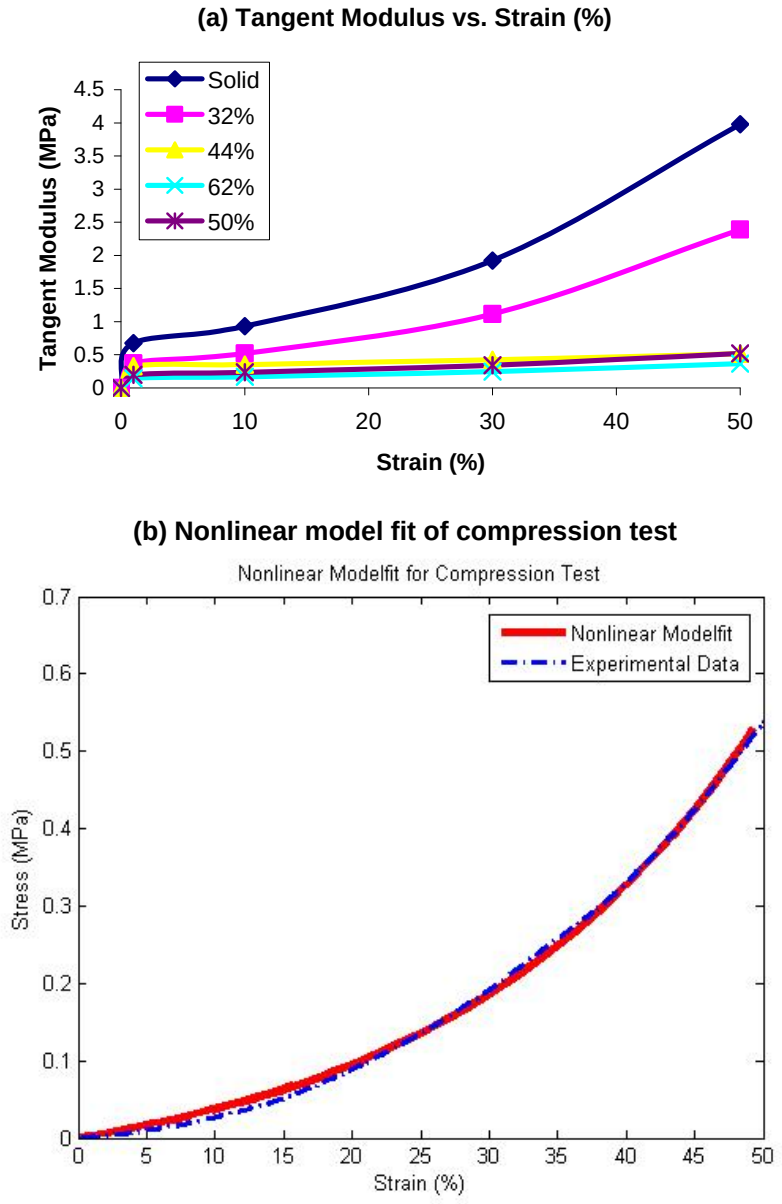

Figure 4.2: (a) a tangent moduli (MPa) vs. Strain (%) curve from unconfined compression tests and nonlinear model fit (N=7, $p<0.05$ for all porosities) (b) an example of compressive test data and corresponding nonlinear model fit for a 44% porous scaffold

Table 4.1 and 4.2 summarize tangent moduli and compressive young's moduli for each design at various strain levels (%). Porous POC scaffolds could provide load bearing within cartilage defect sites as their mechanical properties fall either within or close to the ranges of native cartilage's compressive young's moduli. However, when implanting scaffolds *in vitro* into *in vivo* or actual defect sites, it is probably better to choose a slightly lower range of designed scaffold stiffness as the tissue matrix will add more stiffness to the overall tissue/scaffold constructs after cell infiltration and tissue in-growth. For this application, we also need to consider other factors such as permeability, surface area, pore shape etc., which will affect degradation and tissue matrix formation along with the initial stiffness of scaffolds. In the following chapters, two designs (S50 and C62) were chosen to compare their performance for *in vitro* and *in vivo* subcutaneous models of cartilage regeneration. These two designs have distinctively different permeabilities mainly due to pore shape differences, but have similar porosity, pore size and initial mechanical stiffness (tangent modulus) at 10% strain (Table 4.2) which is close to native cartilage equilibrium modulus.

Tangent Moduli (MPa)					
(N=4-7)	Scaffold Design (Pore Shape, Porosity)				
Strain (%)	Solid[a]	C32%[b]	C44%[c]	S50%[d]	C62%[e]
1	0.674 ± 0.147	0.372 ± 0.048	0.327 ± 0.046	0.199 ± 0.010	0.147 ± 0.046
10	0.933 ± 0.209	0.523 ± 0.061	0.355 ± 0.037	0.235 ± 0.004	0.170 ± 0.052
30	1.922 ± 0.475	1.115 ± 0.123	0.427 ± 0.035	0.344 ± 0.019	0.244 ± 0.089
50	3.977 ± 1.113	2.392 ± 0.343	0.519 ± 0.082	0.504 ± 0.062	0.365 ± 0.182

Table 4.1: Tangent moduli (MPa) of POC sold and scaffolds at various strain (%) presented as average ± standard deviation (N=7, $p<0.05$ for a-e)

Design	Compressive Tangent Modulus (MPa)	Compressive Young's Modulus (MPa)
Solid	0.93-1.92	1.37 ± 0.32
C32	0.52-1.12	0.78 ± 0.08
C44	0.35-0.43	0.39 ± 0.03
C62	0.17-0.24	0.24 ± 0.04
S50	0.13-0.40	0.29 ± 0.01
Human Articular Cartilage*	-	0.4-0.8

Table 4.2: Summary of tangent moduli and compressive young's moduli at 10% strain for solid and all scaffold designs with comparative value of human articular cartilage, which was measured by Moutos et al.[35].

In cartilage engineering, many researchers have tried to design and fabricate scaffolds with stress relaxation properties mimicking the poroelastic biomechanics of cartilage. In order to determine if POC solid cylinders or scaffolds were also either viscoelastic or poroelastic, we have performed confined compressive tests as described as [19-21]. Results of stress-relaxation tests demonstrated that POC does not exhibit significant stress relaxation and thus can be considered as a nonlinear elastic material and not viscoelastic. Porous scaffolds also did not demonstrate stress relaxation, indicating that pores of the designed size did not exhibit poroelastic behavior.

Tensile test data for solid coupons exhibited nonlinear elastic behavior and was fit well with the Neohookean model (Figure 4.3). The coefficients differed with synthesis conditions, with 1 day of curing at 100^{o}C followed by 4 days at 120^{o}C giving a μ_1 value of 0.172 ± 0.022 MPa while 5 days of 100^{o}C giving a μ_1 value of 0.142 ± 0.013 MPa. The coefficient of determination for all fits was greater than 0.99, indicating good fits for the nonlinear model[27]. In addition, all coefficients satisfied the Baker- Eriksen criteria for material stability. This demonstrates higher curing temperature gives an overall stiffer behavior for solid POC. These results also demonstrate that POC can be considered as a nonlinear elastic elastomeric material.

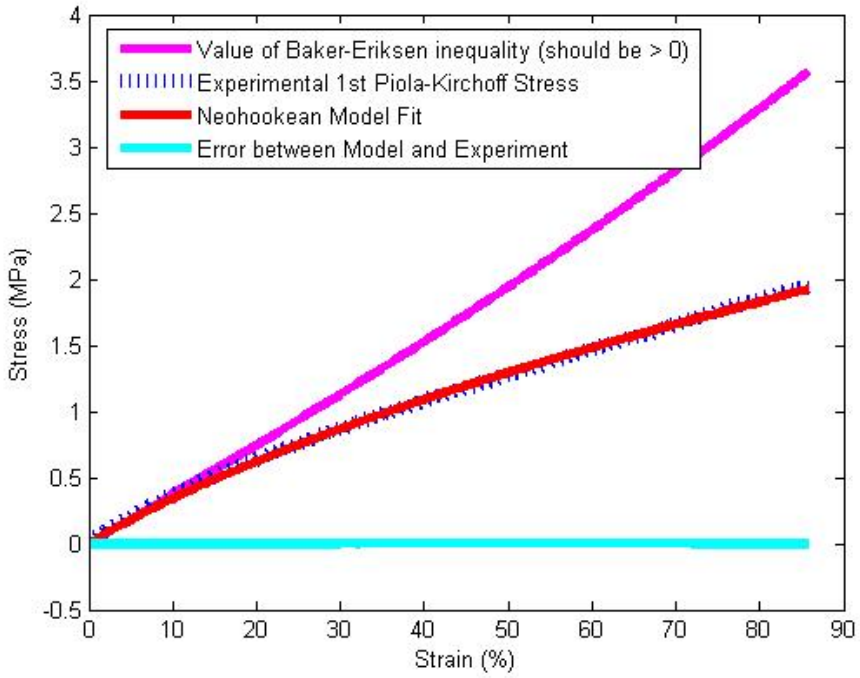

Figure 4.3: An example of tensile test data and corresponding Neohookean model fit

The major difference between linear and non-linear elasticity is that in linear elasticity the material modulus is constant over the entire deformation while for non-linear elasticity the modulus will change with deformation. In general, soft tissues including cartilage are shown to exhibit strain stiffening in which the tangent modulus increases with increasing strain.[27] If we accept the fact that mechanical strain magnitude can affect tissue regeneration in that cells may modulate matrix synthesis in response to strain levels, matching only the linear versus non-linear behavior could have significant consequences for tissue regeneration. If only a material exhibiting linear behavior is used for a scaffold, we are faced with the choice of matching either the low modulus under small strains or the higher modulus under large strains. Matching the small strain low modulus may provide sufficient strain to stimulate cells under small deformation, but if large deformations are seen than the cells may be damaged. If we match the large

deformation higher modulus with a linear scaffold, this may protect the chondrocytes under large strain, but may shield the chondrocytes for sufficient mechanical stimulus under small strain. A nonlinear material that can match both regions may provide better strain microenvironments to chondrocytes. Of course, this is currently conjecture, but such hypotheses can only be tested if we can engineer scaffolds with both linear and nonlinear elastic behavior.

Based on previous reports[29-34], aggregate modulus of human articular cartilage ranges from 0.1 to 3.10 MPa and unconfined compressive modulus ranges from 0.4 to 0.8 MPa with 10~30% strain depending on ages and health conditions. POC scaffold tangent moduli range from 0.13 MPa (62% porosity at 1% strain) to 1.12 MPa (33% porosity at 30% strain). Thus, POC tangent moduli encompass the range of human articular equilibrium moduli.

Permeability

Table 4.3 shows permeability of scaffolds without and with hydrogels for various porosities. Generally, it is known that an increase in interconnected porosity results in an increase in permeability. However, permeability depends not only on scaffold architecture, but also on base materials due to the presence of micropores, hydrophilicity, and number of crosslinkages. The spherical pore shaped scaffold shows the lowest permeability out of all designs despite having higher porosity than the 32 and 44% porous scaffolds. This is probably due to the small pore to pore necking areas and the irregular shape of the pores compared to the regular cylindrical channel type of pores.

Design (N=7-9)	S50, Low	C32	C44	C62, High
Pore Size (μm)	902 ± 6			
Pore Shape	Spherical	Cubical		
Porosity (%)	50.0 ± 1.6	32.7 ± 2.3	44.0 ± 1.9	62.3 ± 2.4
Expt Permeability without gel (10^{-7} m^4/N·s)	3.5 ± 1.0	5.4 ± 1.2	29.8 ± 2.1	47.4 ± 1.2
Expt Permeability with gel (10^{-7} m^4/N·s)	1.7 ± 0.5	3.11 ± 0.4	3.7 ± 0.3	4.1 ± 0.7

Table 4.3: Permeability of scaffold designs with and without collagen I gel is presented based on the designs which have the lowest to highest permeability values. (N=7, $p<0.05$ for both with and without gel)

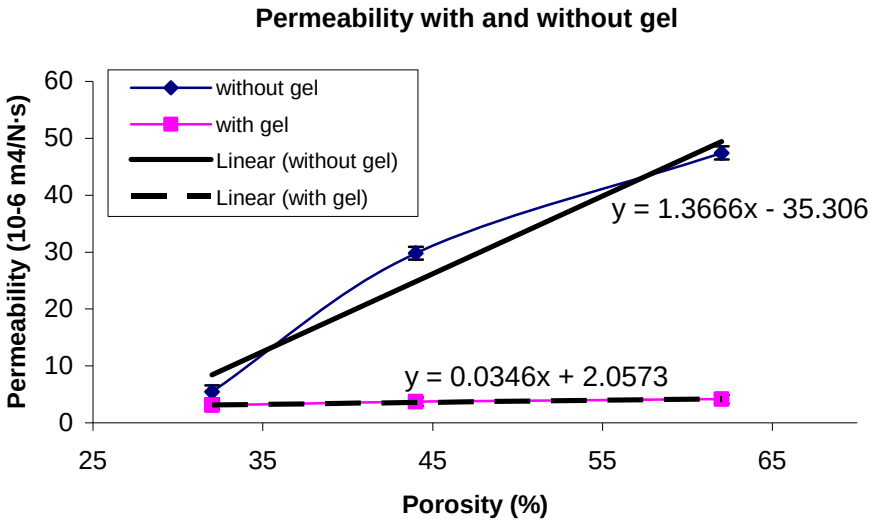

Figure 4.4: POC scaffold permeability with and without gel for different porosity designs is accompanied with a linear regression lines (N=7, $p<0.05$).

Without gels, permeability increased dramatically with a linear regression coefficient of 0.1524 whereas permeability did not vary substantially between different designs with gel, having a linear regression coefficient of 0.0032 (Figure 4.4). The differences in permeability between cases with and without gel become more critical when cells are seeded onto scaffolds for tissue in-growth. Even though scaffold architectures may have significantly different permeabilities, the use of gels for scaffold cell seeding may temporarily cause a significant drop in permeability. However as the

relatively quick hydrogel degradation will cause a steady increase in scaffold permeability.

In Vitro Degradation

Yang J et al. [3]demonstrated that the degradation rate could be adjusted by varying synthesis and fabrication conditions of POC solids. They demonstrated that increased curing temperature and post-polymerization time resulted in a higher tensile strength and a higher Young's modulus due to higher crosslink density and fewer un-reacted monomer groups, but those synthesis conditions tend to make a material that degrades slower. However, they did not investigate how different scaffold architectures could affect POC degradation and associated changes in compressive mechanical properties. The data for degradation of POC scaffolds with various porosities are presented in Figure 4.5. Both fast (0.1M NaOH) and slow (PBS) degradation showed a similar trend in terms of different degradation profiles for each design.

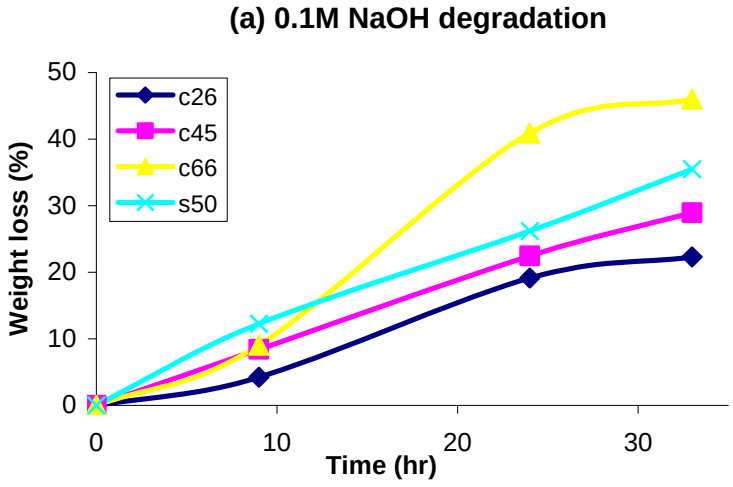

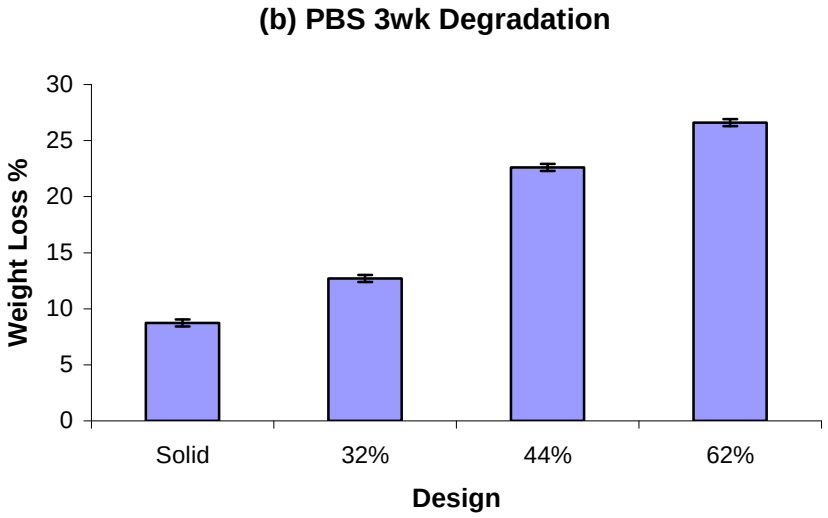

Figure 4.5: Degradation studies of POC solid and scaffolds with various porosities in (a) 0.1M NaOH solution at room temperature (N=9, each porosity) (all designs are statistically significant each other at 32h; $p \leq 0.05$) and (b) PBS at 37 °C for 3 weeks (N=4, each porosity) (all designs are statistically significant each other; $p \leq 0.05$).

Degradation, perhaps due to both bulk and surface erosion for scaffolds, was highly dependent on scaffold porosity and permeability (Figure 4.5). Both the 32% and 44% scaffolds showed loss of architecture and complete pore collapse after 3 week degradation in PBS (Figure 4.5(b)). Of note, only the cylindrical pored scaffold designs were used in the 3 week PBS degradation study as we wanted to see a general profile of degradation due to porosity difference (without any pore shape effects taken account). But for the 0.1M NaOH accelerated degradation study, the spherical pore design (S50) was also included to see a general profile compared to other cylindrical pored designed scaffolds as well (Figure 4.5 (b)). All designs showed loss of architecture after 24 hours in 0.1M NaOH. A significant portion of the 62% porous scaffold showed pore collapse, although the top layer of the scaffold maintained the pore structure. Based on these results, it is not possible to make a definitive conclusion as to the mechanism of

degradation, bulk versus surface. The nature of the pore collapse suggests that both mechanisms may be involved.

In this study, the lower porosity scaffolds with thicker struts showed a greater degree of collapse than the 62% porous scaffolds with the thinnest struts. If the sole mechanism of degradation was surface erosion, one would expect that the 62% porous scaffold with the thinnest struts would collapse sooner, as the struts would lose thickness and geometry first. However, the thinnest struts did not collapse first, suggesting that bulk degradation with autocatalysis could play a role in POC porous architecture degradation.

Tangent Young's modulus (10-20% strain range) for 62% scaffolds decreased from 0.070 to 0.037 MPa after PBS degradation. In Figure 6(a), initial degradation rate did not seem to vary much depending on different porosities, however permeability effects were associated with higher degradation rates at longer time periods as determined by weight loss.

Biocompatibility Evaluation

Cartilaginous-like tissue was formed within POC scaffolds and chondrocytes in lacuna were evenly distributed within the tissue. These cells maintained a rounded form indicating maintenance of the chondrocytes phenotype (Figure 4.6 (B)). The void spaces shown in Figure 4.6 (A & B) are areas occupied by POC scaffolds. The chondrocytic morphology and tissue formation confirm the biocompatibility of the POC scaffolds.

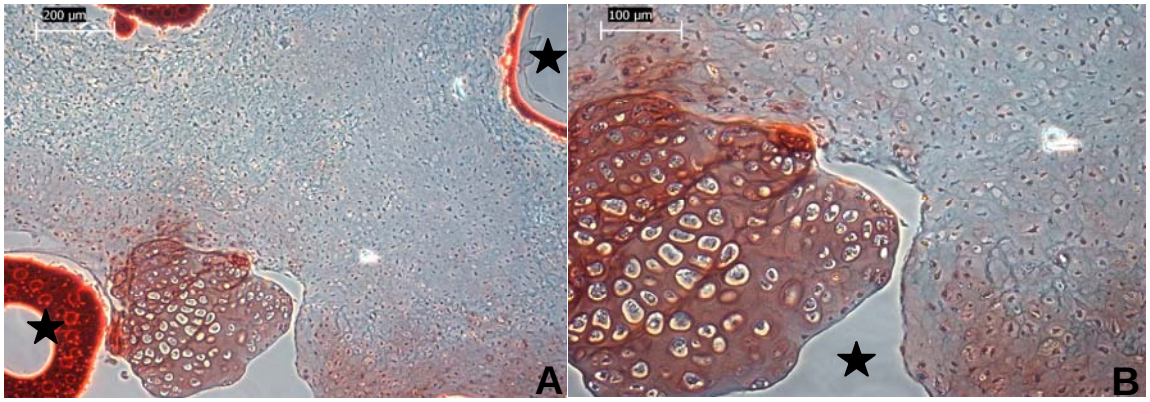

Figure 4.6: Histological image of a POC scaffold with chondrocytes cultured for 4 weeks. The sections were stained with safranin-O/Fast Green counter staining. Stars indicate areas occupied by scaffold materials.

4.4 Discussion and Conclusions

The success in development of novel biodegradable polymers for scaffolds relies on appropriate mechanical properties, degradation rates, and biocompatibility. It is critical to understand how scaffold architectures affect mechanical, mass transport and degradation properties of scaffolds as these properties will significantly influence tissue regeneration. A typical solid elastomer shows nonlinear behavior in compression and tension[3]. However, the degree of nonlinearity in compression depended significantly on scaffold porosity. As porosity increased, nonlinear behavior decreased and 44, 50 and 62% porous scaffolds had a trend towards more linear behavior without any significantly noticeable pore shape effect. Due to the inherent POC nonlinear behavior, solid and 32% porous scaffolds showed a distinct increase in compressive tangent moduli compared to higher porosities.

Permeability showed a more complex relationship to scaffold architecture, depending on the presence or absence of gel cell carriers. Scaffold permeability without gel showed a linear relationship with porosity (Figure 4.4) for the same pore shape;

however the effect of pore shape on permeability seemed to be more influential than porosity such that 50% porous spherical pore shape scaffold had the lowest permeability despite not having the lowest porosity. Based on permeability without gel, we may deduce that water could penetrate through both gel and POC itself at similar rates because the regression coefficients did not depend significantly on porosity when the scaffold contained gel. This data is especially important when considering seeding cells with gels onto POC scaffolds. The degradation rates were also highly dependent on porosity and permeability especially within the same pore shape designs. 62% porous scaffolds exhibited faster and accelerated degradation rates with time whereas 32, 44 and 50% porous scaffolds showed a steady linear increase in degradation rates with time, which suggests that pore shape or permeability does not play much in the degradation profiles especially when there is no cell involved (Figure 4.5a). Data for bulk degradation with PBS for 3 week *in vitro* showed an interesting phenomenon in that only 62% porous scaffolds maintained some porous architecture at 3 week time point while other designs all exhibited distorted inner architectures due to degradation. For compressive modulus, Young's modulus of 62% porous scaffolds was decreased by up to 47% after 3 weeks.

In vitro histological evaluation of POC scaffolds with gel confirmed that they supported synthesis of cartilage matrix by chondrocytes. Also, chondrocytic morphology of scaffold was also maintained showing its promising potential as a scaffold for cartilage regeneration.

The above characterization provides us with a comprehensive understanding of the physical properties of POC scaffolds and proves that POC scaffolds can be fabricated successfully with desired porosity, permeability, and architectures via SFF fabrication.

POC scaffolds hold promise for serving as a supporting template for cartilage and other soft tissue regeneration with tunable biodegradation and nonlinear compliant mechanical properties. Also, this characterization provides us with a foundation to study cell behavior and tissue in-growth on different scaffold architectures in order to elucidate the relation between scaffold architectures, mechanical properties, biodegradation, and consequent cell growth and morphology, and matrix formation, which will be discussed in next following chapters.

Acknowledgements

This work was funded in part by a NIH grant R01 AR 053379. The authors thank Alisha Diggs and Eiji Saito for help with HA mold fabrication, Jessica M. Kemppainen for help with permeability measurements, and Chris Strayhorn for assistance with histology.

References

1. Safran MR, Kim H, Zaffagnini S. The use of scaffolds in the management of articular cartilage injury. J Am Acad Orthop Surg 2008 Jun;16(6):306-11.

2. Yang J, Webb AR, Ameer GA. Novel citric acid-based biodegradable elastomers for tissue engineering. Adv Mater 2004 March 18;16(6):511-16.

3. Yang J, Webb AR, Pickerill SJ, Hageman G, Ameer GA. Synthesis and evaluation of poly(diol citrate) biodegradable elastomers. Biomaterials 2006 Mar;27(9):1889-98.

4. Hidalgo-Bastida LA, Barry JJ, Everitt NM, Rose FR, Buttery LD, Hall IP, Claycomb WC, Shakesheff KM. Cell adhesion and mechanical properties of a flexible scaffold for cardiac tissue engineering. Acta Biomater 2007 Jul;3(4):457-62.

5. Kim K, Jeong CG, Hollister SJ. Non-invasive monitoring of tissue scaffold degradation using ultrasound elasticity imaging. Acta Biomater 2008 Jul;4(4):783-90.

6. Wang Y, Ameer GA, Sheppard BJ, Langer R. A tough biodegradable elastomer. Nat Biotechnol 2002 Jun;20(6):602-6.

7. Motlagh D, Yang J, Lui KY, Webb AR, Ameer GA. Hemocompatibility evaluation of poly(glycerol-sebacate) in vitro for vascular tissue engineering. Biomaterials 2006 Aug;27(24):4315-24.

8. Sundback CA, Shyu JY, Wang Y, Faquin WC, Langer RS, Vacanti JP, Hadlock TA. Biocompatibility analysis of poly(glycerol sebacate) as a nerve guide material. Biomaterials 2005 Sep;26(27):5454-64.

9. Gao J, Ensley AE, Nerem RM, Wang Y. Poly(glycerol sebacate) supports the proliferation and phenotypic protein expression of primary baboon vascular cells. J Biomed Mater Res A 2007 Dec 15;83(4):1070-5.

10. Gao J, Crapo PM, Wang Y. Macroporous elastomeric scaffolds with extensive micropores for soft tissue engineering. Tissue Eng 2006 Apr;12(4):917-25.

11. Chen QZ, Bismarck A, Hansen U, Junaid S, Tran MQ, Harding SE, Ali NN, Boccaccini AR. Characterisation of a soft elastomer poly(glycerol sebacate) designed to match the mechanical properties of myocardial tissue. Biomaterials 2008 Jan;29(1):47-57.

12. Wang S, Kempen DH, Simha NK, Lewis JL, Windebank AJ, Yaszemski MJ, Lu L. Photo-cross-linked hybrid polymer networks consisting of poly(propylene fumarate) and poly(caprolactone fumarate): Controlled physical properties and regulated bone and nerve cell responses. Biomacromolecules 2008 Apr;9(4):1229-41.

13. Kang Y, Yang J, Khan S, Anissian L, Ameer GA. A new biodegradable polyester elastomer for cartilage tissue engineering. J Biomed Mater Res A 2006 May;77(2):331-9.

14. Hollister SJ, Maddox RD, Taboas JM. Optimal design and fabrication of scaffolds to mimic tissue properties and satisfy biological constraints. Biomaterials 2002 Oct;23(20):4095-103.

15. Hollister SJ. Porous scaffold design for tissue engineering. Nat Mater 2005 Jul;4(7):518-24.

16. Liao E, Yaszemski M, Krebsbach P, Hollister S. Tissue-engineered cartilage constructs using composite hyaluronic acid/collagen I hydrogels and designed poly(propylene fumarate) scaffolds. Tissue Eng 2007 Mar;13(3):537-50.

17. Taboas JM, Maddox RD, Krebsbach PH, Hollister SJ. Indirect solid free form fabrication of local and global porous, biomimetic and composite 3D polymer-ceramic scaffolds. Biomaterials 2003 Jan;24(1):181-94.

18. Kemppainen JM, Hollister, SJ. Tailoring the mechanical properties of 3D-Designed Poly(glycerol Sebacate) scaffolds for cartilage applications, J. Biomed. Mat. Research. in press.

19. Ateshian GA, Warden WH, Kim JJ, Grelsamer RP, Mow VC. Finite deformation biphasic material properties of bovine articular cartilage from confined compression experiments. J Biomech 1997 Nov-Dec;30(11-12):1157-64.

20. Soltz MA, Ateshian GA. Experimental verification and theoretical prediction of cartilage interstitial fluid pressurization at an impermeable contact interface in confined compression. J Biomech 1998 Oct;31(10):927-34.

21. Soltz MA, Ateshian GA. Interstitial fluid pressurization during confined compression cyclical loading of articular cartilage. Ann Biomed Eng 2000 Feb;28(2):150-9.

22. Guilak F, Best BA, Ratcliffe A, Mow VC. Instrumentation for load and displacement controlled studies on soft connective tissues. AMD 1989;98:113-6.

23. Hollister SJ, Liao EE, Moffitt EN, Jeong CG, Kemppainen JM. Defining design targets for tissue engineering scaffolds. In: Fundamentals of tissue engineering and regenerative medicine. Meyer U. Ed. ed. Berlin: Springer Verlag.

24. Holzapfel GA. Nonlinear solid mechanics a continuum approach for engineering. ; 2000. 235~239

25. Kemppainen JM., (2008) Mechanically stable solid freeform fabricated scaffolds with permeability optimized for cartilage tissue engineering. Unpublished thesis (Ph.D.), University of Michigan, Ann Arbor, MI, U.S.A.

26. Liao E, Yaszemski M, Krebsbach P, Hollister S. Tissue-engineered cartilage constructs using composite hyaluronic acid/collagen I hydrogels and designed poly(propylene fumarate) scaffolds. Tissue Eng 2007 Mar;13(3):537-50.

27. Humphrey JD. Cardiovascular Solid Mechanics. 2002. 198~201

28. Nugent GE, Schmidt TA, Schumacher BL, Voegtline MS, Bae WC, Jadin KD, Sah RL. Static and dynamic compression regulate cartilage metabolism of PRoteoGlycan 4 (PRG4). Biorheology. 2006;43(3-4):191-200.

29. Demarteau O, Wendt D, Braccini A, Jakob M, Schafer D, Heberer M, Martin I. Dynamic compression of cartilage constructs engineered from expanded human articular chondrocytes. Biochem Biophys Res Commun 2003;310:580-588.

30. Boschetti F, Pennati G, Gervaso F, Peretti GM, Dubini G. Biomechanical properties of human articular cartilage under compressive loads. Biorheology 2004;41:159-166.

31. Huang CY, Mow VC, Ateshian GA. The role of flow-independent viscoelasticity in the biphasic tensile and compressive responses of articular cartilage. J Biomech Eng 2001;123:410-417.

32. Armstrong CG, Mow VC. Variations in the intrinsic mechanical properties of human articular cartilage with age, degeneration, and water content. J Bone Joint Surg Am 1982;64:88-94.

33. Armstrong CG, Mow VC. The mechanical properties of articular cartilage. Bull Hosp Jt Dis Orthop Inst 1983;43:109-117.

34. Mansour JM. Biomechanics of cartilage. . C.A. Oatis ed.: Lippincott Williams and Wilkins, 2003.p. CH 5: 68-77.

35. Moutos FT, Freed LE, Guilak F. A biomimetic three-dimensional woven composite scaffold for functional tissue engineering of cartilage. Nat.Mater. 2007;6:162-7. doi: 10.1038/nmat1822.

CHAPTER 5

THE EFFECTS OF 3D POC SCAFFOLD PORE SHAPE AND PERMEABILITY ON *IN VITRO* CHONDROGNESIS

5.1 Introduction

The field of tissue engineering continues to advance with the discovery of new biomaterials, growth factors, and scaffold fabrication techniques. The use of biodegradable scaffolds as a template on which cells differentiate, proliferate, and grow new tissues has been crucial in the recent advances of cartilage tissue engineering. However, there is still no definitive conclusion as to how scaffold design factors affect chondrogenesis. The choice of scaffold material and geometry will determine the effective scaffold structural and mass transport properties that can significantly influence cartilaginous tissue regeneration. As thoroughly reviewed in chapter 3, the structural, mechanical and mass transport properties of scaffolds are determined by combination of many factors such as pore size, pore shape, porosity, pore interconnectivity, permeability, scaffold surface area, scaffold effective stiffness and scaffold material. These factors cannot be rigorously controlled unless scaffolds are designed with specific architecture and this architecture is realized by controlled fabricated techniques such as solid freeform fabrication (SFF). Many previous studies examining the effect of scaffold designs on chondrogenesis have not rigorously controlled scaffold design parameters like pore shape

and permeability, making it difficult to assess what specific design factor had the most influence on chondrogenesis [1-8].

Based on our own previous work [2], designed PCL scaffolds with lower permeability enhanced chondrogenesis using primary chondrocytes. However, this study examined one pore shape in polycaprolactone (PCL) scaffolds and did not examine changes in scaffold/tissue construct mechanical properties with tissue in-growth. We also have demonstrated that chondrocytes cultured in ellipsoidal pores produced more robust ECM with higher sGAG concentrations in comparison to cubical pores due to increased aggregation of local chondrocytes inside each pore of poly (propylene furmarate) (PPF) [9,10]. However, the permeability of these scaffolds was not experimentally characterized, making it difficult to determine if permeability was significantly different between designs. Poly(1,8-octanediol-co-citrate) (POC) has been shown to be a good candidate for cartilage tissue engineering due to its biocompatibility, biodegradability, and mechanical properties [11-13], yet there is no data on how POC scaffolds with rigorously controlled pore architectures (i.e. pore shape, pore size, permeability, and regular pore interconnectivity) influence chondrogenesis and how mechanical properties of POC scaffolds change with tissue development. The goal of this study was to determine how POC scaffolds with designed and rigorously controlled scaffold permeability and pore shape influence chondrogenesis as determined by chondrogenic gene expression, matrix production and tissue/scaffold mechanical properties. Scaffold design parameters including permeability, pore shape, and surface area were controlled by computational design, and control of these parameters in the final fabricated scaffolds was verified by micro-computed tomography (micro-CT).

Additionally, since type I collagen gel was used as a cell carrier within the POC scaffolds, we determined how collagen I gel concentration affected chondrogenesis prior to assessments of the 3D tissue/scaffold constructs.

5.2 Materials and Methods

Collagen I/Hyalurinoic Acid (Hya) Hydrogel

High concentration collagen I hydrogels and hyaluronic acid were purchased from BD Bioscience Discovery Labs (San Jose, CA) and Hyalogic LLC (Edwardsville, KS) respectively. High concentration collagen I hydrogels were diluted with 0.02N sterile acetic acid for desired concentration (9.92mg/ml, 6mg/ml, and 4mg/ml) and 5% (w/w) hyaluronic acid was combined with collagen I hydrogel based on our previous results showing that collagen I gel with 5% hyaluronic acid enhanced chondrogenesis.

Scaffold Design & Fabrication

Poly (1, 8 Octanediol-*co*-Citrate) pre-polymer (pPOC) was synthesized as previously described (chapter 4) [13]. The scaffolds were designed and fabricated in the same way as previously described in chapter 4. Porous POC scaffolds (6.35mm Diameter, 4.0mm Height), with 900μm interconnected spherical or cylindrical pores, (porosity: 50 %(spherical (S50)), 62 %(cubical (C62)), permeability: High (C62) = Low x 13.5 (S50)) were designed using custom IDL programs (RSI, Boulder, CO).

Scaffold Characterizations

For mechanical tests, four to six porous scaffolds or tissue grown scaffolds per each design were tested in unconfined compression (Alliance RT/30 electromechanical test frame, 50N load cell with 0.5% error range, MTS Systems Corp., MN) and

TestWorks4 software (MTS Systems Corp., MN) was used to collect data during compression testing. The data was analyzed and processed the same way using the nonlinear elasticity model fit as previously described in chapter 4. Tangent moduli (=AB $e^{B\varepsilon}$) were calculated at 1, 10, and 30% strain from fit data and all residuals between model and experimental stress were below 1%. Also, all porosity and permeability measurements were performed under the same conditions as described in chapter 4 following the same methods.

In Vitro Cell Culture & Histology

Primary porcine chondrocytes (pChon) were isolated and seeded onto scaffolds following the methods previously published with some modifications [19]. The detailed gelation and cell seeding procedure was as follows: 770μL of Col I hydrogels (stock concentration: 9.92, 6, or 4mg/mL; BD Bioscience Discovery Labs, San Jose, CA) with 77 μL HyA (stock concentration: 3 mg/mL in 1.5M sodium chloride (NaCl), molecular weight 2.4~3 million Da; Hyalogic LLC, Edwardsville, KS) were well-mixed. The pH of the HyA/Col I suspension was increased with the addition of 11μL of 0.5N sodium hydroxide with 220 mg/mL sodium bicarbonate to initiate gelation. As soon as 0.5N sodium hydroxide is added to HyA/Col I gel mixture, gel contents were evenly re-suspended. Chondrocytes at a density of ~$30x10^6$ cells/mL well-suspended in ~50μL of culture medium were well-mixed with composite hydrogels immediately. The cell/hydrogel mixtures were then dripped down onto pre-prepared sterile scaffolds placed inside the well of a sterile Teflon mold until scaffolds were fully soaked and filled with gel to the top surface. This was followed by incubation at 37°C for at least 30 min to

solidify gels further. Roughly, 121 and150µl of cell/gel mixtures were used for 50 and 62% porous scaffolds respectively in order to keep the same cell density per volume.

Scaffolds seeded with pChon were cultured with chondrogenic medium (basal medium (DMEM, 10% fetal bovine serum (FBS), 1% P/S, Gibco) supplemented with 50 mg/mL 2-phospho-L-ascorbic acid (Sigma)), 0.4mM proline (Sigma), 5 mg/mL insulin (Gibco), and 0.1mM non-essential amino acids (Gibco)) in 12-well plates. Chondrocytes were cultured for 0 (1d), 2 or 4 weeks under gentle agitations on an orbital shaker and the media was changed every other day. All POC scaffolds were sterilized in an autoclave and presoaked in DMEM for 24 hours and briefly rinsed with PBS prior to cell seeding. Cell culture was maintained in a water-jacket incubator equilibrated with 5% CO_2 at 37°C. For histology, constructs (N=3/material) at each time point were fixed in 10% buffered formalin overnight, dehydrated with a series of graded ethanol, and embedded in paraffin. Tissue sections were stained with safranin-O/Fast Green counterstaining, to assess cell distribution, morphology and sGAG production. Eight to ten slides (4 sections/slide) were obtained from the center of each scaffold (top to bottom and left to right).

sGAG and DNA quantification

For comparing the effects of collagen I gel concentration on chondrocytes, at 7 days sGAG and DNA contents of collagen/cell hydrogels (N=4-5/concentration) were quantified using the same methods as for scaffolds. At 2 and 4 weeks, scaffolds (N=8) at each time point or each design were removed from culture, finely diced, and placed immediately into 1ml of pre-prepared papain solution (papain (10 units/mg: Sigma Aldrich #P4762), 1X PBS, 5mM cysteine HCL, 5mM EDTA, pH=6.0; mixed for 2h at

37°C then filtered). Scaffolds were digested in papain solution for 24 hours at 60°C then immediately stored at -20°C. The digested tissue-scaffold solution was analyzed by a dimethylmethylene blue (DMMB) assay. Briefly, 10ul of sample was mixed with 200ul of DMMB reagent and absorbance was read on a plate reader (MultiSkan Spectrum, Thermo, Waltham, MA) at 525 nm. A standard curve was established from chondroitan 6-sulfate from shark (Sigma, C4384) to compare absorbance for samples [20,21]. The total sGAG were normalized by DNA content which was measured using Hoechst dye 33258 methods (Sigma, #DNA-QF). In brief, 10ul digested sample was added to 200ul pre-prepared Hoechst solution and read with excitation at 355nm and emission at 460nm (Fluoroskan Ascent FL, Thermo, Waltham, MA) in a 96 well plate. Readings were compared to standard curves made from calf thymus DNA (Sigma, #DNA-QF) [22].

Quantitative-PCR

Cartilage specific gene (Type II collagen & aggrecan),chondrocyte de-differentiation marker gene (Type I & X collagen) and glycerol-dehyde-3-phosphate dehydrogenase (GAPDH) gene expression were determined by quantitative PCR (qtPCR) using a Gene Amp 7700 sequence detection system (Applied Biosystems, Foster City, CA USA). For different concentration of collagen gels (N=4-5), only Type II & I collagens and aggrecan gene expressions were quantified with normalization with GAPDH at 7 days. Collagen hydrogels or scaffolds (N=8-10/design) at each time point were removed from culture, briefly rinsed with PBS, chopped into smaller pieces, and then placed into RNAlater (Qiagen, Inc., Valencia, CA). Scaffolds immersed in RNAlater were kept at 4°C for 24 hours and stored at -20°C until analysis. Total RNA was extracted using a RNeasy Mini Kit (Qiagen, Inc., Valencia, CA) and reverse transcription

was carried out using the SuperScript First-Strand synthesis kit (Invitrogen). A positive standard curve for each primer was obtained by qtPCR with serially-diluted cDNA sample mixtures. Samples were prepared using a Taqman universal PCR master mix (Applied Biosystems) and custom designed porcine primers. The quantity of gene expressions was calculated with standard samples and normalized with GAPDH or/and low permeable design (S50).

Statistical Analysis

Data are expressed as mean ± standard deviation. The statistical significance among different materials was calculated using linear regressions and one way ANOVA with post-hoc comparison (Tukey) or student t-test using SPSS software (SPSS for Windows, Rel 14.0. 2005 Chicago: SPSS Inc.). Data were taken to be significant, when a *P*-value of 0.05 or less was obtained.

5.3 Results

The effects of collagen I gel concentration on chondrogenesis

Before examining the design effects of scaffolds on chondrogenesis *in vitro*, we wanted to optimize the microenvironment conditions for cells to grow in 3D POC scaffold. Previously, the effects of hyaluronic acid combined with collagen I gel have been elucidated in our lab [9], yet the effects of collagen I gel concentration on chondrogenesis using chondrocytes has not been studied. As our goal for this study was to provide a favorable microenvironment for chondrocytes to form cartilage tissues in our 3D scaffolds, the effects of collagen I gel concentrations on chondrogenesis were in terms of matrix production and the messenger RNA expression relevant to chondrogenesis.

When comparing 4mg/ml, 6mg/ml, and 9.92mg/ml collagen I gel concentrations (Figure 5.1(top)), there was a significant difference in terms of matrix production between 6mg/ml and 9.92mg/ml only with 6mg/ml Col I gel supporting formation of the highest amount of matrix.

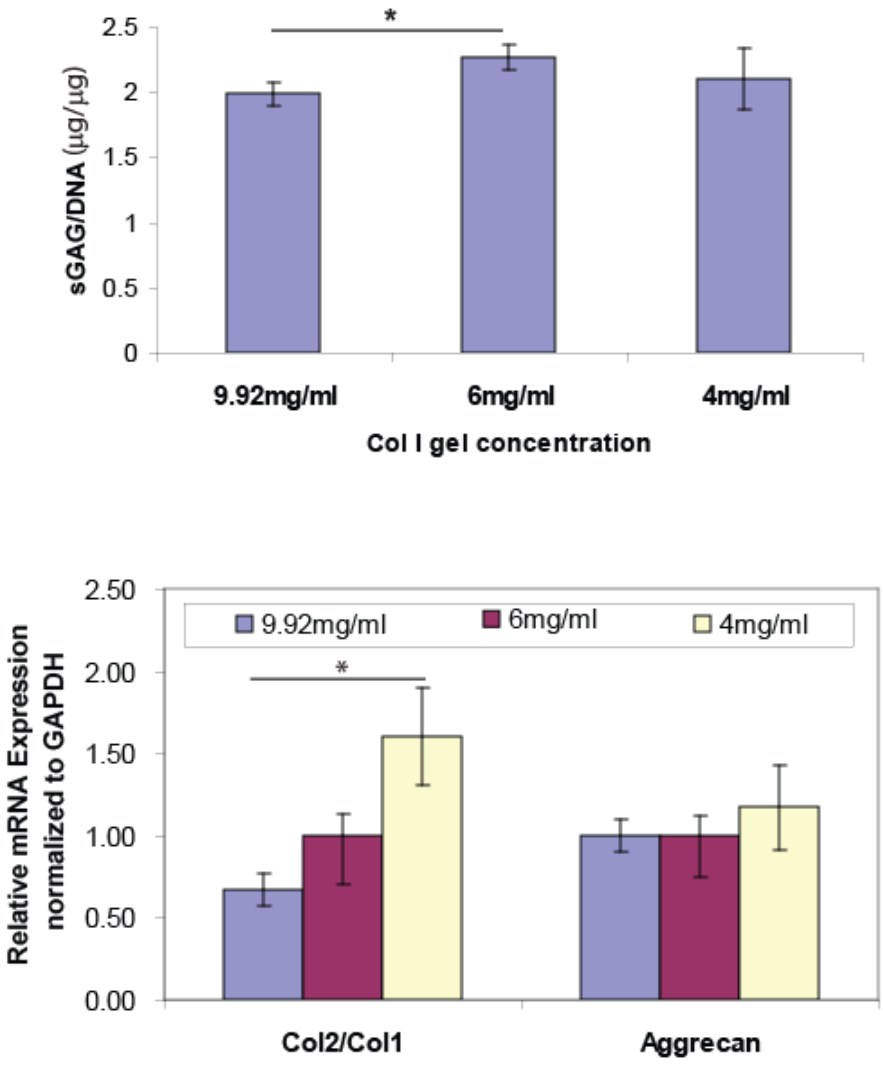

Figure 5.1: The effects of collagen I gel concentration on porcine chondrocytes for 7 days are evaluated by quantification of sGAG/DNA and mRNA expressions. The content of sGAG/DNA (top) represents the overall matrix production for different concentration of collagen I gels (N=4-5, *p≤0.05, One way ANOVA). The relative mRNA expression (bottom) is normalized to endogenous GAPDH for different collagen I gel concentrations (N=4-5, *p≤0.05, One way ANOVA).

However in mRNA gene expression (Figure 5.1 (bottom)), lower concentrations of Col I gels caused less de-differentiation indicated by an increasing trend of the ratio of collagen 2 gene expressions to collagen 1 gene expression of cells (Col2/Col1, known as "chondrocyte differentiation index (DI) [23,24]). Aggrecan expression was not significantly affected by Col I concentration although the 4mg/ml concentration showed a trend for higher aggrecan expression. Overall, 4mg/ml seemed to be the best concentration out of three concentrations and our results showed that lower Col I gel is preferred by chondrocytes in terms of differentiation. However, the gelation time of 4mg/ml collagen I gel was too long to keep cells evenly distributed from top to bottom (cells tended to sink down at the bottom before complete gelation), thus we decided to use 6mg/ml instead of 4mg/ml still for evenly distributed cell seeding in 3D POC scaffolds.

Scaffold design, fabrication, and Mechanical characterization

Three dimensional (3D) scaffolds were fabricated from poly (1, 8 Octanediol-co-citrate) (POC), which imparted variations in pore shape (either spherical or cubical) while maintaining a consistent pore size and a regular interconnectivity (Table 5.1). Example scaffolds are shown in Figure 5.2. For description purposes, the scaffolds with a cubical pore design and 62% porosity are labeled C62, and the scaffolds with a spherical pore design and 50% porosity are labeled S50.

Table 5.1- Scaffold Descriptions

Design Name (N=8)	S50, Low*	C62, High*
Porosity (%)	50 ± 1.62	62 ± 2.36
Permeability without gel (10^{-7} m^4/N·s)**	3.51 ± 0.95	47.4 ± 1.15
Permeability with gel (10^{-7} m^4/N·s)**	1.72 ± 0.45	4.14 ± 0.73
Surface Area (mm^2)***	288 ±38	243 ± 15
Pore Shape	Spherical	Cubical
Pore Size	900μm	900μm

*Note that design names are based on its pore shape and porosity, for example 'S' in S50 is from 'spherical pore shape' and '50' indicates its porosity. It is the same for C62 with 'C' from 'cubical pore shape.' Low and high are based on relative permeabilities.
** Significant ($p \leq 0.05$, t-test)
*** Not significant ($p \leq 0.05$, t-test)

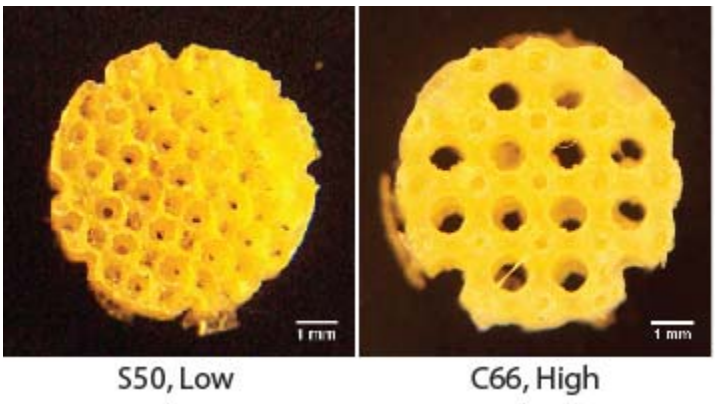

Figure 5.2: Digital pictures of two different scaffold designs

By varying pore shape and porosity, fabricated scaffold permeability was significantly different between designs (Low = 3.51 ± 0.95 × 10^{-7} m^4/N s (S50), High = 47.4 ± 1.15 ×10^{-7} m^4/N s (C62, 13.6 × Low) (t-test, $p \leq 0.05$)). With collagen I/HyA hydrogel, scaffold permeability values all decreased from the original scaffold permeability as expected yet continued to exhibit a similar trend between designs (Low, High = 2.4 × Low). Since collagen gels degrade typically in a week, permeability without gel most likely represents the permeability of scaffolds at 2-4 weeks without tissue ingrowth whereas permeability with gel represents the scaffolds at 0 wk with initial cell

seeding. Thus, permeability is dynamically changing within the 4 week period. However it is likely that the trend of different permeability between the different designs remains. Table 5.2(a) and (b) summarize the nonlinear model fit coefficients and compressive tangent moduli for different scaffold designs.

Table 5.2(a) - $T = A*(e^{B\varepsilon}-1)$ Nonlinear model fit coefficients & Tangent Moduli

Empty Scaffolds	Nonlinear model Coefficients		
Design\Coefficients or Strain (%)	A	B	fval
S50	0.11 ± 0.03	1.89 ± 0.36	8.88E-04
C62	0.013 ± 0.004	4.34 ± 0.58	6.92E-04

Table 5.2(b) - Tangent Moduli (MPa) at 1, 10, 30% Strain

Design\Strain (%)	1	10	30
S50	0.199 ± 0.010	0.235 ± 0.004	0.344 ± 0.019
C62	0.057 ± 0.014	0.085 ± 0.021	0.201 ± 0.048

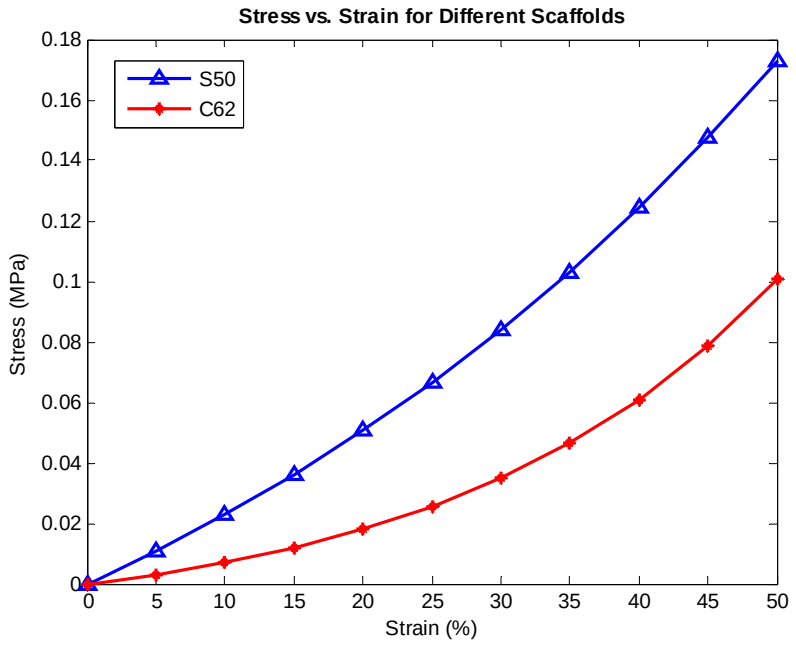

Figure 5.3(a): Comparison of compressive stress vs. strain model fit for low (S50) and high (C62) permeable scaffold designs

As Figure 5.3(a) shows, the more porous scaffold, the more linear behavior with lower stiffness representing the reduction of POC material (which is nonlinear elastic) supporting load. Unlike the relation between porosity and stiffness, there was no significant trend or relation between permeability and scaffold stiffness.

Table 5.3(a) - Model fit for scaffolds with cells:
control (gel, no cell) vs. scaffolds (gel + cell) for 2, 4wk (fval is within 0.000-0.005 so not shown)

Scaffold Design\conditions (N=4)	Control		Cells	
	A	B	A	B
S50 2wk	0.003 ± 0.001	6.51 ± 1.08	0.060 ± 0.014	2.24 ± 0.41
C62 2wk	0.003 ± 0.000	6.55 ± 0.37	0.024 ± 0.027	4.13 ± 2.08
S50 4wk	0.023 ± 0.006	3.79 ± 0.23	0.28 ± 0.33	3.00 ± 1.15
C62 4wk	0.011 ± 0.005	4.55 ± 1.26	0.114 ± 0.175	3.35 ± 1.65

Table 5.3(a) and (b), and Figure 5.3(b - c) summarize nonlinear model fit coefficients and compare compressive tangent moduli for different scaffold designs with or without cells at different time points (2 and 4 weeks).

Table 5.3(b) - Tangent Moduli at 10% Strain

Scaffold Design(N=4)\conditions	Control	Cells
S50 2wk	0.038 ± 0.006	0.161 ± 0.005
C62 2wk	0.042 ± 0.003	0.095 ± 0.061
S50 4wk	0.125 ± 0.027	0.550 ± 0.045
C62 4wk	0.072 ± 0.002	0.156 ± 0.055

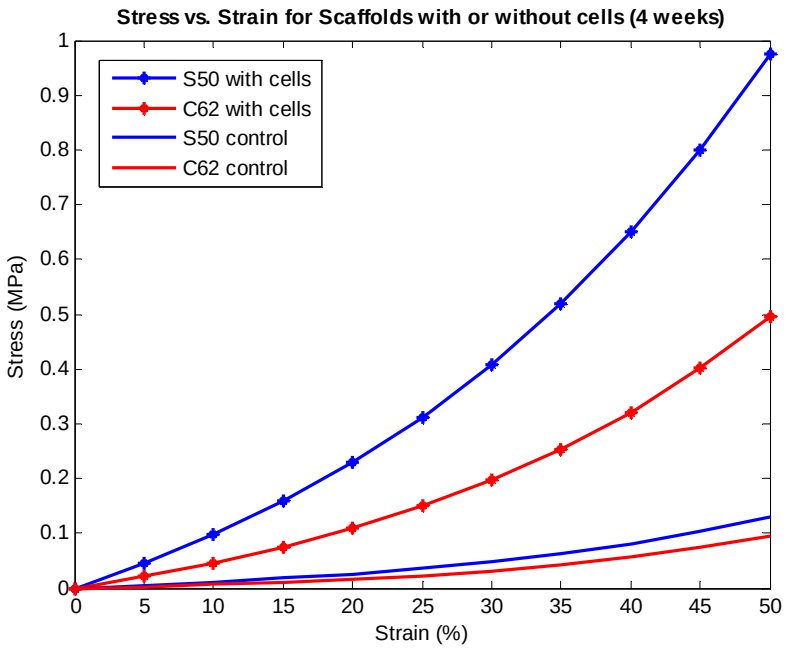

Figure 5.3(b) Comparison of compressive stress vs. strain model fit of different scaffold designs for with or without cells (control) at 4 week time point. Control represents scaffolds that were NOT seeded with cells yet they were subjected to degradation by culture media over 4 weeks whereas scaffolds with cells represent that cells were seeded onto scaffolds and were subject to both degradation and tissue formation for 4 weeks.

Control here represents scaffolds seeded with gels only which were subjected to the same conditions as those scaffolds seeded with cells/gels. At 2 weeks, there was no significant difference in control vs. cell seeded scaffolds, however at 4 weeks both designs with cells have shown a significant increase in tangent moduli compared to control scaffolds (Figure 5.3b). The lower permeability (S50) scaffold design showed a higher increase (~10 times) in tangent moduli from control and this is probably due to the faster tissue formation rate over scaffold degradation rate compared to the higher permeable design (C62). It is also interesting to see that as more tissue formed, the mechanical behavior became more nonlinear with higher strain stiffening.

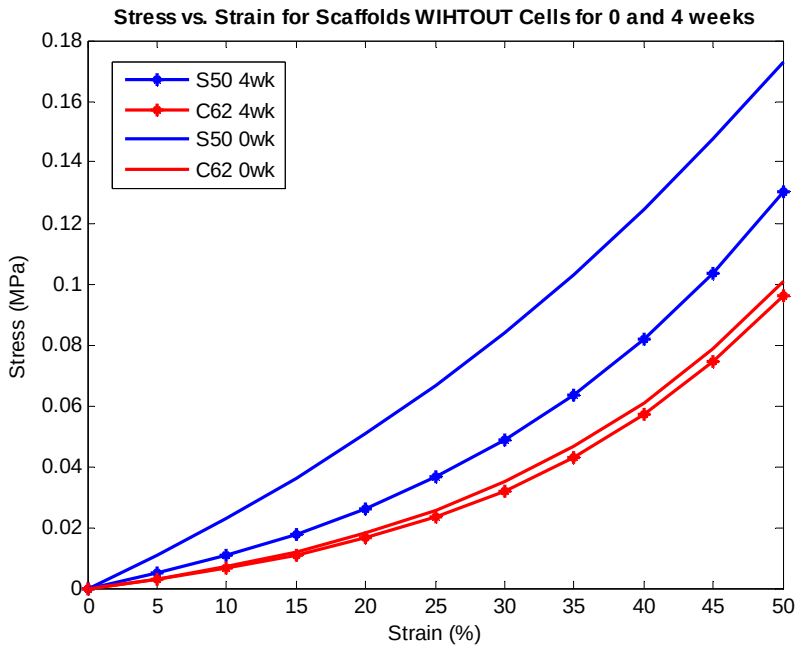

Figure 5.3(c): Comparison of compressive stress vs. strain model fit for different scaffold designs at 0 and 4 week time points without cells (control). This represents a sole degradation effect on mechanical strength of the scaffolds. High permeable design (C62) causes less acid accumulation resulting in slower and less degradation overall.

Figure 5.3c showed the effects of architectural scaffold design on scaffold degradation when no cells were involved; it is interesting that low permeability design decreased its stiffness significantly over 4 weeks but not the high permeability design. From 2 weeks to 4 weeks, both designs increased in stiffness and nonlinearity indicating active tissue formation inside scaffold pores for those two weeks period. Overall, all three figures (5.3b-d) suggest that tissue formation is dominant over scaffold degradation in determining overall scaffold/tissue construct mechanical properties up to 4 weeks, especially in the low permeable design.

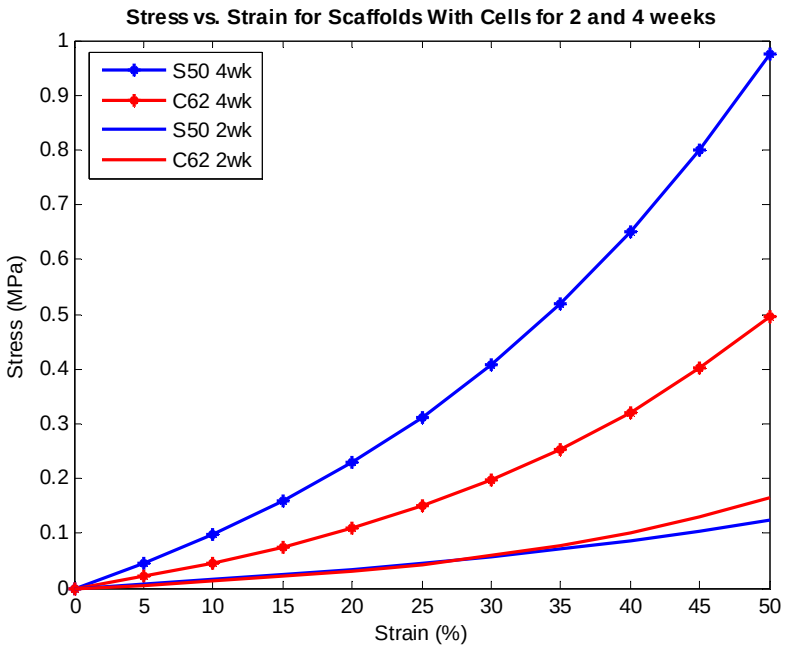

Figure 5.3(d): Comparison of compressive stress vs. strain model fit for different scaffold designs at 2 and 4 week time points with cells. More matrix formation and lower permeability reformed by tissues result in increases in mechanical strength of tissue/scaffold construct. Greater increase in stiffness of low permeable design (S50) represents more tissue formed, which is reflective of sGAG/DNA content shown in Figure 5.4.

In vitro cell culture - matrix production and mRNA expression

Chondrocytes proliferated and produced cartilaginous matrix during the 2 and 4 weeks *in vitro* culture periods (Figure 5.4). The low permeable design (S50) attained significantly higher sGAG/DNA content at both time points and showed a significant increase of sGAG/DNA content from 2 to 4 weeks (39.62 -> 55.94, ~140% increase) whereas the high permeable design (C62) did not show a significant increase in matrix production from 2 to 4 weeks. An increase in sGAG/DNA content implies that a single cell is more geared towards chondrocytic phenotype with more matrix production. At 2 weeks sGAG/DNA content of S50 was 1.6 times higher than that of C62 and at 4 weeks sGAG/DNA content of S50 was 2.3 times higher than that of C62.

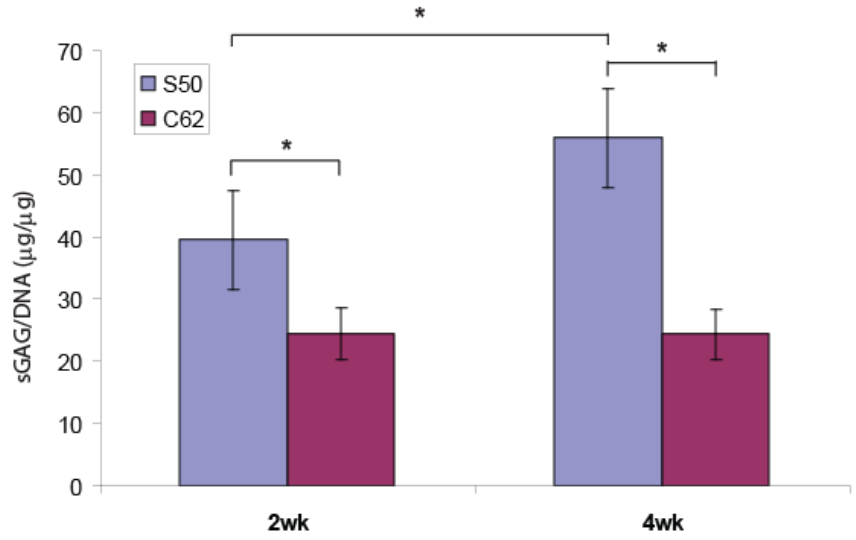

Figure 5.4: The representation of scaffold matrix production for different architectures: The sGAG/DNA content was normalized to that of 0wk. (N=7-8, One way ANOVA, *p≤0.05)

Quantitative-PCR was used to measure the messenger RNA expression for collagens by cells and for aggrecan found in cartilage at 4 week time point (Figure 5.5). The collagen types II, IX, XVIII, & Q and the proteoglycans aggrecan, fibromodulin, & chondroadherin are considered to be markers of differentiation with the increase in relative mRNA expression levels, while the collagen types I, III, IV, & XI, and the proteoglycans biglycan, decorin, & versican are suggested to be markers of dedifferentiations with the increase in relative mRNA expression levels. The ratio of collagen type II/I or aggrecan/versican is therefore proposed as a differentiation index (DI).[31] Only Col2/Col1 (DI) and Col10 expression showed a significant difference between two designs, yet we can certainly see a trend with other gene expressions as well. The main components of healthy articular cartilage are a highly organized network of collagens and proteoglycans. Type II collagen is the main collagen type of hyaline cartilage responsible for the stability and cell biological functions of healthy articular

cartilage[32], accounting for 90–95% of the overall collagen content and determining mechanical behavior [25] hence it is often used as a marker for cartilaginous like tissues. When Type II collagen is destroyed, it is replaced with a type I collagen fibro-cartilage that does not have the same functional properties as type II collagen and again this is why DI is frequently used as a marker for chondrocytic differentiation. The low permeable design (S50) showed higher collagen 2 and lower collagen 1 expression resulting in DI to be 1.6 times higher than the DI of the high permeable design (C62) implying that the low permeable scaffold design yielded more hyaline-like cartilage (or less fibro-cartilage) than the high permeable scaffold design.

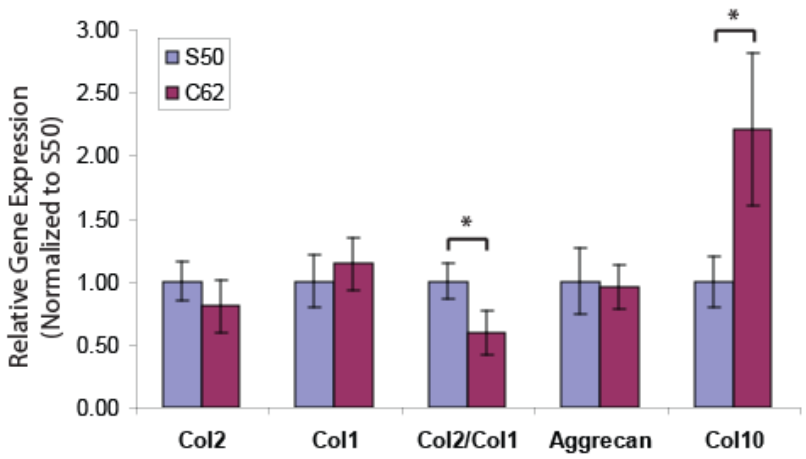

Figure 5.5: Relative mRNA expression ratio comparisons between different scaffold designs at 4 weeks: mRNA expression levels were first normalized to endogenous GAPDH then further normalized to S50 for comparison (N = 8-10, t-test, * $p \leq 0.05$).

Aggrecan is the main proteoglycan found in cartilage, and is a typical marker of differentiated chondrocytes along with collagen II. Even though the aggrecan expressions of both designs were not significantly different, S50 was slightly higher than C62. Type X collagen serves as a marker of the terminally differentiated (hypertrophic) chondrocyte phenotype, and detection of the type X collagen gene transcript and translation product

are useful for studies of chondrocyte growth and de-differentiation [26,27]. The type X collagen expression of C62 was significantly higher than that of S50 (2.2 times higher than S50) implying a greater tendency to hypertrophy.

Histology

Safranin-O staining (Figure 5.6) supported the sGAG quantification data such that low permeable design (S50) showed a larger area of sGAG staining overall and each pore was more packed with sGAG containing tissues. Also, even for outer layer tissues formed around the edges of scaffolds, low permeable design had darker sGAG staining with more vivid chondrocytic cell phenotypes (i.e. round shape with lacuna) than high permeable design, consistent with the results in Figure 5.4.

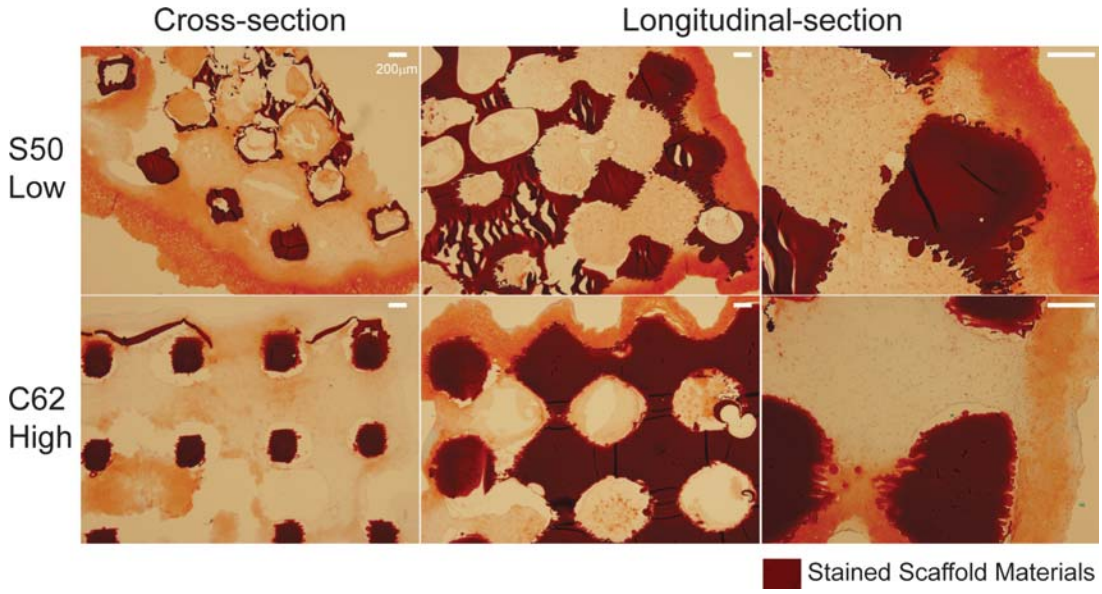

Figure 5.6: Safranin-O/Fast-Green staining of scaffolds at 4 weeks: more chondrocytic cells with vivid lacunae and darker sGAG staining were present in the low permeable design with spherical pore shape (S50). All the sections were taken from the center of the scaffolds cross-sectionally and longitudinally.

5.4 Discussion and Conclusion

There are many structural parameters which characterize and affect the overall function and performance of 3D scaffolds including pore size, porosity, pore shape, degrees of interconnectivity, and scaffold surface area. Each of these structural parameters influences permeability and their aggregate combination determines the final permeability, which in turn affects mass transport. Because of these interrelated structural parameters, it is almost impossible to look at a sole effect of one structural parameter on cartilage regeneration [28]. In our study, we designed scaffolds such that pore size, surface area and degrees of interconnectivity were rigorously controlled within narrow ranges. Thus, the effects of porosity, pore shape and surface area on permeability and mass transport were minimized. In our previous study [2], we examined the effects of scaffold permeability on chondrogenesis by varying both porosity and surface area within a spherical pore shape. This study demonstrated that scaffolds with reduced permeability improved in vitro chondrogenesis by primary chondrocytes. However, since permeability was decreased by changing the spherical neck connection size, lower permeable scaffolds would have increased surface area. Although we postulated that surface area was not a major factor in that study since the chondrocytes were not seen on histology to attach to the scaffold surface, it nonetheless raises the question as to whether increased surface area played a role in the increased chondrogenesis with decreased permeability.

In this work, we designed scaffolds to examine the effects of permeability due to pore shape while eliminating surface area as a potential confounding factor. In addition, the porosity difference between the two designs was minimal (1.2 x between designs) compared to the permeability differences (13.5x between designs). Thus, in this work,

we have isolated the major differences in scaffold architecture to permeability and pore shape (cylindrical versus spherical). Since the overall impact of scaffold design on cartilage regeneration should not just be measured in terms of cartilage matrix production and gene expression, we also determined how scaffold architecture affected scaffold degradation and scaffold mechanical behavior with and without seeded cells. Scaffold behavior with seeded cells obviously represents the overall mechanics of the scaffold/regenerated tissue construct.

The lower permeability with spherical pore shape design scaffold (S50) led to increased cartilage matrix production and increased cartilage gene expression (Figure 5.4, 5.5, and 5.6). The spherical pore shape may have helped creating denser cell aggregation within the pore volume, conditions that would be favorable to chondrogenesis. In addition, as we have earlier suggested [2], lower permeability may enhance chondrogenesis due to decreases in oxygen tension and lower reactive oxygen species (ROS) around cells that results from lower permeability and higher cell concentration. Finally, lower permeable design may demonstrate enhanced cartilage matrix production due to retained sGAG molecules that could diffuse out from lower permeable designs. These three factors, 1) increased cell aggregation, 2) decreased O_2 tension resulting from lower permeability, and 3) increased sGAG retention in lower permeable designs, could all contribute to enhanced chondrogenesis in the spherical pore shapes. Thus, the spherical pore shape may enhance chondrogenesis due to its unique capability of generating a larger pore volume for cell aggregation while maintaining low permeability for sGAG retention and low O_2 tension.

In addition to significantly affecting cartilage matrix production, scaffold architecture design had significant affects on scaffold mechanics (empty without cells) and scaffold degradation (empty without cells). Architecture design significantly affected the inherent effective nonlinear elastic properties. Despite having only 12% less porosity, the stiffness of the S50 (low permeable) design as measured by tangent modulus (Figure 5.3a and Table 5.2b) was from 1.5 to 4 times greater than the C62 (high permeable) design depending on strain magnitude. The C62 design exhibited greater nonlinear behavior, as seen in Figure 5.3a and as demonstrated that the larger B coefficient in the nonlinear elastic model $\sigma = A(e^{b\varepsilon}-1)$, where a higher B coefficient indicates greater nonlinear behavior. Thus, it is clear that 3D arrangement of material greatly affects the stiffness and nonlinearity of scaffold mechanics for nonlinear elastomers like POC, even when the amount of material used in the scaffolds is very similar.

Architecture design greatly influenced *in vitro* scaffold degradation as well (Figure 5.3c). The S50 design without cells demonstrated a significant decrease in effective tangent moduli, but the nonlinearity of the stress-strain curve increased. The C62 design demonstrated slight overall decrease in tangent moduli between 0 and 4 weeks, although the nonlinearity appeared unchanged. These mechanical results would suggest a significant change in polymer crosslinking and molecular weight for the S50 (Low) design, but not for the C62 (High) design. Again, given that the amount of material is similar between designs, it is likely the arrangement of material in 3D space as well as the permeability that most influenced degradation.

Of significant interest for eventual *in vivo* application is the combined effect of cartilage matrix production and scaffold material degradation on overall scaffold/tissue construct mechanical properties. Here again, there is a significant influence of scaffold architecture design. There is a tremendous increase in both the stiffness (tangent moduli) and nonlinearity of both designs with seeded cells, although the increase is even more dramatic for the S50 design. This reflects the greater increase in cartilaginous matrix within the S50 design over the C62 design. This increased cartilaginous matrix is reflected in the increased mRNA expression (Figure 5.5), sGAG/DNA quantification data (Figure 5.4) and sGAG staining of different scaffold designs (Figure 5.6). Higher expressions of collagen 2 and aggrecan and lower expressions of collagen 1 creating a higher differentiation index (higher collagen 2 to collagen 1 ratio), coupled with low collagen 10 expression of low permeable design (S50) are all positive indications of higher chondrocytic differentiation and matrix production, and less hypertrophy. Damage to the collagen type II meshwork is reported as a critical event in the early development and pathology of osteoarthritis[33] and some previous *in vitro* studies[34, 35] have shown a significant switch in production from collagen type II to collage type I in de-differentiating chondrocytes in cell culture[32]. The high permeable design (C62) seemed to cause more rapid de-differentiation marked by higher expression of collagen 1 with high tendency towards hypertrophy. Thus, in both cases, the ability to rapidly generate cartilage matrix within the pores more than overcame the material degradation effects on mechanical properties.

The final component in our system that can affect cartilage matrix production is the cell seeding gel. The use of collagen gels allows cells to be evenly seeded through

the 3D architecture. Our results (Figure 5.1) showed that lower collagen I gel concentration provided a more preferable microenvironment for porcine chondrocytes in terms of matrix production and chondrocytic differentiation and this founding becomes more important and useful when collagen I gel is used as a primary scaffold. This can be explained by comparing to the environments of chondrocytes in normal cartilage. Chondrocytes are known to be sensitive to the macromolecular organization of collagen fibrils and the spherical chondrocytes in normal cartilage are surrounded by a network of hyaluronan and glycosaminoglycan molecules containing Type II collagen fibrils [29,30]. The abundance of Type I collagen instead of hyaluronan, glycosaminoglycan, and Type II collagen surrounding chondrocytes may have led to morphological changes of chondrocytes and unbalanced ECM demonstrating that lower content of collagen I gel was actually better in production and maintenance of matrix (sGAG) than higher content of collagen I gel.

Our study clearly shows that chondrocytes prefer lower permeable scaffolds in terms of matrix production and differentiation; pore shape not only plays a role in determining effective scaffold permeability but also it may play an additive role ensuring abounded pore space for enhancing cell aggregation and sGAG retention. The enhanced cartilage matrix production in the low permeable design resulted in superior mechanical properties for the scaffold/tissue construct for this design. In addition, designed pores architecture significantly influenced empty scaffold degradation kinetics in addition to effective mechanical and permeability properties. The results of this study motivate further investigation to separate pore shape and permeability effects on chondrogenesis. It further suggests that designed scaffold architecture is a component affecting the

success or failure of tissue engineered cartilage that should be further studied in appropriate *in vivo* cartilage defect models.

Acknowledgements

This work was funded in part by a NIH grant R01 AR 053379. The authors thank Gregory A. Bratkovich and Carolyn Slope for help with scaffold fabrication and cell harvest, Huina Zhang for advices with data analysis, and Chris Strayhorn for assistance with histology.

References

1. Liao, E., Yaszemski, M., Krebsbach, P., and Hollister, S. Tissue-engineered cartilage constructs using composite hyaluronic acid/collagen I hydrogels and designed poly(propylene fumarate) scaffolds. Tissue engineering 13, 537, 2007.

2. Kemppainen, J.M., and Hollister, S.J. Differential effects of designed scaffold permeability on chondrogenesis by chondrocytes and bone marrow stromal cells. Biomaterials 31, 279, 2010.

3. Yamane, S., Iwasaki, N., Kasahara, Y., Harada, K., Majima, T., Monde, K., Nishimura, S., and Minami, A. Effect of pore size on in vitro cartilage formation using chitosan-based hyaluronic acid hybrid polymer fibers. Journal of biomedical materials research.Part A 81, 586, 2007.

4. Alves da Silva, M.L., Crawford, A., Mundy, J.M., Correlo, V.M., Sol, P., Bhattacharya, M., Hatton, P.V., Reis, R.L., and Neves, N.M. Chitosan/polyester-based scaffolds for cartilage tissue engineering: Assessment of extracellular matrix formation. Acta biomaterialia, 2009.

5. Lien, S.M., Ko, L.Y., and Huang, T.J. Effect of pore size on ECM secretion and cell growth in gelatin scaffold for articular cartilage tissue engineering. Acta biomaterialia 5, 670, 2009.

6. Woodfield, T.B., Malda, J., de Wijn, J., Peters, F., Riesle, J., and van Blitterswijk, C.A. Design of porous scaffolds for cartilage tissue engineering using a three-dimensional fiber-deposition technique. Biomaterials 25, 4149, 2004.

7. Bhardwaj, T., Pilliar, R.M., Grynpas, M.D., and Kandel, R.A. Effect of material geometry on cartilagenous tissue formation in vitro. Journal of Biomedical Materials Research 57, 190, 2001.

8. Yang, S., Leong, K.F., Du, Z., and Chua, C.K. The design of scaffolds for use in tissue engineering. Part I. Traditional factors. Tissue engineering 7, 679, 2001.

9. Liao, E., Yaszemski, M., Krebsbach, P., and Hollister, S. Tissue-engineered cartilage constructs using composite hyaluronic acid/collagen I hydrogels and designed poly(propylene fumarate) scaffolds. Tissue engineering 13, 537, 2007.

10. Liao, E.E. Enhancement of chondrogenesis by directing cellular condensation through chondroinductive microenvironments and designed solid freeform fabricated scaffolds. , 2007.

11. Yang, J., Webb, A.R., Pickerill, S.J., Hageman, G., and Ameer, G.A. Synthesis and evaluation of poly(diol citrate) biodegradable elastomers. Biomaterials 27, 1889, 2006.
12. Kang, Y., Yang, J., Khan, S., Anissian, L., and Ameer, G.A. A new biodegradable polyester elastomer for cartilage tissue engineering. Wiley Periodicals, Inc. published online (www.interscience.wiley.com), 2006.

13. Jeong, C.G., and Hollister, S.J. Mechanical, Permeability, and Degradation Properties of 3D Designed Poly(1,8 Octanediol-co-Citrate)(POC) Scaffolds for Soft Tissue Engineering. Journal of Biomedical Materials Research: Part B , 2010 Jan 20.

14. Hollister, S.J., Maddox, R.D., and Taboas, J.M. Optimal design and fabrication of scaffolds to mimic tissue properties and satisfy biological constraints. Biomaterials 23, 4095, 2002.

15. Hollister, S.J. Porous scaffold design for tissue engineering. Nature materials 4, 518, 2005.

16. Kim, K., Jeong, C.G., and Hollister, S.J. Non-invasive monitoring of tissue scaffold degradation using ultrasound elasticity imaging. Acta biomaterialia 4, 783, 2008.

17. Taboas, J.M., Maddox, R.D., Krebsbach, P.H., and Hollister, S.J. Indirect solid free form fabrication of local and global porous, biomimetic and composite 3D polymer-ceramic scaffolds. Biomaterials 24, 181, 2003.

18. Kemppainen, J.M. Mechanically stable solid freeform fabricated scaffolds with permeability optimized for cartilage tissue engineering. , 2008.

19. Liao, E., Yaszemski, M., Krebsbach, P., and Hollister, S. Tissue-engineered cartilage constructs using composite hyaluronic acid/collagen I hydrogels and designed poly(propylene fumarate) scaffolds. Tissue engineering 13, 537, 2007.

20. Farndale, R.W., Buttle, D.J., and Barrett, A.J. Improved quantitation and discrimination of sulphated glycosaminoglycans by use of dimethylmethylene blue. Biochem Biophys Acta 883, 173-7, 1986.

21. Chandrasekhar, S., Esterman, M.A., and Hoffman, H.A. Microdetermination of proteoglycans and glycosaminoglycans in the presence of guanidine hydrochloride. Analytical Biochemistry 161, 103, 1987.

22. Kim, Y.J., Sah, R.L., Doong, J.Y., and Grodzinsky, A.J. Fluorometric assay of DNA in cartilage explants using Hoechst 33258. Analytical Biochemistry 174, 168, 1988.

23. Martin, I., Jakob, M., Schafer, D., Dick, W., Spagnoli, G., and Heberer, M. Quantitative analysis of gene expression in human articular cartilage from normal and

osteoarthritic joints. Osteoarthritis and cartilage / OARS, Osteoarthritis Research Society 9, 112, 2001.

24. Martin, I., Jakob, M., Schafer, D., Dick, W., Spagnoli, G., and Heberer, M. Quantitative analysis of gene expression in human articular cartilage from normal and osteoarthritic joints. Osteoarthritis and cartilage / OARS, Osteoarthritis Research Society 9, 112, 2001.

25. Bruckner, P., and van der Rest, M. Structure and function of cartilage collagens. Microscopy research and technique 28, 378, 1994.

26. Bohme, K., Conscience-Egli, M., Tschan, T., Winterhalter, K.H., and Bruckner, P. Induction of proliferation or hypertrophy of chondrocytes in serum-free culture: the role of insulin-like growth factor-I, insulin, or thyroxine. The Journal of cell biology 116, 1035, 1992.

27. Shen, G. The role of type X collagen in facilitating and regulating endochondral ossification of articular cartilage. Orthodontics & craniofacial research 8, 11, 2005.

28. Li, S.H., de Wijn, J.R., Layrolle, P., and de Groot, K. Accurate geometric characterization of macroporous scaffold of tissue engineering. Bioceramics 240–2, 541–545, 2003.

29. Farjanel, J., Schurmann, G., and Bruckner, P. Contacts with fibrils containing collagen I, but not collagens II, IX, and XI, can destabilize the cartilage phenotype of chondrocytes. Osteoarthritis and cartilage / OARS, Osteoarthritis Research Society 9 Suppl A, S55, 2001.

30. Terada, S., Yoshimoto, H., Fuchs, J.R., Sato, M., Pomerantseva, I., Selig, M.K., Hannouche, D., and Vacanti, J.P. Hydrogel optimization for cultured elastic chondrocytes seeded onto a polyglycolic acid scaffold. Journal of biomedical materials research.Part A 75, 907, 2005.

31. Schulze-Tanzil, G. Activation and dedifferentiation of chondrocytes: implications in cartilage injury and repair. Ann Anat. 2009; 191; 325-338.

32. Hagiwara, Y., Ando, A., Chimoto, E., Tsuchiya, M., Takahashi, I., Sasano, Y. et al. Expression of collagen types I and II on articular cartilage in a rat knee contracture model. Connect Tissue Res. 2010;51(1):22-30.

33. Henrotina, Y,. Addisonb, S., Krausb, V., and Deberg, M. Type II collagen markesr in osteoarthritis: what do they indicate? Curr. Opin. Rheumatol., 2007; 19, 444-450.

34. Layman, D.L., Sokoloff, L., and Miller, E.J. Collagen synthesis by articular chondrocytes in monolayer culture. Exp. Cell, Res. 1972; 73, 107-112.

35. Von der Mark, K., Gauss, V., von der Mark, H., and Muller, P. Relationship between cell shape and type of collagen synthesized as chondrocytes lose their cartilage phenotype in culture. Nature, 1977; 267, 531-532.

CHAPTER 6

THE EFFECTS OF 3D POC SCAFFOLD PORE SHAPE AND PERMEABILITY ON *IN VIVO* CHONDROGNESIS

6.1 Introduction

Current therapeutic strategies such as microfracture, osteochondral transplantation and autologous chondrocyte implantation (ACI) have been applied with relative success for more than a decade, yet are still limited to small defect sizes, and suffer from donor-site morbidity restricting their clinical application [1-5]. These limitations have increased interest in tissue engineering approaches combining degradable biomaterial scaffolds with or without cell therapy. While it is widely postulated that scaffolds play a major role in the success or failure of cartilage repair, there is very limited data on how scaffold architecture and material should be designed to enhance cartilage repair using tissue engineered approaches. Specifically, the mechanical and mass transport environments provided to seeded cells or host cells by implanted scaffolds may significantly affect cell activity, dictating the outcome of cartilage repair. These environments are determined by scaffold structural parameters including pore geometry, pore size, porosity, pore interconnectivity, etc. To create scaffolds that enhance chondrogenesis, we must first be able to test hypotheses concerning how scaffolds design affects chondrogenesis, which requires fabricating scaffolds with controlled architectures. In this chapter, we have taken one step further from chapter 5 to implant pre-cultured chondrocytes/ poly (1, 8 Octanediol-co-Citrate) (POC) scaffold constructs *in vivo* subcutaneously to examine the

coupled effects of designed pore shape and permeability on matrix production, mRNA gene expression, and differentiation of chondrocytes *in vivo*, as well as the resultant mechanical property changes of scaffold/tissue constructs due to tissue formation and scaffold degradation. As thoroughly illustrated in chapter 4 and 5, POC has been shown to support cell attachment, proliferation, and matrix production with chondrocytes [6] and POC scaffolds had compressive mechanical properties similar to native articular cartilage (Table 6.2) [8].

Our previous work[7, 9-11] demonstrated that a low permeable design with a spherical pore shape promotes chondrogenesis *in vitro* for different materials using chondrocytes and the *in vitro* study of POC scaffolds in chapter 5 also showed that chondrocytes responded more favorably towards the low permeable design with a spherical pore shape. The purpose of this part was to investigate whether low permeable spherical pore designs also supported enhanced chondrogenesis *in vivo* at an ectopic site. Specifically, we tested the hypothesis that POC scaffolds designed with a spherical pore shape and low permeability would enhance chondrogenesis *in vivo* in a sub-cutaneous model as well. Chondrogenesis in chondrocytes seeded POC scaffolds was assessed by cartilaginous matrix production, cartilage specific gene expression and tissue/scaffold compressive mechanical properties, including how tissue formation and scaffold degradation interact in determining final construct mechanics in the same way we evaluated chondrogenesis in chapter 5 for the *in vitro* study. For this purpose, we first cultured seeded primary chondrocytes in designed POC scaffolds using collagen I/hyaluronic acid hydrogels as a cell carrier cultured for one week *in vitro*. These

cell/scaffold constructs were then implanted for six weeks *in vivo* in a sub-cutaneous model [12].

6.2 Materials and Methods

Collagen I/Hyaluronic Acid (Hya) Hydrogel

High concentration collagen I hydrogels and hyaluronic acid were purchased from BD Bioscience Discovery Labs (San Jose, CA) and Hyalogic LLC (Edwardsville, KS) respectively. High concentration collagen I hydrogels were diluted with 0.02N sterile acetic acid for 6mg/ml concentration and 5% (w/w) hyaluronic acid was combined with collagen I hydrogel based on our previous results that showed that collagen I gel with 5% hyaluronic acid enhanced chondrogenesis [12].

Synthesis of pre-Poly (1,8 Octanediol-co-Citrate) (POC)

All chemicals were purchased from Sigma-Aldrich (Milwaukee, WI). Poly (1, 8 Octanediol-*co*-Citrate) pre-polymer (pPOC) was synthesized as previously described [13]. Briefly, equimolar amounts of citric acid and 1,8-octanediol were added and the mixture was melted at 160–165 °C for 15 mins under a flow of nitrogen gas while stirring and then further lowered to 140 °C for 40 mins to create a pre-polymer.

Scaffold Design & Fabrication

3D POC scaffold architecture was designed using previous methods and software [12, 14-16]. Porous POC scaffolds (6.35mm Diameter, 4.0mm Height) with 900µm interconnected spherical or cubical pores (porosity: 50% (spherical (S50)), 62% (cubical (C62)), permeability: High (C62) = 13.5 x Low (S50)) were designed. The details of POC scaffold fabrication were the same as previously described in chapter 5 [13,16,17].

Mechanical Tests

Porous scaffolds (N=4-6/design/time), gel seeded scaffolds (N=4-6/design/time), or scaffolds with tissue in-growth (after *in vitro* pre-culture (=0 week *in vivo*) or 3 or 6 weeks of *in vivo* implantation, N=4-6/design/time) were tested in unconfined compression (Alliance RT/30 electromechanical test frame, 50N load cell with 0.5% error range, MTS Systems Corp., MN, data collected using TestWorks4 software) . MATLAB (The MathWorks Inc., MA) software (LSQNONLIN) was used to fit a nonlinear elasticity model, $\sigma = A[e^{B\varepsilon} - 1]$ to experimental data where σ is the 1st Piola-Kirchoff stress, ε is large strain and A and B are model coefficients. Tangent moduli ($=AB\, e^{B\varepsilon}$) were calculated at 10 % strain from the fit.

Porosity and Permeability Measurements & cell seeding

Porosity and permeability measurements were performed the same way as described in chapters 4 and 5. Scaffold permeability (N=6-7, each material) with and without composite HyA/collagen I (6mg/ml) gel and for tissue/scaffold constructs after 6 week *in vivo* implantation was measured using a permeability test set up[13, 18]. The cell seeding and gelation procedures were performed the same way as described in chapter 5.

In vitro pre-culture & In vivo implantation

Porcine chondrocytes were isolated from the joints of domestic pigs and seeded onto scaffolds following previous methods[12] with some modifications [12]. Cells were re-suspended at a density of ~$30x10^6$ cells/mL in 770µL of composite HyA/Col I with ~50µL of culture medium. The remaining steps were the same as previously described (chapter 5). Twenty four scaffolds per design (15/design for 6 week *in vivo* implantation, 9/design (*in vivo* 0 week)) seeded with pChon were pre-cultured with chondrogenic

medium (basal medium (DMEM, 10% fetal bovine serum (FBS), 1% P/S, Gibco) supplemented with 50 mg/mL 2-phospho-L-ascorbic acid (Sigma)), 0.4mM proline (Sigma), 5 mg/mL insulin (Gibco), and 0.1mM non-essential amino acids (Gibco)) in 12-well plates for 1 week before *in vivo* implantation. Chondrocytes were cultured under gentle agitations on an orbital shaker and the media was changed every other day. All POC scaffolds were sterilized in an autoclave, presoaked in DMEM for 24 hours and rinsed with PBS prior to cell seeding. For observing mechanical stiffness changes over time due to degradation gel seeded scaffolds with no cells (N = 4-6/design/time) were subjected to the same *in vitro* conditions as cell/gel seeded scaffolds.

After pre-culture *in vitro*, thirty cell-seeded POC scaffolds (15/design) and twenty gel-seeded POC scaffolds (no cell) (10/design: N = 4/design for 3 week, N=6/design for 6 week) were implanted subcutaneously in 6-8 week-old immuno-compromised mice (N:NIH-bg-nu-xid; Charles River, Wilmington, MA). The mice implantation procedure was following the methods previously published with some modifications[12]. Four dorsal subcutaneous pockets were created by blunt dissection, and a POC scaffold from each group (cell, no cell, spherical, cubical pores) was placed in each pouch and in a different pouch location in each mouse (Figure 1b) [12]. The animals were housed in groups with free access to food and water and killed after 3 or 6 weeks for evaluation.

sGAG and DNA quantification and Quantitative-PCR

The sGAG content of the dissolved solution at each time point (0 and 6 weeks *in vivo* implantation) for scaffolds (N=3/design 0 week, N=4/design 6 week) tested was assayed using the DMMB method and the total sGAG were normalized by DNA content which was measured using Hoechst dye 33258 method.[7, 19-21]

For quantitative-PCR, cartilage matrix specific genes (Type II collagen & aggrecan),chondrocyte de-differentiation marker genes (Type I & X collagen), matrix degradation indicator genes (matrix metalloproteinases 3 and 13 (MMP3, MMP13) and glyceraldehyde-3-phosphate dehydrogenase (GAPDH) gene expressions were determined by quantitative PCR (qtPCR) using a Gene Amp 7700 sequence detection system (Applied Biosystems, Foster City, CA USA) for scaffolds (N=4-6/design at each time point) after removal from culture *in vitro* or *in vivo* implantation following the procedures described in chapter 5. The quantity of gene expression was calculated with standard samples and normalized with GAPDH and then further normalized to low permeable design (S50) for easy comparison.

Histology

For histology, constructs (N=3/design) at each time point were fixed in 10% buffered formalin overnight, dehydrated with a series of graded ethanol, and embedded in paraffin. Tissue sections were stained with hematoxylin and eosin (H&E) for scaffolds without cells or Safranin-O/Fast Green counterstaining for scaffolds with cells, to assess cell and tissue distribution, cell morphology and sGAG production. Eight to ten slides (4 sections/slide) were obtained from the center of each scaffold (top to bottom and left to right) [12].

Statistical Analysis

Data are expressed as mean ± standard deviation. The statistical significance among different designs or time points was calculated using linear regressions and one way ANOVA with post-hoc comparison (Tukey) or student t-test using SPSS software (SPSS

for Windows, Rel 14.0. 2005 Chicago: SPSS Inc.). Data were taken to be significant when a *P*-value of 0.05 or less was obtained.

6.3 Results

Scaffold design and Permeability, Mechanical characterization

Three dimensional (3D) scaffolds were fabricated from poly (1, 8 Octanediol-co-citrate) (POC) using solid freeform fabrication methods. The scaffolds were designed with either a spherical or cubical pore shape, with resultant significant differences in permeability. Pore size and a regular interconnectivity were maintained between scaffold designs (Figure 6.1a, Table 6.1).

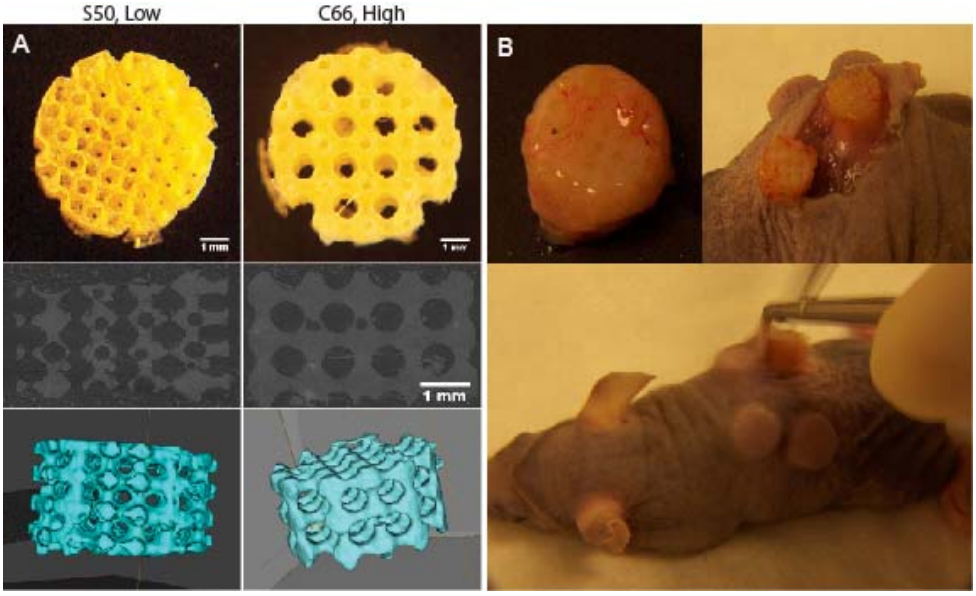

Figure 6.1: (a) scaffold design pictures (top: digital pictures, mid: center cut of side view of scaffold micro CT images, bottom: isosurfaced 3D scaffold microCT images) (b) a digital picture of a scaffold with tissues taken out of mice after 6 week *in vivo* implantation and digital pictures of scaffold removal from subcutaneous sites of mice

The fabricated scaffold permeability was the same as shown in chapter 5, which was significantly different between designs (Low = $3.51 \pm 0.95 \times 10^{-7}$ m^4/N s (S50),

High = 47.4 ± 1.15 $\times 10^{-7}$ m^4/N s (C62 (high) = 13.6 × S50 (Low)) (t-test, $p \leq .05$)). The difference in permeability is far greater than the difference in porosity (High = Low x 1.2). Surface area was also not significantly different between designs (S50 = 288 ± 38 vs. C62 = 243 ± 15 mm^3). Thus, among design parameters permeability and pore shape exhibited the greatest variations between designs.

Table 6.1- Scaffold Descriptions

Design Name (N=8)	S50, Low	C62, High
Porosity (%)	50 ± 1.62	62 ± 2.36
Permeability without gel (10^{-7} m^4/N·s)	3.51 ± 0.95	47.4 ± 1.15
Permeability with gel (10^{-7} m^4/N·s)	1.72 ± 0.45	4.14 ± 0.73
Permeability with tissues (in vivo) (10^{-7} m^4/N·s)*	0.52 ± 0.01	0.51 ± 0.01
Surface Area (mm^2)**	288 ±38	243 ± 15
Pore Shape	Spherical	Cubical
Pore Size	900μm	

* N=4/design, t-test, $p \leq 0.05$, not statistically significant (after 6 weeks of *in vivo* implantation)
** Not statistically significant (t- test, $p \leq 0.05$)

Even though both POC and gels are subjected to degradation, hydrogels degrade much faster than POC, being completely degraded by 1-2 weeks. Hence, the permeability without gels most likely represents the permeability of scaffolds during 6 weeks of *in vivo* implantation without tissue in-growth whereas permeability with gels represents the scaffolds at 0 wk with initial cell seeding. As most of collagen gels are degraded in a week during tissue formation, scaffold permeability is dynamically changing within the 6 week *in vivo* implantation period with scaffold degradation, tissue in-growth from seeded chondrocytes, and tissue formation around the scaffold by cells from mice. The permeabilities measured with tissues grown after 6 week *in vivo* implantation for both designs were significantly lower than the permeabilities with gels indicating extensive growth of tissue into scaffolds during *in vivo* implantation. The gel seeded scaffold permeability for the low permeable design (S50: 1.72 x 10^{-7} m^4/N·s) was 3.3 times higher

than the permeability of scaffold with tissue in-growth (0.52 x 10^{-7} $m^4/N{\cdot}s$), whereas that for the gel-seeded high permeable design (C62: 4.14 x 10^{-7} $m^4/N{\cdot}s$) was 8.1 times higher than the permeability of scaffold with tissue in-growth (0.51 x 10^{-7} $m^4/N{\cdot}s$). However, there was no significant difference in permeability between tissue/scaffold constructs between designs after 6 week *in vivo* implantation.

In order to observe mechanical stiffness changes due to scaffold degradation and tissue formation *in vivo*, we implanted gel seeded scaffolds (which are also cultured *in vitro* for 1 week before implantation) in mice and measured their stiffness at 0, 3, and 6 weeks *in vivo* to determine changes in effective nonlinear scaffold stiffness.

Table 6.2 - Tangent Moduli (MPa) at 10% strain

Time\Design (*In vivo* implantation, N=4-6)*	S50, Low		C62, High	
	without cells	with cells	without cells	with cells
0wk	0.059 ± 0.019	0.192 ± 0.047	0.054 ± 0.015	0.122 ± 0.022
3wk	0.531 ± 0.159	-	0.185 ± 0.026	-
6wk	0.525 ± 0.173	0.701 ± 0.131	0.202 ± 0.097	0.467 ± 0.092

* Note that all of the scaffolds were pre-cultured for 1 week *in vitro* with the same condition before *in vivo* implantation no matter whether the cells are present or not.

Table 6.2 summarizes compressive tangent moduli at 10% strain for different scaffold designs after applying the nonlinear model fit for gel seeded or tissue grown scaffolds at each time point. For both designs, the tangent modulus increased from 0 to 3 or 6 weeks when cells were not seeded. The low permeable design demonstrated greater increase over the 6 week implantation period (9 times vs. 3.4 times increase) than the high permeable design. There were no significant changes in stiffness from 3 to 6 week period for both designs. Unlike the case without cells, both designs with cells showed roughly the same increase (~3.8 x) in stiffness from 0 to 6 weeks *in vivo*. When comparing cases with and without cells, scaffolds with cells all showed higher mechanical stiffness.

In Figure 6.2a, the stress-strain curve presents the pattern of how the nonlinear mechanical stiffness curve changes over time for each design without cells. The stress-strain curve for low permeable design (S50) increases from 0 to 3 weeks whereas it drops down from 3 to 6 weeks. However, the curve for high permeable design (C62) keeps on increasing from 0 to 3 week and then from 3 to 6 weeks.

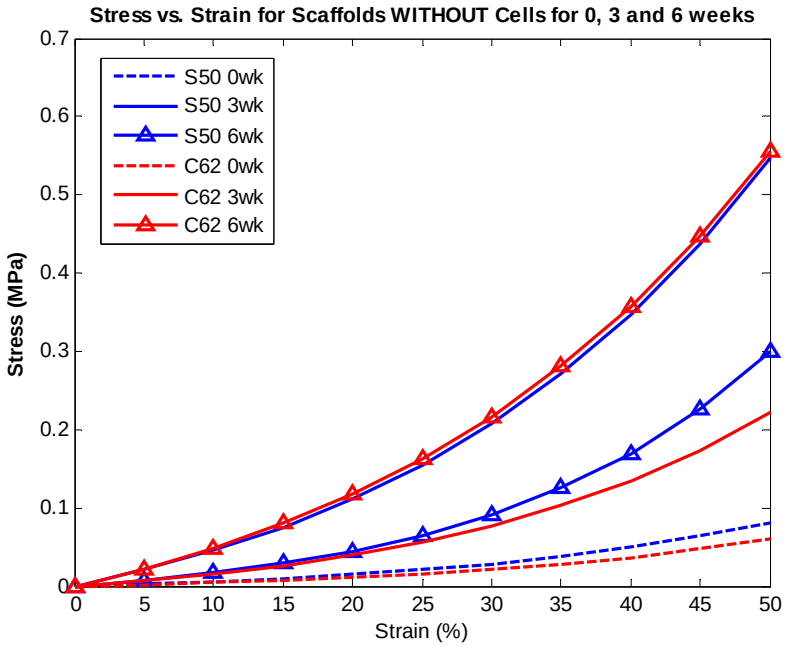

Figure 6.2(a): Comparison of compressive stress vs. strain nonlinear model fit for different scaffold designs at 0, 3 and 6 week time points without cell seeded *in vivo*. This represents a sole degradation effect on mechanical strength of the scaffolds with minor influences of fibroblastic cell infiltration of mice.

C62 (high) shows less nonlinear behavior than S50 (low) at 3 week time point but at the 6 week time point the C62 (high) shows more nonlinear behavior due to possible increased tissue matrix deposition from host cells within the pores, coupled with slower scaffold degradation. When cells were present (Figure 6.2b), both designs increased in its stiffness over 6 weeks and showed more nonlinear behavior after implantation due to tissue formation inside pores. However when comparing scaffold with cells vs. without

cells at 6 weeks, the low permeable design (S50) showed a larger increase in nonlinear stiffness than the high permeable design (C62).

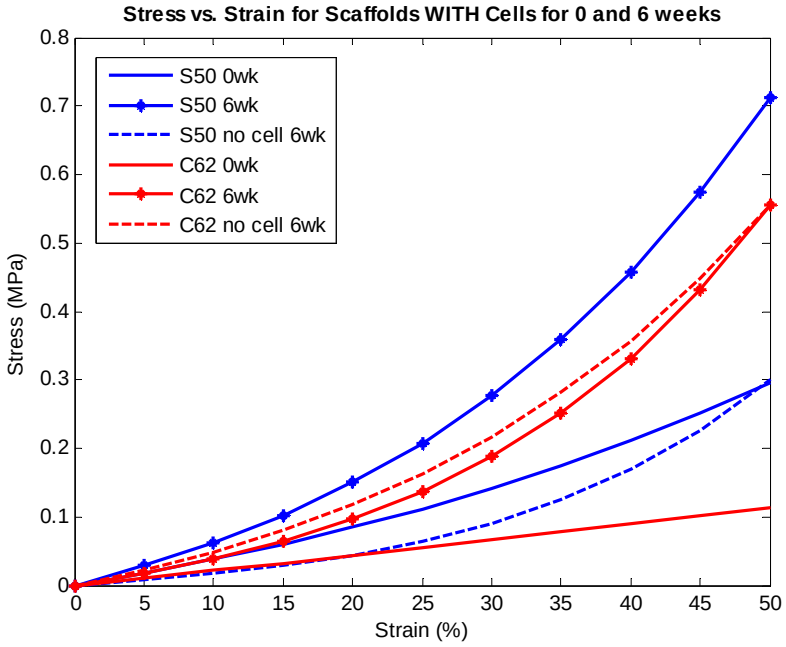

Figure 6.2(b): Comparison of compressive stress vs. strain nonlinear model fit for different scaffold designs at 0 and 6 week time points with cells seeded and pre-cultured 1 week *in vitro* followed by *in vivo* implantation. Both designs formed matrix noted by increase in mechanical stiffness curve however when comparing cell-seeded vs. control (no cell) at 6 weeks high permeable design with cubical pore shape did not show any significant difference whereas cell-seeded low permeable design showed a higher stiffness and more nonlinear behavior with cells than control.

Matrix production and mRNA expression before and after in vivo implantation

Chondrocytes seeded in low permeable design (S50) showed a significant increase in matrix formation (sGAG/DNA contents) over 6 week *in vivo* implantation whereas high permeable design (C62) did not (Figure 6.3). An increase in sGAG/DNA content implies that a single cell is more geared towards chondrocytic phenotype with higher matrix production/maintenance rate. Even though it was not significantly different, the low permeable design (S50) showed a 22% higher matrix production than high permeable design (C62) at 6 weeks, which were opposite of the results at 0 week (right

after 1 week *in vitro* pre-culture), where the high permeable design formed 35% higher matrix than the low permeable design. This flipping pattern between the designs over the 6 week implantation period happens again for relative mRNA expression.

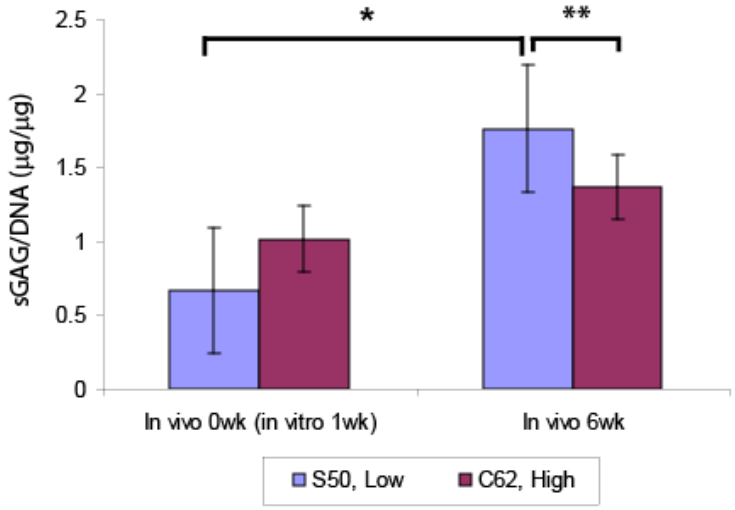

Figure 6.3: Matrix production is quantified by amount of sGAG per DNA for different scaffold designs at each time point *in vivo* (*p≤0.05, **p≤0.1, N=4). Low permeable design with spherical pore shape (S50) showed higher matrix amount at 6 week *in vivo* and significantly higher increase in matrix formation from 0 to 6 weeks *in vivo*.

Quantitative-PCR was used to measure the messenger RNA expression for collagens by cells and for aggrecan found in cartilage at 0 and 6 week *in vivo* implantation (Figure 6.4a & b). All mRNA expressions except col10 (a typical marker for terminally differentiated chondrocytes[28]), the typical biomarkers of differentiated chondrocytes and cartilaginous tissues [23-26] such as col2 and aggrecan as well as the typical marker of the de-differentiated [27] chondrocytes (col1), showed higher ratios for the low permeable design than the high permeable design at 0 week *in vivo* (Figure 6.4a). The differentiation index (DI, col2/col1), and the aggrecan expressions for the low permeable design (S50) in particular were significantly higher than the expressions for

the high permeable design (C62). A higher DI value indicates a more chondrocytic genotype, while a lower value indicates a more fibroblastic gene expression [22].

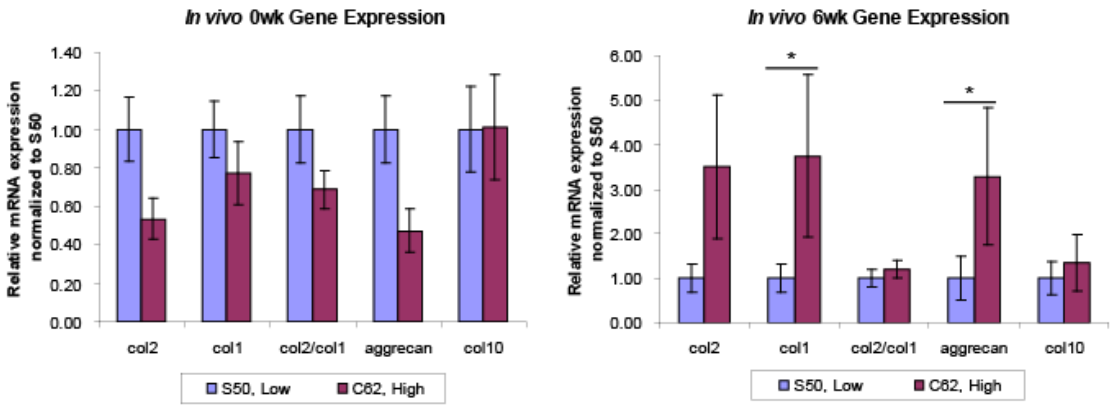

Figure 6.4: Relative mRNA expression comparison for cartilage or hypertrophy related proteins among different scaffold designs at 0 (left) and 6 (right) weeks of *in vivo* implantation. Data are first normalized to GAPDH and then normalized to Low, S50 design in order to compare ratios between designs (*p≤0.05, N=4/design/time points).

In contrast, the high permeable design (C62) showed higher values than the low permeable design (S50) after 6 week *in vivo* implantation for all expressed genes (Figure 6.4b). Type I collagen and aggrecan expressions for C62 were significantly higher (~4 times) than those for S50. Thus, results for all gene expression were higher for the C62 design after 6 weeks *in vivo*, whereas all gene expression was higher for the S50 design after 1 week *in vitro* culture (Figure 6.5a & b).

Since total sGAG (Figure 6.3) is a result of not only matrix formation and secretion but also matrix degradation and sGAG leaching out of the scaffolds, mRNA expressions of matrix degradation proteins are also important to investigate; hence evaluation of MMP mRNA expressions was added to further elucidate the results for sGAG quantification data. MMP-13 and MMP-3 play critical roles in extracellular matrix degradation in cartilage. MMP-13 appears to be the primary collagenase of articular

cartilage and is also critical for cartilage turnover and chondrocyte hypertrophy in the growth plate[29, 30]. MMP-3 is elevated in arthritis, which degrades non-collagen matrix components of the joints. In addition to collagen, MMP-13 also degrades the proteoglycan molecule, aggrecan, giving it a dual role in matrix destruction[31-33].

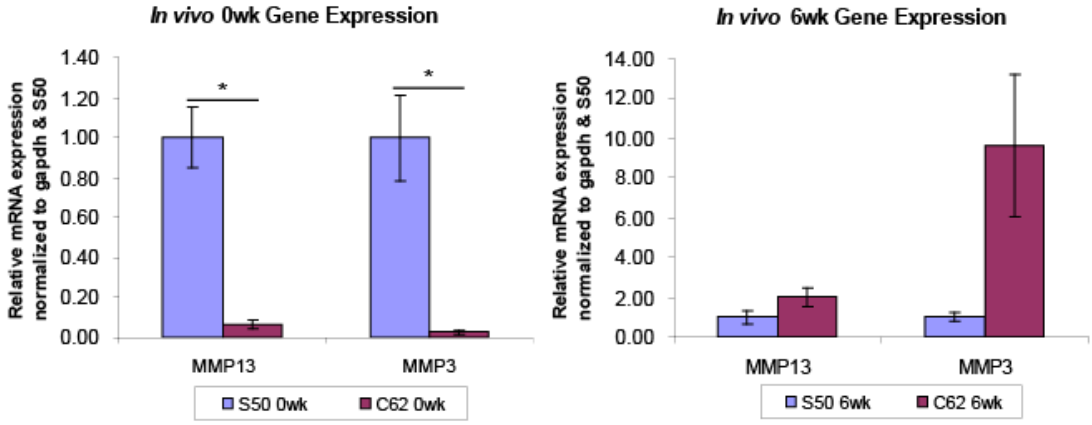

Figure 6.5: Relative mRNA expression comparison for matrix degradation proteins among different scaffold designs at 0 (left) and 6 (right) weeks of *in vivo* implantation. Data are first normalized to GAPDH and then normalized to Low, S50 design in order to compare ratios between designs (*p≤0.05, N=4-6/design/time points).

Both MMP-13 and MMP-3 mRNA expressions for low permeable design (S50) were significantly higher than high permeable design (C62) at 0 week, which then reversed after 6 week *in vivo* implantation. Over 6 weeks, both MMPs expressions greatly increased for high permeable design whereas the low permeable design maintained relatively constant mRNA expression levels of MMPs. In general, mRNA expression levels were high for low permeable designs at 0 week whereas mRNA expression levels were high for high permeable designs at 6 week *in vivo*.

Histology

Safranin-O staining (Figure 6.6) supported the sGAG quantification data (Figure 6.3) in that more vivid and darker sGAG staining inside the scaffolds was observed after 6 weeks for both designs compared to the 0 week time point.

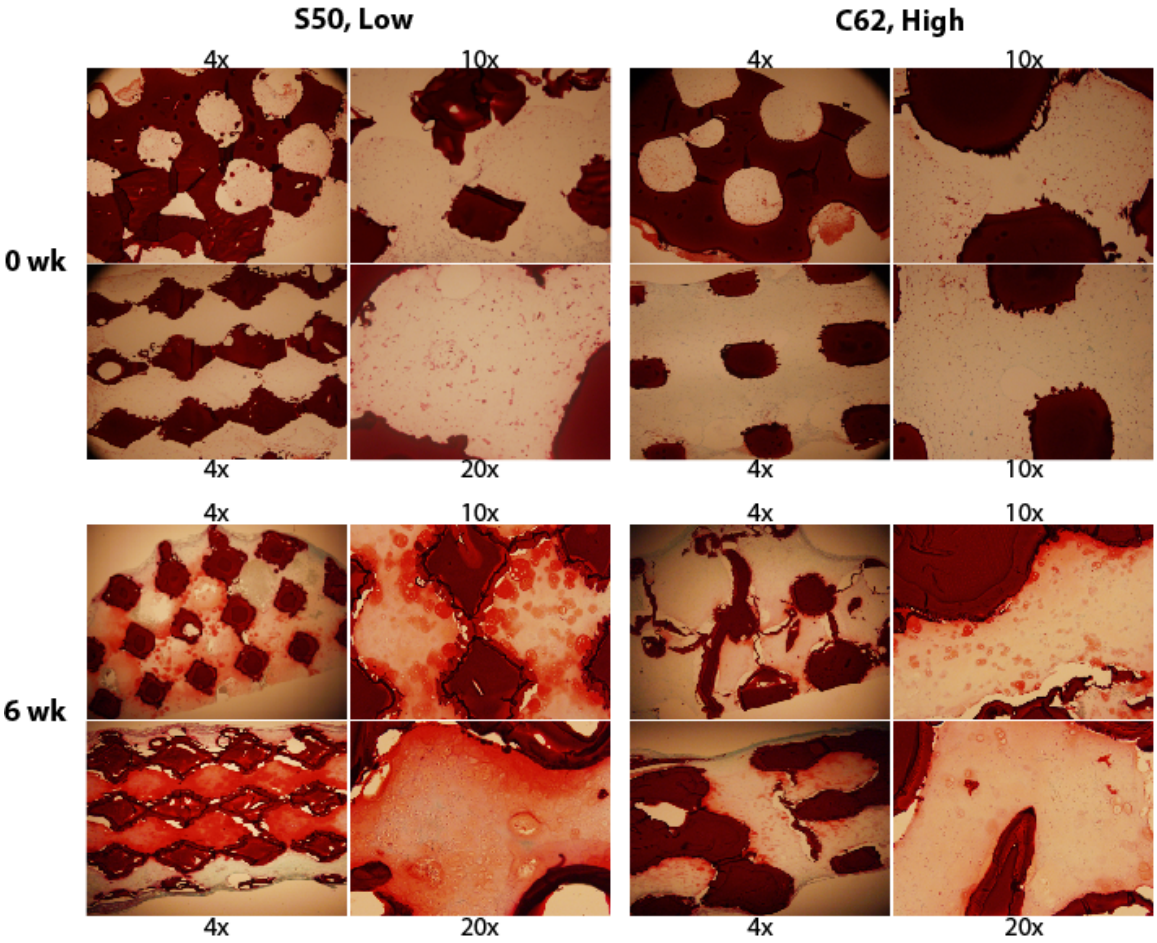

Figure 6.6: Safranin-O/Fast-Green staining of scaffolds at 6 weeks *in vivo* implantation for both designs showed chondrocytic cell phenotype with vivid lacunae but low permeable design with spherical pore shape (S50) contained darker sGAG staining with wider staining area. Dark reddish purple color represents POC materials.

For the 0 week time point, it was hard to determine which scaffold design contained more sGAG inside the scaffold. However, after 6 weeks of implantation, the low permeable design (S50) showed wider staining areas over the entire scaffold with

darker sGAG staining compared to the high permeable design (C62). Especially the most inner parts of the low permeable scaffolds (top to bottom and right to left) had rich Saf-O staining, demonstrating that sGAG were formed and maintained inside the scaffold. The chondrocytic phenotype was easily observed with lacunae as well for both designs at 6 weeks.

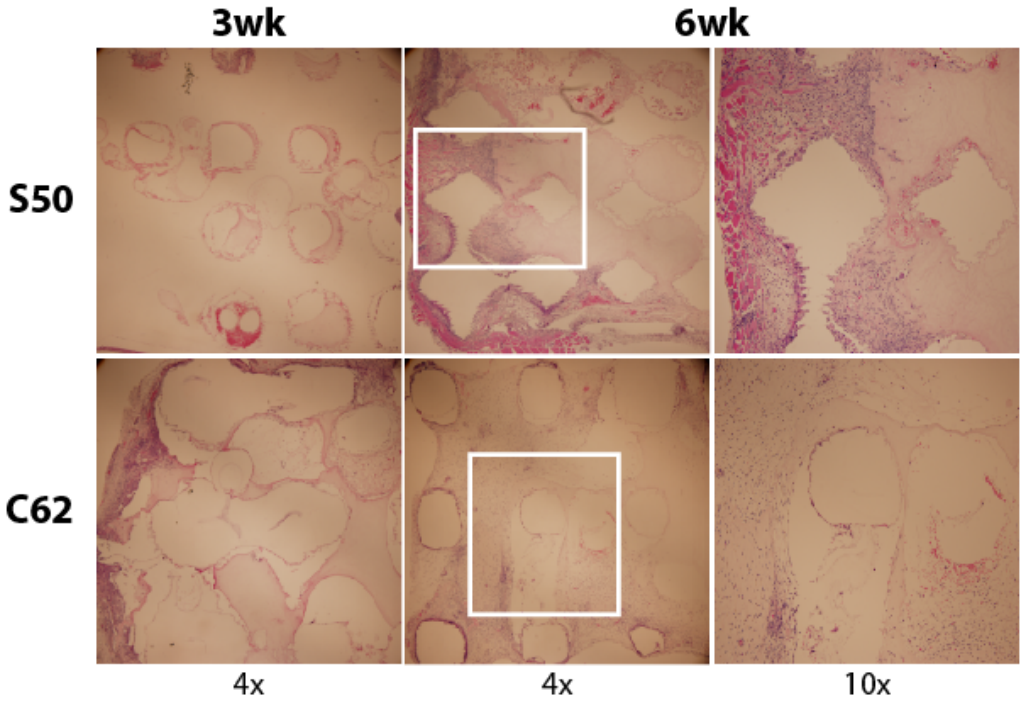

Figure 6.7: H & E staining for scaffolds implanted without cells, which are subjected to scaffold degradation and cell infiltration from surrounding mice skin at 3 and 6 weeks *in vivo* implantation for both designs. Magnification is noted at the bottom. 4x magnification images show the entire scaffold center sections from top to bottom section. The 10x magnification area is marked by a white box in the 4x magnification 6 week-implantation image.

H & E stained images (Figure 6.7) for scaffolds without cells at 3 and 6 weeks were similar between designs. This infiltrated tissue was likely fibrous tissue resulting from in-growth of surrounding host tissue fibroblasts. The combination of fibrous tissue formation with scaffold degradation likely dictated the change in mechanical properties of scaffolds without seeded chondrocytes. The C62 (High) showed deeper cell

infiltration into the pore architecture towards the scaffold center, likely due to the higher permeability allowing greater and more rapid cell migration.

6.4 Discussion and Conclusion

The focus of this study was to determine effects of 3D POC controlled scaffold pore shape and permeability on chondrogenesis *in vivo*. Our previous *in vitro* studies [7, 9] demonstrated that scaffolds with lower permeability and spherical pore shapes increased cartilage matrix production and gene expression. The question then is whether scaffold permeability and pore shape still influence chondrogenesis *in vivo*. Although the ultimate test for *in vivo* chondrogenesis would be an articular defect, such a defect would also entail mechanical compression and stimulus effects on chondrogenesis, confounding the investigation of pore shape and permeability influences on chondrogenesis. Thus, we chose a subcutaneous mouse model for the *in vivo* chondrogenesis, to better isolate the pore shape and permeability affects on chondrogenesis using scaffolds with different controlled designs manufactured from the same material. Using the same scaffold material also helps isolate design effects, since we have also shown that scaffold material significantly influences chondrogenesis [7]. In order to evaluate the effects of POC scaffold pore architectures and resulting permeability on tissues and the quality of engineered cartilage/scaffold constructs, we examined constructs before and after *in vivo* implantation. Specifically, in this way, we would be able to tell how scaffold architectures and resulting permeabilities may affect chondrogenesis differently *in vitro* and *in vivo*. Some studies have reported that cells are predominantly distributed in the outer or surface zones of scaffolds when cultured *in vitro* via static seeding. [34]Thus we

tested pre-cultured POC/cell constructs *in vitro* before implantation to ensure that cells deposited in the scaffold pores and synthesized cartilage ECM (Figure 6.3 & 6.6). Both designs showed the capability to form matrix (Figure 6.3) and to synthesize articular cartilage specific proteins (Figure 6.4a & 5a) before *in vivo* implantation.

For the *in vitro* pre-culture period, there was no significant difference between designs in terms of matrix production (Figure 6.3). The high permeable design (C62) produced slightly more matrix. However for relative mRNA expressions, the low permeable design (S50) demonstrated a trend of having relatively high mRNA expressions for all proteins except the collagen type 10 (col10). Of note, the differentiation index (col2/col1) and aggrecan expressions were significantly higher in S50 scaffolds. This can be explained related to permeability. For initial cell seeding and with regular supply of nutrients during 1 week of *in vitro* culture, cells in both designs are exposed to excessive nutrients and permeabilities that differ in relative magnitude between designs as regulated by permeability and pore shape (Table 6.1). The low permeable design had higher expressions of type 2 collagen, type 2 collagen/type 1 collagen, and aggrecan, which are indicators of differentiated chondrocytes closely related to sGAG formation, than the high permeable design (Figure 6.4a). In addition both MMP13 and 3 expression levels for low permeable design (S50) were almost 10 times higher than high permeable design (C62) indicating active matrix remodeling. Hence overall sGAG/DNA content at 0 week for the low permeable design attained lower values than that for the high permeable design since sGAG/DNA would be an outcome of sGAG secretion/production inside the scaffolds, matrix degradation, and possible sGAG loss by leaching out of scaffolds.

At 6 weeks after implantation however, the results were opposite of the short term 1 week *in vitro* results. At 6 weeks after implantation, the low permeable design (S50) produced more matrix than the high permeable design (C62) and demonstrated a significant increase in matrix production compared to the 1 week *in vitro* data (Figure 6.3). However for relative mRNA expressions, the high permeable design (C62) showed a trend of having relatively high mRNA expressions for all proteins, with type I collagen and aggrecan expressions significantly higher (Figure 6.4b & 5b). This again can be explained by scaffold permeability. The environment of native articular cartilage is well known for its low permeability, avascularization (thus low nutrient supply), and hypoxic conditions. Unlike the *in vitro* conditions, there is probably limited chondrogenic nutrient supply around scaffolds *in vivo*. The low permeable design with spherical pore shape likely allows even lower nutrient exchange from outside. The scaffold permeability differences between designs would increase with time due to gel and POC degradation (Table 6.1) while tissue production would fill up pore spaces lowering the entire tissue/scaffold construct permeability still more. For low permeable design, sGAG would be deposited and maintained inside the scaffold better due to low permeability and chondrocytes inside the spherical pores would tend to aggregate further, limiting sGAG leaching out of tissue/scaffold constructs.

Several studies[36-38] have demonstrated phenotypical changes in OA chondrocytes *in vivo* compared with normal chondrocytes; the expression of genes belonging to hypertrophic cartilage (collagen type X) and more primitive cartilage (collagen type I and III) was increased, while the expression of genes characteristic for a mature articular cartilage phenotype (aggrecan) was significantly decreased in comparison with normal

cartilage[37,38]. Also some reported that the OA-related alterations affect bioactivity and matrix gene expression negatively when cultured *in vitro*[39,40].

In addition, even though mRNA expressions of relevant cartilage-like tissue formation proteins such as type II collagen and aggrecan are lower for the low permeable design, the activities of MMP-13 and -3 are also lower (2 fold lower for MMP-13 and 10-fold lower for MMP-3). Given that the elevation or overexpression of several MMPs in cartilage and synovial tissues are considered as an early sign of OA development [41], the lower activities of MMP-13 and -3 in the tissues grown from S50 at 6 weeks *in vivo* should be taken as a positive sign for our engineered cartilage. Furthermore, mRNA expressions of both MMPs remain relatively constant over 6 weeks after implantation for the low permeable design (Figure 6.4b & 5b). This suggests that the low permeable design may be better at retaining sGAG due to its limited nutrient flux coupled with lower matrix degradation. These results are in line with histological data (Figure 6.6) clearly showing darker staining present in the wider area of the middle of the low permeable scaffolds. There is especially intense sGAG staining near the necks of the spherical pores, further support for the postulate that the spherical pore shape helps retain cartilage matrix. Regardless of scaffold pore architectures and permeabilities though, Figure 6.6 proves that the pores of the POC scaffold *in vivo* appear to be filled with cartilaginous tissue produced by the implanted chondrocytes and the scaffold still maintains its architecture after 6 weeks implantation. Along with biochemical and histological assessments, mechanical assessments such as changes in nonlinear mechanical properties of entire tissue/scaffold constructs before and after implantation are important as mechanical performance is another important factor determining the

success of regenerated tissues. Martinez-Diaz et al.[35] recently demonstrated that rabbit articular cartilage had nonlinear elastic properties and more successful repair strategies better replicated the nonlinear elastic cartilage behavior. POC itself behaves nonlinearly elastic[13, 16] and exhibits nonlinear elastic properties ranging up to the low end of articular cartilage, depending on scaffold architecture. With increasing matrix production, both scaffold designs demonstrated increased nonlinear elastic properties. Compared to data from the study by Martinex-Diaz et al.[35], our spherical design scaffold/tissue constructs matched normal rabbit articular cartilage nonlinear elasticity up to 25% strain while our cubical pore design matched nonlinear elastic properties up to approximately 10% strain. Scaffolds with no cells or after one week *in vitro* culture had nonlinear elastic properties below those of normal cartilage. Thus, even though placed subcutaneously, the nonlinear elastic properties of both designs increased into the range of normal articular cartilage. The spherical pore design demonstrated a greater increase in nonlinear elastic properties, closer to those of articular cartilage than the cubical pore design.

When there were no implanted cells inside scaffolds, both high and low permeable designs demonstrated significant scaffold stiffness increases over 3 weeks showing stronger nonlinear behavior and shifting the stress-strain curve upwards. However, from 3 to 6 weeks of implantation period, the C62 (high permeable) design kept on increasing its stiffness with more nonlinear behavior while the S50 (low permeable) design showed a significant drop in the nonlinear elastic properties. This may reflect a deposition of fibroblastic tissues that would cause an increase in the mechanical properties and relatively different rates of scaffold degradation (Figure 6.2a & 7). For the low permeable design, cell infiltration and fibroblastic tissue formation may be

responsible for an increase in nonlinear elastic properties over the first 3 weeks, followed by a decrease in mechanical properties over the next 3 weeks due to more rapid degradation of the spherical pore design over cubical design (also seen in our *in vitro* studies in chapter 5). Based on Figure 6.7, we could not see any significant differences in cell infiltration and tissue formation by surrounding cells between two designs especially at 6 weeks. Even though there was active cell infiltration and formation of fibroblastic or fat-like tissues within both scaffolds, there were no cartilaginous-like tissues formed, which was confirmed by the lack of sGAG for any designs at any time points (data not shown). While cell infiltration takes place over 6 weeks, during the first 3 weeks, cell infiltration and tissue formation are possibly more dominant than scaffold degradation in determining scaffold mechanical properties. Over the next 3 weeks, scaffolds become more vulnerable to degradation due to acid accumulation inside scaffolds leading to a decrease in mechanical properties. However it should be borne in mind that this stress-strain curve rise and fall pattern is taking place within very small stress ranges. Examining changes in tangent moduli at 10% strain (Table 6.2) from 0, 3, & 6 weeks, reveals no significant differences between 3 and 6 weeks results within the same design. Furthermore, all designs without cells showed the same increased trend in mechanical properties, indicating cell infiltration into scaffolds and tissue formation around scaffolds. Figure 6.2b is more relevant to the effect of chondrogenesis by seeded chondrocytes on tissue/scaffold mechanical properties. Both designs demonstrated increased mechanical stiffness with neotissues packed into pores after 6 week implantation. However, the low permeable design (S50) showed higher absolute stiffness and a greater relative stiffness increase than the high permeable design (C62). This increase in mechanical properties at

6 weeks reflects the overall cartilage matrix production results (Figure 6.3). In comparison between cell-seeded vs. empty scaffolds at 6 weeks, the high permeable design showed no significant difference implying that tissue formation and scaffold degradation are taking place at the same rates balancing out each other in terms of stiffness. However, low permeable design results suggest that cartilage tissue formation is occurring more rapidly than scaffold degradation, giving stiffer and more nonlinear behavior of entire tissue/scaffold constructs (Figure 6.2b). Regardless, both designs proved to give sufficient mechanical support for cells to grow in and form tissue organization and the tangent moduli of entire constructs after 6 weeks implantation were within the ranges of articular cartilage stiffness.

Results of this study parallel those of our earlier *in vitro* work (chapter 5) demonstrating that lower permeability and a spherical pore design were beneficial for chondrogenesis using primary chondrocytes as assessed mechanically, histologically, and with gene expression. Although both POC scaffold designs supported chondrogenesis, the spherical pore design demonstrated enhanced chondrogenesis over the cubical pore design. This is particularly interesting given the implantation in a sub-cutaneous site. The results suggest that pre-seeded POC controlled scaffolds are capable of providing mechanical integrity and suitable microenvironments for cartilage tissue regeneration. Pore shape plays an additive role by ensuring pore volume for keeping ECM and chondrocytes phenotype around pore necking areas and preventing any extra leakage of sGAG out of the scaffolds. Given that low permeability and spherical pore shapes enhance chondrogenesis *in vitro* and sub-cutaneously, the next step is to investigate these

factors in a cartilaginous defect where mechanical environment will exhibit a significant interactive role with designed scaffold pore shape, permeability and scaffold material.

Acknowledgements

This work was funded in part by a NIH grant R01 AR 053379. The authors thank Carolyn Slope for help with scaffold fabrication, cell harvest, and mechanical tests, Eiji Saito for help with mice surgery and Chris Strayhorn for assistance with histology.

References

1. Hangody L, Kish G, Karpati Z, Udvarhelyi I, Szigeti I, Bely M. Mosaicplasty for the treatment of articular cartilage defects: application in clinical practice. Orthopedics 1998;21:751-6.

2. Hunziker EB. Articular cartilage repair: basic science and clinical progress. Osteoarthritis Cartilage 2001; 10: 432-463.

3. Smith GD, Richardson JB, Brittberg M, Erggelet C, Verdonk R, Knutsen G*, et al*. Autologous chondrocyte implantation and osteochondral cylinder transplantation in cartilage repair of the knee joint. J.Bone Joint Surg.Am. 2003;85-A:2487,8; author reply 2488.

4. Knutsen G, Engebretsen L, Ludvigsen TC, Drogset JO, Grontvedt T, Solheim E*, et al*. Autologous chondrocyte implantation compared with microfracture in the knee. A randomized trial. J.Bone Joint Surg.Am. 2004;86-A:455-64.

5. Knutsen G, Drogset JO, Engebretsen L, Grontvedt T, Isaksen V, Ludvigsen TC*, et al*. A randomized trial comparing autologous chondrocyte implantation with microfracture. Findings at five years. J.Bone Joint Surg.Am. 2007;89:2105-12. doi: 10.2106/JBJS.G.00003.

6. Kang Y, Yang J, Khan S, Anissian L, Ameer GA. A new biodegradable polyester elastomer for cartilage tissue engineering. 2006;published online (www.interscience.wiley.com):.

7. Jeong CG and Hollister SJ. A comparison of the influence of material on *in vitro* cartilage tissue engineering with PCL, PGS, and POC 3D scaffold architecture seeded with chondrocytes. Biomaterials 2010 in press.

8. Moutos FT, Freed LE, Guilak F. A biomimetic three-dimensional woven composite scaffold for functional tissue engineering of cartilage. Nat.Mater. 2007;6:162-7. doi: 10.1038/nmat1822.

9. Kemppainen JM and Hollister SJ. Differential effects of designed scaffold permeability on chondrogenesis by chondrocytes and bone marrow stromal cells. Biomaterials 2010;31:279-87. doi: 10.1016/j.biomaterials.2009.09.041.

10. Kemppainen JM and Hollister SJ. Tailoring the mechanical properties of 3D-Designed Poly(glycerol Sebacate) scaffolds for cartilage applications. J Biomed Mater Res A. 2010 Jan 20.

11. Liao EE. Enhancement of chondrogenesis by directing cellular condensation through chondroinductive microenvironments and designed solid freeform fabricated scaffolds. 2007.

12. Liao E, Yaszemski M, Krebsbach P, Hollister S. Tissue-engineered cartilage constructs using composite hyaluronic acid/collagen I hydrogels and designed poly(propylene fumarate) scaffolds. Tissue Eng. 2007;13:537-50. doi: 10.1089/ten.2006.0117 [doi].

13. Jeong CG and Hollister SJ. Mechanical, Permeability, and Degradation Properties of 3D Designed Poly(1,8 Octanediol-co-Citrate)(POC) Scaffolds for Soft Tissue Engineering. J Biomed Mater Res B Appl Biomater. 2010 Jan 20.

14. Hollister SJ, Maddox RD, Taboas JM. Optimal design and fabrication of scaffolds to mimic tissue properties and satisfy biological constraints. Biomaterials 2002;23:4095-103.

15. Hollister SJ. Porous scaffold design for tissue engineering. Nat.Mater. 2005;4:518-24. doi: 10.1038/nmat1421.

16. Kim K, Jeong CG, Hollister SJ. Non-invasive monitoring of tissue scaffold degradation using ultrasound elasticity imaging. Acta Biomater. 2008;4:783-90. doi: 10.1016/j.actbio.2008.02.010.

17. Taboas JM, Maddox RD, Krebsbach PH, Hollister SJ. Indirect solid free form fabrication of local and global porous, biomimetic and composite 3D polymer-ceramic scaffolds. Biomaterials 2003;24:181-94.

18. Kemppainen JM. Mechanically stable solid freeform fabricated scaffolds with permeability optimized for cartilage tissue engineering. 2008.

19. Farndale RW, Buttle DJ, Barrett AJ. Improved quantitation and discrimination of sulphated glycosaminoglycans by use of dimethylmethylene blue. Biochem. Biophys. Acta 1986;883:173-7.

20. Chandrasekhar S, Esterman MA, Hoffman HA. Microdetermination of proteoglycans and glycosaminoglycans in the presence of guanidine hydrochloride. Anal.Biochem. 1987;161:103-8.

21. Kim YJ, Sah RL, Doong JY, Grodzinsky AJ. Fluorometric assay of DNA in cartilage explants using Hoechst 33258. Anal.Biochem. 1988;174:168-76.

22. Martin I, Jakob M, Schafer D, Dick W, Spagnoli G, Heberer M. Quantitative analysis of gene expression in human articular cartilage from normal and osteoarthritic joints. Osteoarthritis Cartilage 2001;9:112-8. doi: 10.1053/joca.2000.0366.

23. Birmingham JD, Vilim V, Kraus VB. Collagen biomarkers for arthritis applications. Biomark Insights 2007;1:61-76.

24. Bruckner P and van der Rest M. Structure and function of cartilage collagens. Microsc.Res.Tech. 1994;28:378-84. doi: 10.1002/jemt.1070280504.
25. Henrotin Y, Addison S, Kraus V, Deberg M. Type II collagen markers in osteoarthritis: what do they indicate? Curr.Opin.Rheumatol. 2007;19:444-50. doi: 10.1097/BOR.0b013e32829fb3b5.

26. Tabassi CB and Garnero P. Monitoring cartilage turnover. Curr Rheumatol Rep. 2007 Apr;9(1):16-24.;.

27. Bohme K, Conscience-Egli M, Tschan T, Winterhalter KH, Bruckner P. Induction of proliferation or hypertrophy of chondrocytes in serum-free culture: the role of insulin-like growth factor-I, insulin, or thyroxine. J.Cell Biol. 1992;116:1035-42.

28. Shen G. The role of type X collagen in facilitating and regulating endochondral ossification of articular cartilage. Orthod.Craniofac.Res. 2005;8:11-7. doi: 10.1111/j.1601-6343.2004.00308.x.

29. Takaishi H, Kimura T, Dalal S, Okada Y, D'Armiento J. Joint diseases and matrix metalloproteinases: a role for MMP-13. Curr Pharm Biotech 2008, 9, 47-54.

30. Zhang L, Yang M, Yang D, Cavey G, Davidson P, Gibson G. Molecular Interactions of MMP-13 C-Terminal Domain with Chondrocyte Proteins. Connect.Tissue Res. 2010; doi: 10.3109/03008200903288902.

31. Burrage PS, Mix KS, Brinckerhoff CE. Matrix metalloproteinases: role in arthritis. Front.Biosci. 2006;11:529-43.

32. Malemud CJ. Matrix metalloproteinases: role in skeletal development and growth plate disorders. Front.Biosci. 2006;11:1702-15.

33. Cawston TE and Wilson AJ. Understanding the role of tissue degrading enzymes and their inhibitors in development and disease. Best Pract.Res.Clin.Rheumatol. 2006;20:983-1002. doi: 10.1016/j.berh.2006.06.007.

34. Holy CE, Shoichet MS, Davies JE. Engineering three-dimensional bone tissue in vitro using biodegradable scaffolds: investigating initial cell-seeding density and culture period. J.Biomed.Mater.Res. 2000;51:376-82.

35. Martinez-Diaz S, Garcia-Giralt N, Lebourg M, Gomez-Tejedor JA, Vila G, Caceres E, *et al*. In Vivo Evaluation of 3-Dimensional Polycaprolactone Scaffolds for Cartilage Repair in Rabbits. Am.J.Sports Med. 2010; doi: 10.1177/0363546509352448.

36. Schulze-Tanzil, G. Activation and dedifferentiation of chondrocytes: implications in cartilage injury and repair. Ann Anat. 2009; 191; 325-338.

37. Aigner T, Bertling W, Stoss H, Weseloh G, Mark K von der. Independent expression of fibril-forming collagens I, II, and III in chondrocytes of human osteoarthritic cartilage. The Journal of clinical investigation 1993; 91: 829-837

38. Mark K von der, Kirsch T, Nerlich A, Kuss A, Weseloh G, Gluckert K, Stoss H. Type X collagen synthesis in human osteoarthritic cartilage: indication of chondrocyte hypertrophy. Arthritis Rheum 1992 35: 806-811.

39. Acosta CA, Ixal I, Ripalda P, Douglas-Price AL, Forriol F: Gene expression and proliferation analysis in young, aged, and osteoarthritic sheep chondrocytes effect of growth factor treatment. J Orthop Res 2006 24: 2087-2094.

40. Dehne, T., Karlsson, C. Ringe, J., Sittinger, M. And Lindahl, A. Chondrogenic differentiation potential of osteoarthritic chondrocytes and their possible use in matrix-associated autologous chondrocyte transplantation. Arthritis Research & Therapy 2009; 11:5;

41. Nagase, H., Kashiwagi, M. Aggrecanases and cartilage matrix degradation Arthritis Research & Terapy, 2003; 5;2

CHAPTER 7

THE INFLUENCE OF SCAFFOLD MATERIALS ON *IN VITRO* CARTILAGE TISSUE ENGINEERING WITH PCL, PGS, AND POC 3D SCAFFOLDS

7.1 Introduction

The biomaterial and scaffold architecture design that best enhances chondrogenesis for Matrix Assisted Chondrocyte Implantation (MACI) remains an open yet critical question. So far, we have explored the feasibility of POC as a cartilage scaffolding material, and evaluated scaffold architectural effects on chondrogenesis using POC scaffolds. As a result we could obtain useful information on how scaffold pore shape and permeability are coupled to affect chondrogenesis *in vitro* and *in vivo*. Then we came to a critical question of whether scaffold architectural effects would still prevail and have the same effects on chondrogenesis when created in any material. In other words, what is the relative influence of scaffold material and design on chondrogenesis? A number of biomaterials with mechanical and surface properties attractive for cartilage regeneration have been put forth. However, there have been almost no head to head comparisons of these different materials as cartilage scaffolds. True material influences can only be ascertained if all materials are fabricated with the exact same architecture, as architecture itself can influence chondrogenesis.

In this chapter, we compare three biomaterials for cartilage tissue engineering: 1) Polycaprolactone (PCL), 2) Poly (Glycerol-co-Sebacate) (PGS), and 3) Poly (Octanediol-co-Citrate)(POC) in terms of mechanical properties, permeability properties, cartilage

matrix production and cartilage-related gene expressions. All three materials were fabricated into the exact same architecture design which was previously found to facilitate matrix production and cellular differentiation of chondrocytes *in vitro*[1]. Thus, we eliminate scaffold architecture as a confounding variable to completely focus on material influences on chondrogenesis. One material, PCL, has a long history in tissue engineering while the other two, PGS and POC are relatively recently developed materials for tissue engineering. The rationale for selection of the three candidate materials was based on their mechanical stiffness (within or close to published ranges for articular cartilage), hydrophilicity, and potential use in the field of cartilage engineering. Furthermore, we wanted to be able to fabricate all chosen materials with the same architecture to remove architecture as a confounding influence on chondrogenesis. All three materials were seeded with primary chondrocytes in the same 3D scaffold design with spherical voids, which was found to enhance chondrogenesis in terms of matrix production and cellular differentiation of chondrocytes *in vitro* from a previous study in our laboratory [1].

Polycaprolactone (PCL) is one of the polyester polymers that have been most frequently used in the field of orthopedic tissue engineering. It is a biocompatible material that is FDA approved for cranial burr hole fillers and trapezoid joint spacers that is readily fabricated and biodegradable. Previous research has shown that PCL is a good candidate for cartilage tissue engineering in terms of cell attachment, proliferation, and matrix production [1-4]. Unlike PCL, PGS and POC are relatively new biomaterials in the field of tissue engineering and there are few published reports on their use for cartilage regeneration [5-7]. Both PGS and POC are rubber-like biodegradable polyester elastomers

which are made by reacting an acid and alcohol monomers via condensation using high temperature and vacuum. Both are degraded by hydrolysis with non-toxic and natural metabolic intermediates degradation products. Due to these characteristics, both materials have been proposed as good scaffold candidates for soft tissue engineering (i.e. cartilage and blood vessels) [5, 7-11].

Due to their recent development, and the lack of controlled 3D scaffold architectures, there has been no direct comparison of PGS and POC for cartilage scaffold materials. Such comparisons are critical to make informed design choices for cartilage tissue engineering matrices for use with autologous chondrocyte therapy or even with current cartilage resurfacing techniques like microfracture or mosaicplasty. However, rationale design decisions to determine optimal cartilage tissue engineering scaffolds will require studying material influences using the same architectures and then studying architectural influences using the same material. The goal of this study was to compare PCL, PGS, and POC material influences on chondrogenesis in terms of mechanical properties, cell activity, cartilage matrix production and gene expression utilizing scaffolds of the same fixed 3D designed architecture.

7.2 Materials and Methods

Synthesis of pre-Polymer

Poly (1, 8 Octanediol-co-Citrate) (POC)

All chemicals were purchased from Sigma-Aldrich (Milwaukee, WI). Poly (1, 8 Octanediol-*co*-Citrate) pre-polymer (pPOC) was synthesized as previously described in previous chapters.[10,12-13]

Poly (glycerol sebacate) (PGS)

PGS pre-polymer (pPGS) was synthesized following methods described by Gao *et al.*[14]. Equimolar sebacic acid and glycerol were reacted under N_2 at 120°C. After 24 hours, the N_2 was removed and a vacuum of 50mTorr was pulled for an additional 48 hours, with a condenser attached.

Scaffold Design & Fabrication

Previously developed image-based design processes and software were used to design 3D POC scaffold architectures [13, 15-18]. Porous polycaprolactone (PCL), PGS, and POC scaffolds (6.35mm diameter, 3.5mm height, 50% porosity, 900μm interconnected spherical pore shape with 310-320μm diameter of the windows between the pores) were designed using custom IDL programs (RSI, Boulder, CO) following previously reported methods[5,13,19]. In brief, wax molds with 3D-image based design architecture were built by a Solidscape Patternmaster™ machine and the wax molds were used directly to melt-cast PCL scaffolds in PTFE molds. PCL powder (43-50 kDa, Polysciences) packed into PTFE molds was melted at 115°C with -30 in.Hg vacuum for 2 hours and then wax molds were pushed into the warm PCL liquid. The wax molds were dissolved by ethanol after cool-down (Figure 3.5).

For PGS and POC scaffolds, inversely solid freeform fabricated hydroxyapatite (HA) molds were prepared before curing pPGS and pPOC into architecture scaffolds. As the wax molds melt at PGS and POC curing temperatures, the HA secondary molds were created from the wax molds as the HA easily withstands the pPGS and pPOC curing temperatures that reach over 100°C. pPGS or pPOC was poured into the wells of a Teflon mold and HA molds were embedded within each pre-polymer. The

pPGS/HA/Teflon mold unit was post-polymerized at 150°C for 3 days. The pPOC/HA/Teflon mold unit was post-polymerized at 100°C for 1 day followed by curing at 100°C for 3 days more with vacuum (-25 in.Hg). The HA mold was removed using a decalcifying reagent (RDO, APEX Engineering Products Corp, Plainfield, IL) followed by incubation in water (Milli-Q water purification system, Billerica, Mass, USA) for 24 hours to obtain the final porous POC scaffolds (Figure 3.3).

Mechanical Tests

For scaffold unconfined compression tests, four to six porous scaffolds per each material were tested in compression (Alliance RT/30 electromechanical test frame, 50N load cell (POC, PGS) or 500N load cell (PCL) with 0.5% error range, MTS Systems Corp., MN) and TestWorks4 software (MTS Systems Corp., MN) was used to collect data during compression testing. MATLAB (The MathWorks Inc., MA) software was used to fit a nonlinear elasticity model, $\sigma = A[e^{B\varepsilon} - 1]$ to experimental data. The sum of least square errors between the model stress and experimental stress was minimized using the LSQNONLIN minimization program in the MATLAB optimization toolbox. Tangent moduli were calculated at 10 and 30% strain from fit data and all residuals between model and experimental stress were below 1%.

***In Vitro* Cell Culture & Histology**

The porosity and permeability measurements were performed with the same procedures and conditions as described in previous chapters. Chondrocytes were seeded into 3D scaffolds by first suspending the cells in media with composite HyA/Col I gels and then pushing the gel into the 3D scaffolds[17]. The gelation procedure is as follows: 625μL of Col I (stock concentration: 8.37mg/mL diluted to 6mg/ml with 0.2N acetic

acid; BD Bioscience Discovery Labs, San Jose, CA) with 62.5 µL HyA (stock concentration: 3 mg/mL in 1.5M sodium chloride (NaCl), molecular weight 2.4-3 million Da; Hyalogic LLC, Edwardsville, KS) were well-mixed. The pH of the HyA/Col I suspension was increased with the addition of 9µL of 0.5N sodium hydroxide with 220 mg/mL sodium bicarbonate to initiate gelation. As soon as 0.5N sodium hydroxide is added to HyA/Col I gel mixture, gel contents were evenly re-suspended. Hydrogel mixtures are then dripped down onto pre-prepared sterile scaffolds until scaffolds were fully soaked and filled with gel to the top surface. This was followed by incubation at 37°C for 30 min to solidify gels further. 125µl of gel mixtures were used for each scaffold.

Porcine chondrocytes (pChon) were isolated from the full depth of metacarpophalangeal joints of domestic pigs and seeded onto scaffolds following methods previously published [17] with some modifications. In short, cells were re-suspended at a density of $20x10^6$ cells/mL in 625µL of composite HyA/Col I (6mg/ml) with ~50µL of culture medium. The cell seeding and gelation procedures of composite HyA/Col I hydrogels were the same as described in chapter 5 & 6 [20]. Before cell culture, PGS and POC scaffolds were sterilized by autoclave and PCL scaffolds were sterilized by incubation in 70% ethanol for 1 hour. After sterilization, all scaffolds were neutralized to physiological pH level by media incubation for 24-48 hours with brief PBS rinse prior to cell seeding. Scaffolds seeded with pChon were cultured with chondrogenic medium (basal medium (DMEM, 10% fetal bovine serum (FBS), 1% P/S, Gibco) supplemented with 50 mg/mL 2-phospho-L-ascorbic acid (Sigma)), 0.4mM proline (Sigma), 5 mg/mL insulin (Gibco), and 0.1mM non-essential amino acids (Gibco)) in 12-well plates.

Chondrocytes were cultured for 0 (1d), or 4 weeks under gentle agitation on an orbital shaker and the media was changed every other day. Cell culture was maintained in a water-jacket incubator equilibrated with 5% CO_2 at 37°C. For histology, constructs (N=3/material) at each time point were fixed in 10% buffered formalin overnight, dehydrated with a series of graded ethanol, and embedded in paraffin. Tissue sections were stained with safranin O/Fast green counterstaining to assess cell distribution, morphology and sGAG production. Six to eight slides (4 sections/slide) were obtained from the center of each scaffold (top to bottom and left to right). Immunohistochemistry was used to detect collagen II following a previously established protocol [20]. Four slides (4 sections/slide) were obtained from the center of each material scaffold.

sGAG and DNA quantification

Before cell analysis, excessive out-layer tissues were removed from PCL scaffolds and analyzed separately for both sGAG/DNA quantification and mRNA gene expression analysis. Scaffolds (N=6) at both the 0 and 4 week time points were removed from the culture and sGAG and DNA were quantified using the same methods as described in chapter 5 & 6. The digested tissue-scaffold solution was analyzed by a dimethylmethylene blue (DMMB) assay following a previously established protocol [5,21,22]. The total sGAG were normalized by DNA content which was measured using Hoechst dye 33258 methods (Sigma, #DNA-QF).[1,23]

Quantitative-PCR

Cartilage matrix specific genes (Type II collagen & aggrecan),chondrocyte de-differentiation marker genes (Type I & X collagen), matrix degradation indicator genes (matrix metalloproteinases 13 and 3 (MMP13, MMP3) and glyceraldehyde-3-phosphate

dehydrogenase (GAPDH) gene expression were determined by quantitative PCR (qtPCR) using a Gene Amp 7700 sequence detection system (Applied Biosystems, Foster City, CA USA) for PCL, PGS, and POC Scaffolds (N=6/material). The remaining procedures were the same as described in chapter 6. The quantity of gene expressions were calculated with standard samples and normalized with GAPDH and further normalized by PCL for easy comparison.

Statistical Analysis

Data are expressed as mean ± standard deviation. The statistical significance among different materials was calculated using linear regressions and one way ANOVA with post-hoc comparison (Tukey) or student t-test using SPSS software (SPSS for Windows, Rel 14.0. 2005 Chicago: SPSS Inc.). Data were taken to be significant, when a *P*-value of 0.05 or less was obtained.

7.3 Results

Scaffold design, fabrication, and characterization

In order to isolate design effects from material effects on chondrogenesis, scaffold designs were kept the same for all three materials in terms of pore shape, pore size, surface area, and porosity (Table 7.1, Figure 7.1). Due to material influences, PCL, PGS, and POC had different effective scaffold modulus and permeability (Table 7.1). Figure 7.1 shows example micro-CT images of scaffolds and a digital picture for the POC scaffold design (other scaffolds are similar in images thus not shown here). With no tissue in-growth, the PCL scaffold tangent modulus was roughly two hundred times the PGS and POC effective scaffold tangent modulus at 10 % strain. However, with in-growth of cartilaginous tissues at 4 weeks *in vitro*, the PCL effective scaffold tangent

modulus was only twice that of the PGS and POC scaffolds at the same strain rate, which is likely due to the composite PCL/tissue tangent modulus being dominated by tissue growing on top of the PCL scaffolds. Even though scaffold designs were kept the same, effective scaffold permeability differed significantly between the different materials. Scaffold design permeability, a single physical design parameter that describes how multiple structural properties including pore size, pore shape, interconnectivity, porosity, and fenestration size affect mass transport, depends not only on scaffold design but also on scaffold material [1, 24].

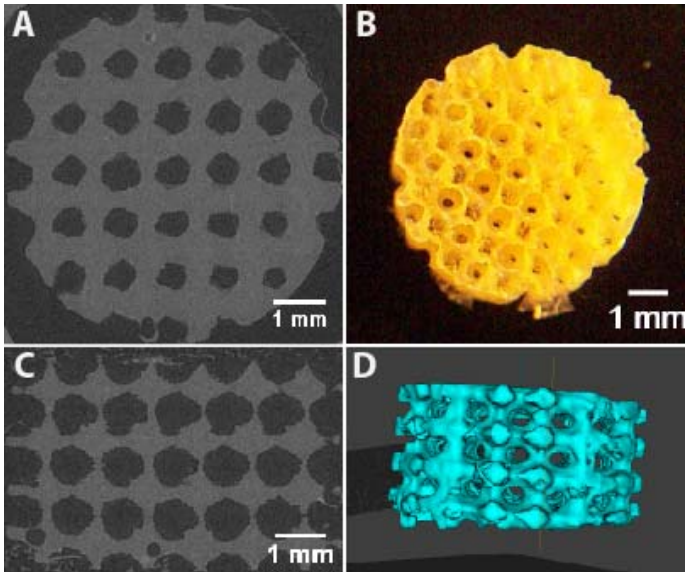

Figure 7.1: (A) Top view of MicroCT image of a scaffold (B) a digital picture of a POC scaffold (C) Side view of MicroCT image of a scaffold (D) Isosurfaced 3D MicroCT image of a scaffold

Table 7.1- Scaffold Descriptions (N=6-8)

Material	PCL	PGS	POC
Porosity (%)	48 ± 3.62	49 ± 2.36	50 ± 1.62
Permeability without gel (10^{-7} m^4/N·s)	2.93 ± 0.73	8.31± 3.91	3.51 ± 0.95
Permeability with gel (10^{-7} m^4/N·s)	0.66 ± 0.24	3.0 ± 0.18	1.72 ± 0.45
Equilibrium Water contact angle (hydrophilicity) (°)	77.0 ± 1.4	60.8 ± 6.3	32.8 ± 2.0
Surface Area (mm^2)	288 ± 38		
Pore Shape	Spherical		
Designed Pore Size	900μm		
Designed Pore Strut Size	315μm		

Permeability without gel likely represents the permeability of scaffolds at 4 weeks without tissue in-growth whereas permeability with gel represents the scaffolds at 0 wk with initial cell seeding. As most of collagen gels are degraded in a week during tissue formation, permeability is dynamically changing within the 4 week period. However it is likely that the trend of different permeability between the different materials remains. PCL, POC, and PGS are in order of increasing permeability without gel, 2.93 ± 0.73, 3.51 ± 0.95, and 8.31± 3.91 (10^{-7} m^4/N·s). With gel, the same permeability rankings hold with PCL, POC, and PGS having 0.66 ± 0.24, 1.72 ± 0.45, and 3.0 ± 0.18 (10^{-7} m^4/N·s) permeability, respectively (Table 7.1).

Table 7.2 - Mechanical Properties (N=4-6)

Material	PCL	PGS	POC
Tangent modulus without tissues (0wk) (MPa)*	21.8 ± 4.43	0.19 ± 0.06	0.13 ± 0.04
Tangent modulus with tissues (4wk) (MPa)*	1.43 ± 0.56	0.89 ± 0.19	0.73 ± 0.37
Tangent modulus with tissues (4wk) (MPa)**	13.49 ± 3.53	2.44 ± 0.69	1.26 ± 0.33

*measured at 10% strain, ** at 30% strain

Table 7.2 summarizes compressive tangent moduli for each material scaffold with or without tissues. PCL is more than 100 times stiffer than PGS and POC whereas PGS and POC have similar effective scaffold tangent moduli at 10% strain rate. After tissues were formed for 4 weeks, the tangent compressive moduli of both PGS and POC were

increased ~ 400% compared to that of PGS and POC without tissues measured at the same strain rate. The effective scaffold tangent moduli of PCL at 4 week were only two times higher than that of PGS and POC at 10% strain. This result is probably due to excessive tissues outgrown on the top of PCL scaffolds. Thus effective scaffold tangent compressive moduli more likely reflected the properties of the formed tissues on the top of PCL scaffolds rather than the combined scaffold and tissue properties. This was not the case for PGS and POC as regenerated cartilaginous tissues were contained within the scaffolds (see Figure 7.2B and C). At 30% strain, tangent moduli of all the scaffolds reflect better the entire tissue/scaffold construct (Table 7.2). The POC/tissue construct was the most compliant at 30% strain, followed by PGS (2x stiffer than POC) and PCL (10x stiffer than POC and 6x stiffer than PGS).

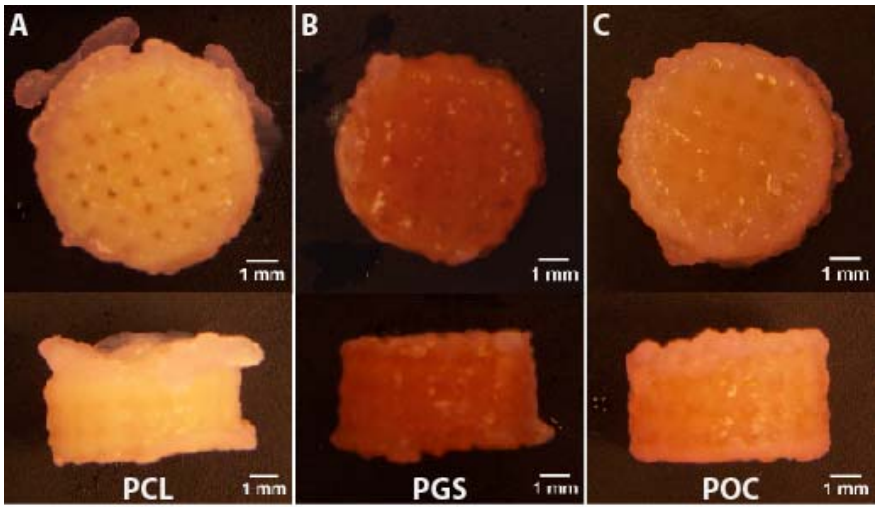

Figure 7.2: Digital pictures of three different material scaffolds with tissues grown for 4 weeks.

In vitro cell culture-proliferation, differentiation, and matrix production

Chondrocytes proliferated and produced cartilaginous matrix during the 4 week *in vitro* culture period (Figure 7.2). Excessive outer tissues were grown on the top and bottom of the PCL scaffold whereas tissue were contained completely within the PGS

and POC scaffolds (Figure 7.2) Since we were interested in the amount of tissues formed inside the scaffold, we separated excessive outer tissues from PCL, denoting assays on tissue within the PCL scaffold as PCL_{in}, assays on tissue outside the PCL scaffold as PCL_{outer}, and assays on complete PCL tissue simply as PCL.

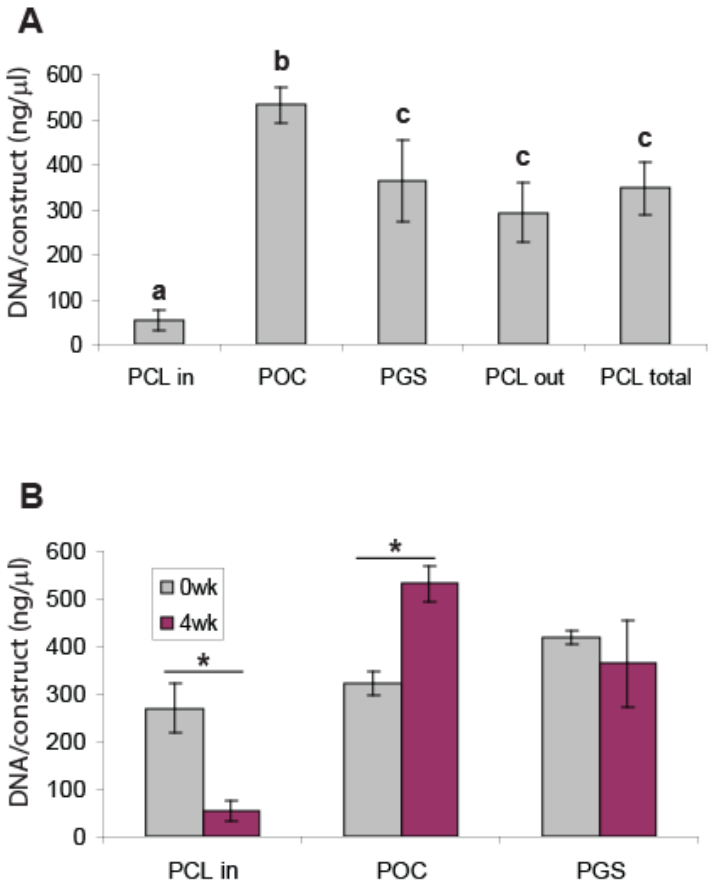

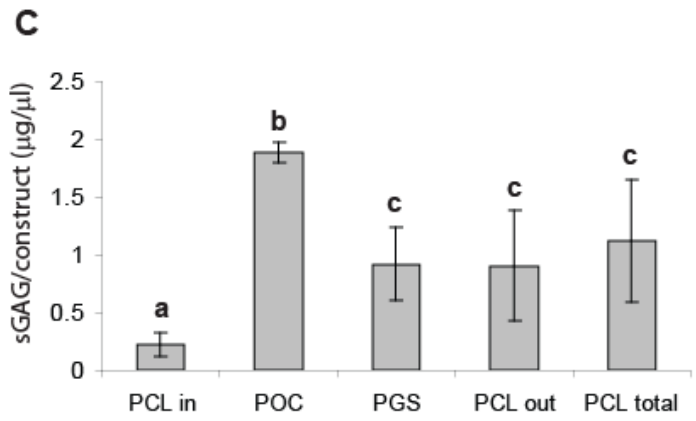

Figure 7.3: (A) Amount of DNAs per construct at 4 weeks for different materials (PCL_{in}: tissues inside PCL scaffolds only, PCL_{out}: excessive outer layers removed from PCL scaffolds, PCL_{total} = PCL_{in} + PCL_{out}) (Annotations 'a', 'b', 'c' shown in the graphs are statistically significant each other; PCL_{in}, POC are significant to all other groups, PGS are significant to PCL_{in} and POC only) (B) Changes in DNA content of chondrocytes for different materials over time is measured by amount of DNAs per scaffold suggesting some possible cell migration (especially for PCL) and exterior tissue growth. (Asterisk represents statistical significance. $p \leq 0.05$, N=6) (C) Matrix production per scaffold is quantified by amount of sGAG per construct for different materials. (PCL_{in}, POC are significant to all other groups, PGS are significant to PCL_{in} and POC, $p \leq 0.05$, N=6)

POC produced the highest DNA content (531 ± 39 ng/µl) per construct, whereas PCL_{in} produced the lowest content (54 ± 22 ng/µl) per construct\. PGS and PCL_{total} showed similar DNA contents (363 ± 22 ng/µl and 346 ± 59 ng/µl respectively) per construct (Figure 7.3a). Over 4 weeks, POC showed highest proliferation rate, with an increase of DNA content from 322 ± 24 ng/µl to 531 ± 39 ng/µl per construct. PGS showed no significant difference in the amount of DNA over time. Note that PCL_{in} showed a decrease from 269 ± 52 ng/µl to 54 ± 22 ng/µl per construct, likely reflecting the fact that more cells grew outside the PCL scaffold than inside (Figure 7.3b). Sulfated-glycosaminoglycan (sGAG) content, measured through a DMMB assay, was used to quantify cartilaginous matrix production by chondrocytes (Figure 7.3c). This showed a similar trend to the DNA content. POC produced the most amount of sGAG per

scaffold (1.88 ± 0.88 μg/μl) which was roughly eight times more than PCL_{in} (0.22 ± 0.10 μg/μl) and two times more than PCL_{total} (1.12 ± 0.53 μg/μl) and PGS (0.92 ± 0.32 μg/μl). However, PGS and PCL_{total} were not significantly different from each other.

In vitro cell culture-gene expression

Quantitative-PCR was used to measure the messenger RNA expression for collagen by cells and for aggrecan and MMPs found in cartilage (Figure 7.4). As mentioned in the previous chapters, healthy articular cartilage is composed of a highly organized network of collagen and proteoglycans. The most abundant and major fibrillar collagen of articular cartilage, Type II collagen, determines the mechanical behavior of native tissue [25]. When Type II collagen is destroyed and replaced by a type I collagen fibro-cartilage, the mechanical behavior subsequently alters as a type I collagen does not have the same functional properties as type II collagen. Of note again, collagen type II and the proteoglycan aggrecan are considered to be markers of chondrocytic differentiation or hyaline-like cartilage with the increase in relative mRNA expression levels, while collagen types I is suggested to be a marker of dedifferentiation or more fibrocartilige with the increase in relative mRNA expression levels [38]. This is why the differentiation index (col2/col1) is used as an indicator for chondrogenesis by comparing col2/col1 values (i.e. chondrocytic if a higher col2/col1 value and fibroblastic if a lower col2/col1 value) [26].

The differentiation index of POC was 4.31, significantly higher than that of PCL_{in}, PGS, and PCL_{out} (0.92, 1.31, 1.21 respectively), reflecting the sGAG quantification data. In contrast, the differentiation indexes of PCL and PGS were not significantly different from each other. PCL and PGS seemed to provide environments for cells to be active

causing elevated expressions of both type II collagen and type I collagen genes. In contrast, POC was good for keeping type I collagen expression low while promoting type II collagen expression.

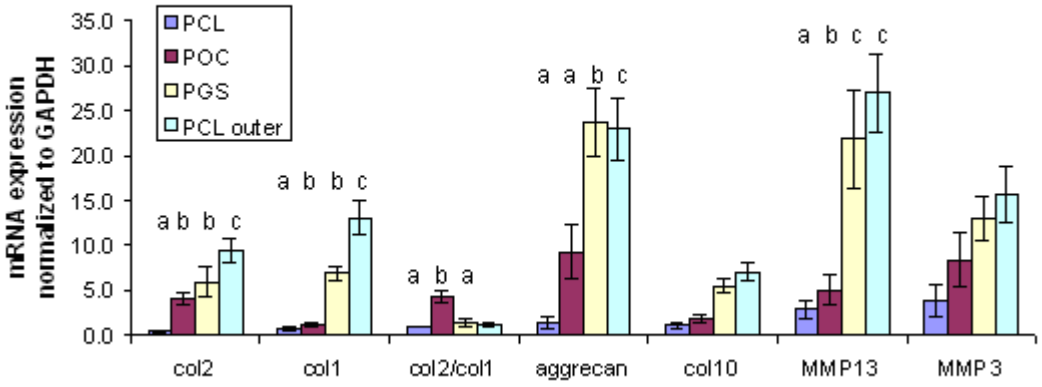

Figure 7.4: Relative mRNA expression comparison for proteins among different materials. (PCL = PCL inner tissues only) (Annotations 'a', 'b', 'c' shown in the graphs are statistically significant each other. N=6, $p \leq 0.05$ for a-c)

As introduced in chapter 6, aggrecan is the main proteoglycan found in cartilage, and is a typical marker of differentiated chondrocytes. The aggrecan expression of PGS and POC_{out} were significantly higher than that of PCL_{in} and POC. The type X collagen expression, a marker of the terminally differentiated (hypertrophic) chondrocyte phenotype [27,28], also showed a similar trend as the type I collagen and aggrecan expressions among different materials with significance ($p<0.1$). PGS and PCL_{out} showed the highest tendency to hypertrophy.

MMP-13 and MMP-3 play critical roles on extracellular matrix degradation but their degradation roles are slightly different. MMP-13 is a product of the chondrocytes that reside in the cartilage and it not only degrades collagen but also degrades the proteoglycan molecule, aggrecan, giving it a dual role in matrix destruction [29-31]. On the

other hand, MMP-3 is elevated in arthritis, which degrades non-collagen matrix components of the joints. When comparing the gene expressions of MMP-13 and MMP-3 for inner tissues, PGS showed the highest MMPs' expressions which were five to ten times higher than PCL_{in} and POC implying that degradation of collagens and aggrecan were actively taking place.

Histology and Immunohistochemistry

Safranin-O staining (Figure 7.5) supported the sGAG quantification data. POC showed the highest sGAG content with pores fully packed with sGAG stained tissues whereas PCL and PGS showed less tissues formed with sGAG stained. Also, even for outer layer tissues of POC, sGAG staining was darker than any other materials showing higher sGAG content. The safranin O staining of PCL confirmed that not much cartilaginous tissues formed inside the scaffold pore (less sGAG staining) and most of cartilage tissues were formed outside the PCL scaffold.

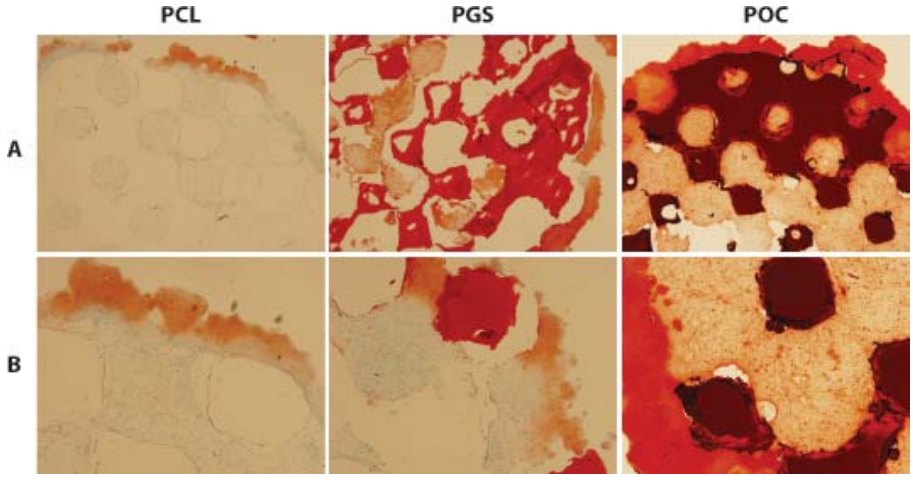

Figure 7.5: Safranin-O/Fast-Green staining for sGAG. Dark crimson colored regions shown in the middle of PGS and POC sections are scaffold materials. (A: 4x magnification, B: 10x magnification)

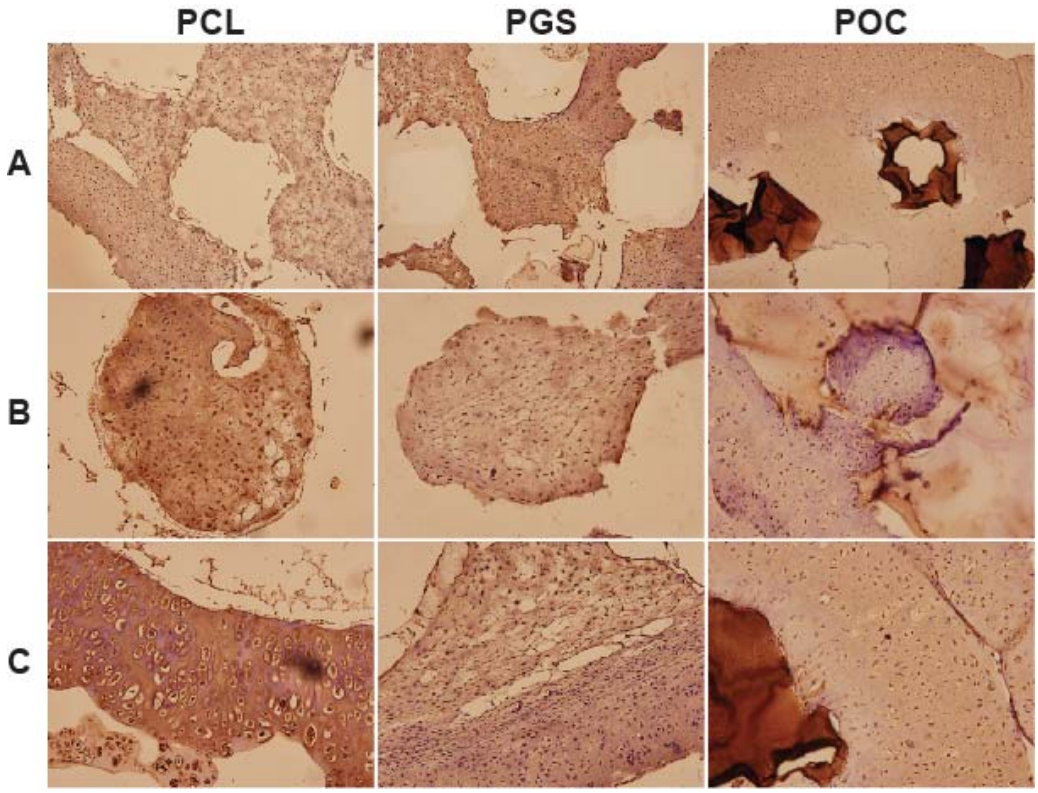

Figure 7.6: Immunohistochemical analysis for Type II collagen (brown) with hematoxylin staining (purple) (A: tissues between pores: 10x magnification, B: tissues inside a pore: 20x magnification, C: Outer layer tissues: 20x magnification).

Immunostaining of type II collagen (Figure 7.6) tracked relative mRNA expression data (Figure 7.4) such that PCL (inner and outer tissues combined) showed the strongest intensity of immunostaining for type II collagen and PGS and POC followed respectively. For cell morphology, PCL and POC showed more vivid chondrocytic phenotype with lacunae inside pore, between pores, and the most outer part of scaffolds, whereas more fibroblastic cells were found across the entire PGS scaffold, which also matched with type I collagen relative mRNA expression data (Figure 7.4) indicating higher de-differentiation. In general, outer tissues for all materials maintained a more chondrocytic cell morphology than the center part of the scaffold.

7.4 Discussion and Conclusions

This is the first time a true apples to apples comparison of scaffold material influence on chondrogenesis has been performed *with the same designed 3D porous architecture*. Many studies have reported how one or two materials affect chondrogenesis yet they cannot make a completely unfounded comparison of material effects due to lack of controlled scaffold design and the resultant differences in scaffold architecture [17,32,33]. Since scaffold design is also a critical factor affecting tissue regeneration within scaffold[1], we cannot isolate material effects on chondrogenesis unless we can test different scaffold materials fabricated with the same 3D architecture. Here, using an identical scaffold design for all three materials, we could make a direct comparison of scaffold material effect on chondrogenesis.

The most significant difference in terms of material effects, PCL, PGS, and POC scaffolds were seen in the permeability, hydrophilicity, and effective scaffold tangent moduli differences. Even though scaffold architectural permeability was kept the same for all materials, there were effective permeability differences among materials themselves. PGS was significantly more permeable than POC and PCL (Table 7.1) PCL showed significantly higher tangent moduli than other two materials (Table 7.2) with or without tissues. In general, the degradation rates of PGS and POC are much faster than that of PCL and the degradation rates and the rates of tissue formation are related to mechanical tangent moduli [8,10,34,35].

PGS and POC tangent moduli increased significantly by 4 weeks, suggesting that tissue formation occurred faster than scaffold degradation. However, the tangent modulus for the PCL/tissue construct decreased greatly from 0 to 4 weeks of tissue

culture. This was more likely because cartilage tissue grew over the scaffold, and thus dominated the compressive properties over the scaffold material. In terms of tangent modulus, PGS and POC were more similar to native cartilage tissues than PCL [5,7], which may be more advantageous when applying these scaffolds in cartilage defects.

Cell proliferation measured by amount of DNA (live cells) per construct at 0 and 4 weeks clearly shows that POC provided the most favorable environment for cell proliferation in terms of overall or inner parts of scaffolds. When considering tissues formed in the inner parts of scaffolds only, PCL seemed to be least favorable material yet when comparing overall effects PGS and PCL_{total} were not significantly different (Figure 7.3A). Proliferation over time (Figure 7.3B) also supports this contention since PGS and POC proliferated or at least kept the same number of cells whereas PCL_{in} showed a significant decrease in cell numbers. This may be explained by low permeability, hydrophobicity and low wettability of PCL scaffolds compared to the other two materials.

As cells started to grow and tissues were formed, less nutrients from the media would flow in and out due to lower permeability for all materials. However, since PGS and POC may better retain fluid due to hydrophilicity, there would be more nutrients from media that are soaked into these materials available to cells inside of the scaffold. Excessive growth of tissue outside the PCL scaffolds may have further prevented nutrient diffusion within the PCL scaffold, leading to reduced cell proliferation.

It was reported that chondrocytes prefer decreased scaffold permeability within PCL scaffolds in terms of cartilaginous matrix production, promoting increases in aggrecan content and collagen 2: collagen 1 gene expression ratios (the differentiation index: DI) [1]. This was true for POC which had a relatively lower permeability than PGS

and showed the highest sGAG contents (Figure 7.3C and 5). Also, in terms of gene expression, its DI (Col2/Col1) was the highest with relatively low type X collagen expression indicating a reduced tendency towards hypertrophy. However, even though PCL had permeability similar to POC, the results for PCL chondrogenesis were more similar to PGS in terms of matrix production and gene expression. When comparing inner tissues only, PCL showed the lowest cell number (Figure 7.3A), proliferation rate (Figure 7.3B), and thus lowest matrix production (Figure 7.3C). This could be again due to the presence of excessive outer tissues preventing sufficient nutrient supply to the innermost cells within the scaffold, causing these cells not to proliferate and to produce less sGAG. However tissues on the outside of the PCL scaffolds exposed to media still proliferated well and had high level of gene expressions, confirming a high level of cell activity. PCL_{out} and PGS showed similar pattern in terms of total amount of DNA, sGAG content, and relative mRNA expressions. Especially for relative mRNA expressions, PCL and PGS seemed to cause lower chondrocyte differentiation (shown by Col2/Col1 ratio) yet higher aggrecan production, higher rates of matrix degradation (shown by MMPs), and a higher tendency towards hypertrophy (shown by Col X). Even though POC did not show the highest expression of type II collagen and aggrecan, it did show a high differentiation index, lower hypertrophy tendency, and lower matrix degradation with the highest DNA and sGAG contents. Thus we could probably conclude that overall POC maybe the material that best enhances chondrogenesis out of the three materials examined. This is probably due to benefits delivered from combined effects of higher hydrophilicity and wettability retaining more media inside, and sufficiently low permeability to keep sGAG inside the scaffold while still allowing media flow. PCL and PGS seemed to promote

chondrocyte proliferation and activity in terms of gene expressions, however these chondrocytes may be more likely to proceed to hypertrophy as seen by the type X collagen expression and increased matrix degradation suggested by increased MMP3 and 13 gene expression.

Histological data (Figure 7.5) supported sGAG quantification data and type II collagen immunostaining supported type II collagen gene expression data. However, from Figure 6 we should note that while type II collagen immunostaining may give some useful qualitative information, it only gave partial information on chondrocytic differentiation. As Figure 7.4 shows, PCL_{total} and PGS had high expression of type II collagen however they also had high expression of type I and X collagen as well compared to POC. It would not be possible to calculate a quantitative differentiation index using type I and type II immunostaining. Combining histological and immunohistological images with sGAG quantification and mRNA expression data likely gives the most complete picture of chondrogenesis.

The *in vitro* results presented here showed a significant dependence of chondrogenesis on scaffold material, eliminating pore architecture as a confounding variable by fabricating all scaffolds with the same architecture. However, these results must obviously be verified in *in vivo* cartilage defects, since mechanical loading, oxygen tension and host cells may affect chondrogenesis in this situation. For instance, engineered cartilage grown in scaffolds may cause chondrocytes to proceed to hypertrophy and matrix degradation such that they would end up promoting endochondral ossification before sufficient cartilage formation. In order to overcome these limitations, more *in-vivo* studies with small and large animals would be necessary

for future clinical applications. Still, *in vitro* results are important since many *in vivo* studies will utilize in vitro culture periods to boost cartilage matrix production before transplantation.

Overall, this work confirms that scaffold material selection is an important factor that affects chondrogenic cellular differentiation and matrix production. It has been widely postulated yet never proven that the choice of material directly affects cell differentiation and chondrogenesis, since previous studies saw variation in both scaffold material and architecture, which confounds interpretation of experimental results. This work points to the capability to modulate and ultimately enhance chondrogenic potential with careful selections of material.

Acknowledgements

This work was funded in part by a NIH grant R01 AR 053379. The authors thank Annie G. Mitsak and Carolyn Slope for help with PGS pre-polymer synthesis and scaffold fabrication, Huina Zhang for advices with data analysis, and Chris Strayhorn for assistance with histology.

References

1. Kemppainen, J.M., and Hollister, S.J. Differential effects of designed scaffold permeability on chondrogenesis by chondrocytes and bone marrow stromal cells. Biomaterials, 2010.

2. Kim, H.J., Lee, J.H., and Im, G.I. Chondrogenesis using mesenchymal stem cells and PCL scaffolds. Journal of biomedical materials research.Part A, 2009.

3. Izquierdo, R., Garcia-Giralt, N., Rodriguez, M.T., Caceres, E., Garcia, S.J., Gomez Ribelles, J.L., Monleon, M., Monllau, J.C., and Suay, J. Biodegradable PCL scaffolds with an interconnected spherical pore network for tissue engineering. Journal of biomedical materials research.Part A 85, 25, 2008.

4. Li, W.J., Tuli, R., Okafor, C., Derfoul, A., Danielson, K.G., Hall, D.J., and Tuan, R.S. A three-dimensional nanofibrous scaffold for cartilage tissue engineering using human mesenchymal stem cells. Biomaterials 26, 599, 2005.

5. Kemppainen, J.M., and Hollister, S.J. Tailoring the mechanical properties of 3D-Designed Poly(glycerol Sebacate) scaffolds for cartilage applications. J Biomed Mater Res A , 2010 Jan 20.

6. Hollister, S.J., Liao, E.E., Moffitt, E.N., Jeong, C.G., and Kemppainen, J.M. Defining Design Targets for Tissue Engineering Scaffolds. In: Anonymous Fundamentals of Tissue Engineering and Regenerative Medicine. Berlin: Springer Verlag.

7. Kang, Y., Yang, J., Khan, S., Anissian, L., and Ameer, G.A. A new biodegradable polyester elastomer for cartilage tissue engineering. Wiley Periodicals, Inc. published online (www.interscience.wiley.com), 2006.

8. Wang, Y., Ameer, G.A., Sheppard, B.J., and Langer, R. A tough biodegradable elastomer. Nature biotechnology 20, 602, 2002.

9. Nijst, C.L., Bruggeman, J.P., Karp, J.M., Ferreira, L., Zumbuehl, A., Bettinger, C.J., and Langer, R. Synthesis and characterization of photocurable elastomers from poly(glycerol-co-sebacate). Biomacromolecules 8, 3067, 2007.

10. Yang, J., Webb, A.R., Pickerill, S.J., Hageman, G., and Ameer, G.A. Synthesis and evaluation of poly(diol citrate) biodegradable elastomers. Biomaterials 27, 1889, 2006.

11. Motlagh, D., Yang, J., Lui, K.Y., Webb, A.R., and Ameer, G.A. Hemocompatibility evaluation of poly(glycerol-sebacate) in vitro for vascular tissue engineering. Biomaterials 27, 4315, 2006.

12. Yang, J., Webb, A.R., and Ameer, G.A. Novel Citric Acid-Based Biodegradable Elastomers for Tissue Engineering. Advanced Materials 16, 511-16, 2004.

13. Kim, K., Jeong, C.G., and Hollister, S.J. Non-invasive monitoring of tissue scaffold degradation using ultrasound elasticity imaging. Acta biomaterialia 4, 783, 2008.

14. Gao, J., Crapo, P.M., and Wang, Y. Macroporous elastomeric scaffolds with extensive micropores for soft tissue engineering. Tissue engineering 12, 917, 2006.

15. Hollister, S.J., Maddox, R.D., and Taboas, J.M. Optimal design and fabrication of scaffolds to mimic tissue properties and satisfy biological constraints. Biomaterials 23, 4095, 2002.

16. Hollister, S.J. Porous scaffold design for tissue engineering. Nature materials 4, 518, 2005.

17. Liao, E., Yaszemski, M., Krebsbach, P., and Hollister, S. Tissue-engineered cartilage constructs using composite hyaluronic acid/collagen I hydrogels and designed poly(propylene fumarate) scaffolds. Tissue engineering 13, 537, 2007.

18. Jeong, C.G., and Hollister, S.J. Mechanical, Permeability, and Degradation Properties of 3D Designed Poly(1,8 Octanediol-co-Citrate)(POC) Scaffolds for Soft Tissue Engineering. Journal of Biomedical Materials Research: Part B , 2010 Jan 20.

19. Kemppainen, J.M. Mechanically stable solid freeform fabricated scaffolds with permeability optimized for cartilage tissue engineering. , 2008.

20. Liao, E., Yaszemski, M., Krebsbach, P., and Hollister, S. Tissue-engineered cartilage constructs using composite hyaluronic acid/collagen I hydrogels and designed poly(propylene fumarate) scaffolds. Tissue engineering 13, 537, 2007.

21. Farndale, R.W., Buttle, D.J., and Barrett, A.J. Improved quantitation and discrimination of sulphated glycosaminoglycans by use of dimethylmethylene blue. Biochem Biophys Acta 883, 173-7, 1986.

22. Chandrasekhar, S., Esterman, M.A., and Hoffman, H.A. Microdetermination of proteoglycans and glycosaminoglycans in the presence of guanidine hydrochloride. Analytical Biochemistry 161, 103, 1987.

23. Kim, Y.J., Sah, R.L., Doong, J.Y., and Grodzinsky, A.J. Fluorometric assay of DNA in cartilage explants using Hoechst 33258. Analytical Biochemistry 174, 168, 1988.

24. Li, S.H., de Wijn, J.R., Layrolle, P., and de Groot, K. Accurate geometric characterization of macroporous scaffold of tissue engineering. Bioceramics 240–2, 541–545, 2003.

25. Bruckner, P., and van der Rest, M. Structure and function of cartilage collagens. Microscopy research and technique 28, 378, 1994.

26. Martin, I., Jakob, M., Schafer, D., Dick, W., Spagnoli, G., and Heberer, M. Quantitative analysis of gene expression in human articular cartilage from normal and osteoarthritic joints. Osteoarthritis and cartilage / OARS, Osteoarthritis Research Society 9, 112, 2001.

27. Bohme, K., Conscience-Egli, M., Tschan, T., Winterhalter, K.H., and Bruckner, P. Induction of proliferation or hypertrophy of chondrocytes in serum-free culture: the role of insulin-like growth factor-I, insulin, or thyroxine. The Journal of cell biology 116, 1035, 1992.

28. Shen, G. The role of type X collagen in facilitating and regulating endochondral ossification of articular cartilage. Orthodontics & craniofacial research 8, 11, 2005.

29. Burrage, P.S., Mix, K.S., and Brinckerhoff, C.E. Matrix metalloproteinases: role in arthritis. Frontiers in bioscience : a journal and virtual library 11, 529, 2006.

30. Malemud, C.J. Matrix metalloproteinases: role in skeletal development and growth plate disorders. Frontiers in bioscience: a journal and virtual library 11, 1702, 2006.

31. Cawston, T.E., and Wilson, A.J. Understanding the role of tissue degrading enzymes and their inhibitors in development and disease. Best practice & research.Clinical rheumatology 20, 983, 2006.

32. Banu, N., Banu, Y., Sakai, M., Mashino, T., and Tsuchiya, T. Biodegradable polymers in chondrogenesis of human articular chondrocytes. Journal of artificial organs : the official journal of the Japanese Society for Artificial Organs 8, 184, 2005.

33. Gong, Y., Ma, Z., Zhou, Q., Li, J., Gao, C., and Shen, J. Poly(lactic acid) scaffold fabricated by gelatin particle leaching has good biocompatibility for chondrogenesis. Journal of biomaterials science.Polymer edition 19, 207, 2008.

34. Wang, Y., Kim, Y.M., and Langer, R. In vivo degradation characteristics of poly(glycerol sebacate). Journal of biomedical materials research.Part A 66, 192, 2003.

35. Lam, C.X., Hutmacher, D.W., Schantz, J.T., Woodruff, M.A., and Teoh, S.H. Evaluation of polycaprolactone scaffold degradation for 6 months in vitro and in vivo. Journal of biomedical materials research.Part A 90, 906, 2009.

36. Tan, P.S., and Teoh, S.H. Effect of stiffness of polycaprolactone (PCL) membrane on cell proliferation. Materials Science and Engineering: C 27, 304-308, 2006.

37. Wang, Y., Sheppard, B.J., and Langer, R. Poly (glycerol sebacate) — A Novel Biodegradable Elastomer for Tissue Engineering. Mat Res Soc Symp Proc 724, N11.1.1, 2002.

38. Schulze-Tanzil, G. Activation and dedifferentiation of chondrocytes: implications in cartilage injury and repair. Ann Anat. 2009; 191; 325-338.

CHAPTER 8

THE CELL-MATERIAL INTERACTION IN 2D DISCS

8.1. Introduction

From the experiments comparing 3D PCL, PGS, and POC scaffolds for chondrogenesis *in vitro* shown in chapter 7, we could conclude that POC is the best choice of scaffold material for chondrogenesis in terms of matrix production, chondrocytic cell phenotype and sGAG staining in histology, and cartilaginous tissue relevant gene expressions for the low permeable scaffold design with the spherical pore shape (S50). However, we still could not elucidate why chondrocytes actually favor POC for chondrogenesis. One postulate is that hydrophilicity could be one factor influencing chondrogenic response on different polymers. In order to compare the direct cell-material interactions for each material without the intermediate gel seeding or 3D architecture, we conducted a short parallel follow-up study of the 3D scaffold study shown in chapter 7 with two dimensional (2D) discs instead of 3D environments. Additionally, one more additional material, the Arg-Gly-Asp (RGD)-modified PCL, was added to examine the possible effects of hydrophilicity on chondrocytes (chondrogenesis). Hence, the four material groups compared in this study were PCL, PGS, POC, and RGD-modified PCL (PCL-RGD). RGD-modified PCL has been shown to have a higher hydrophilicity than PCL and a better cell adhesion, attachment and proliferation for bone

marrow stromal cells in our previous study [1,2] and Hsu et al. reported that RGD-modified substrate could improve the adhesion of chondrocytes [3].

The rationale behind adding RGD-modified PCL is that the hydrophobicity of PCL is known to prevent effective cell aggregation and attachment initially, which can explain why chondrocytes don't favor PCL, given that cell aggregation is desirable for chondrocytes and chondroprogenitor cells to form cartilaginous matrix in [4]. RGD-modified PCL not only has a higher hydrophilicity than PCL but also it has the degree of hydrophilicity closer to POC and PGS. In this set-up, if the hydrophilicity is the main factor providing a favorable environment for chondrocytes, we should be able to see a trend according to different degrees of hydrophilicity among materials. Also, hydrophilic materials tend to absorb and retain media more, which may help chondrocytes by providing more immediate nutrients. Both PGS and POC are relatively highly hydrophilic yet POC is slightly more hydrophilic based on the equilibrium water contact angle than PGS (32.8° vs. 60.8°) (Table 8.1).

Table 8.1 Water contact angle represents hydrophilicity of each material.

Material	PCL	PCL-RGD	PGS	POC
Equilibrium water contact angle (hydrophilicity) (°)*	77.0 ± 1.4	46.4 ± 3.0	60.8 ± 6.3	32.8 ± 2.0

Even though least complicated way in general is to examine cell-material interactions is to directly seed cells in a two dimensional (2D) culture such as discs or films, as mentioned in chapter 2, several studies have confirmed that chondrocytes de-differentiate in a 2D environment even at 7 days [7]. Hence we chose to culture chondrocytes for a short term (1 week) to observe the initial chondrocyte response to each material using the same characterization methods used in previous chapters.

8.2 Materials and Methods

2D discs fabrication

Pre-polymer of PGS and POC were synthesized following the protocol previously described in chapter 7. First, each sheet of PCL, PGS and POC were cured in a tensile specimen Teflon mold using the same curing conditions described in chapter 7. Ten 2D cylindrical discs (7mm (D) x 1.25mm (H)) per each material were punched out of cooled down solid polymer sheets using 7mm biopsy punch for cell culture. PCL discs were modified with RGD following the previously established method in our lab [1] In short, the PCL discs were immersed into a 10% w/v solution of 1, 6-hexanediamine (Sigma) prepared in isopropanol at 37^{o}C for 1 hr for the aminolysis. After the exposure, the discs were thoroughly washed in deionized distilled water for 24 hrs and were dried under vacuum at room temperature. The aminated PCL discs were then pre-washed with activation buffer 3 times (0.1 M phosphate buffered saline contained 0.15 M NaCl, pH 7.2). For conjugation of RGDC peptides to the surface of aminated PCL disc, the heterobifunctional crosslinker sulfosuccinimidyl 4-(N-maleimidomethyl) cyclohexane-1-carboxylate (sulfo-SMCC) (Pierce Biotechnology, Rockford, IL) was used. 4 mg/ml of the sulfo-SMCC solution was pipetted onto aminated PCL discs and incubated for 1 hr at room temperature, followed by washing with conjugation buffer (activation buffer contained 0.1 M EDTA, pH 7.0). The RGDC peptide (Bachem California, Inc., Torrance, CA) was dissolved at a concentration of 0.125 mg/ml in conjugation buffer. The peptide solution was applied onto the sulfo-SMCC-treated PCL disc and incubated overnight at 4 °C. Peptide conjugated PCL discs were washed thoroughly with conjugation buffer twice and PBS for 3 times and dried under vacuum at room temperature. For all

subsequent experiments, the following PCL samples were created and used: untreated PCL (PCL) and RGD-modified PCL (PCL-RGD).

In Vitro Cell Culture

All discs were sterilized by immersion in 70% ethanol for 45 mins followed by neutralization to physiological pH level by incubation in serum-free cell media prior to cell seeding. Porcine chondrocytes were isolated using the same method as in previous chapters and a density of 1 x 10^6cells/cm^2 (3.4 x 10^5 cells/disc) cells suspended in 40μl media were seeded onto the discs directly in the 24 ultra-low attachment well plates and cultured for 1 week *in vitro* with the same conditions described before.

sGAG and DNA quantification & Quantitative-PCR

The sGAG content of the dissolved solution at 1 week for all discs (N=4/design) was assayed using the DMMB method and the total sGAG were normalized by DNA content measured using Hoechst dye 33258 method as described previously in chapter 5. For quantitative PCR, Type II, I, X collagens, aggrecan, matrix metalloproteinases 3, 13 (MMP3, MMP13), and glyceraldehyde-3-phosphate dehydrogenase (GAPDH) mRNA expressions were quantified by real-time PCR using Gene Amp 7700 sequence detection system (Applied Biosystems). A positive standard curve for each primer was obtained by quantitative PCR with serially-diluted cDNA sample mixture. The quantity of gene expression was calculated with standard samples and normalized with GAPDH then further normalized to PCL for easy comparison.

Statistical Analysis

Data are expressed as mean ± standard deviation. The statistical significance among different materials was calculated using linear regressions and one way ANOVA with

post-hoc comparison (Tukey) using SPSS software (SPSS for Windows, Rel 14.0. 2005 Chicago: SPSS Inc.). Data were taken to be significant, when a *P*-value of 0.05 or less was obtained.

8.3 Results

sGAG and DNA quantification

For DNA quantification shown in Figure 8.1, POC discs had the statistically significant higher DNA contents than the other four materials, by a factor of nearly 100 (4267 ± 63 ng/µl). PCL discs showed the lowest DNA contents (24.56 ± 8.88 ng/µl) and the amount of DNA present in PGS and RGD-modified PCL (PCL-RGD) discs were very similar each other (44.2 ± 10.5, 42.6 ± 8.83 ng/µl, respectively). However PCL, PGS, and RGD-PCL discs were still not significantly different in terms of total amount of DNA per dick.

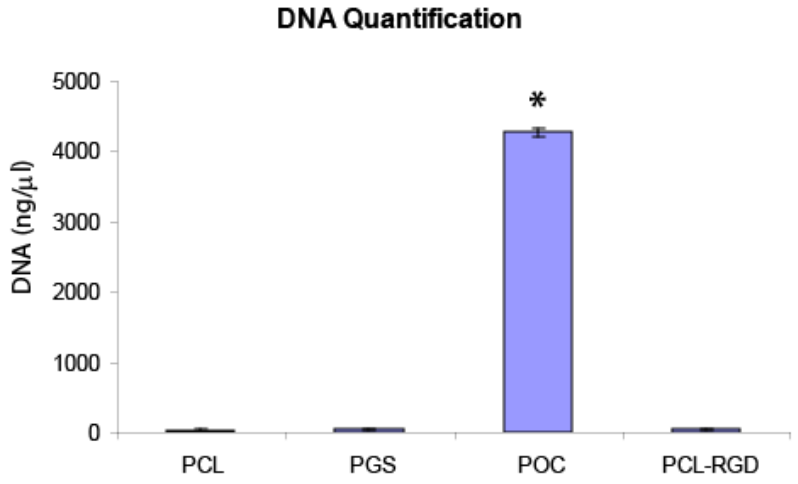

Figure 8.1: The amount of DNA per disc was quantified (N = 4-5, *p ≤ 0.05).

For the amount of total sGAG produced per disc, the same pattern as DNA was shown (Figure 8.2). The amount of sGAG secreted on POC disc was significantly higher

than any other materials (11.4 ± 1.85 μg/μl, 10 folds higher), yet there was no significant difference among PCL, PGS and PCL-RGD discs (0.17, 0.23, 0.70 μg/μl, respectively).

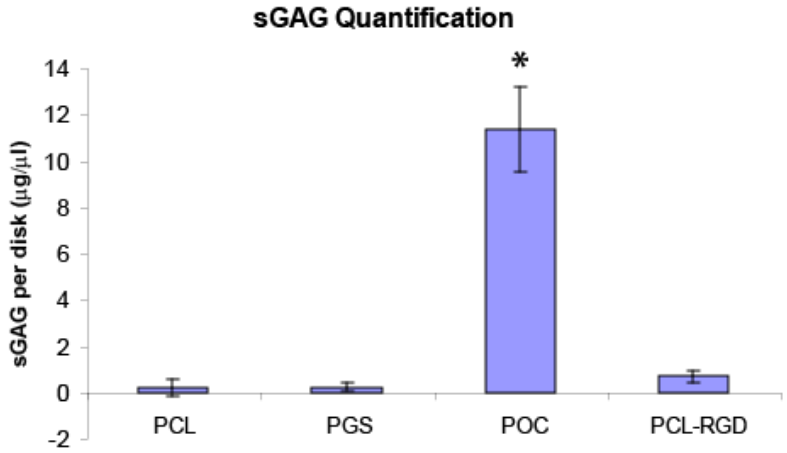

Figure 8.2: The total amount of sGAG per disc was quantified (N = 4-5, *p ≤ 0.05).

When the amount of sGAG was normalized to the amount of DNA (sGAG/DNA shown in Figure 8.3) however, which represents a tendency of single cell towards chondrogenesis, PCL-RGD showed a significantly (5 times) higher tendency towards chondrogenic differentiation than any other materials. Among PCL, PGS, and POC, there was no trend or significance shown.

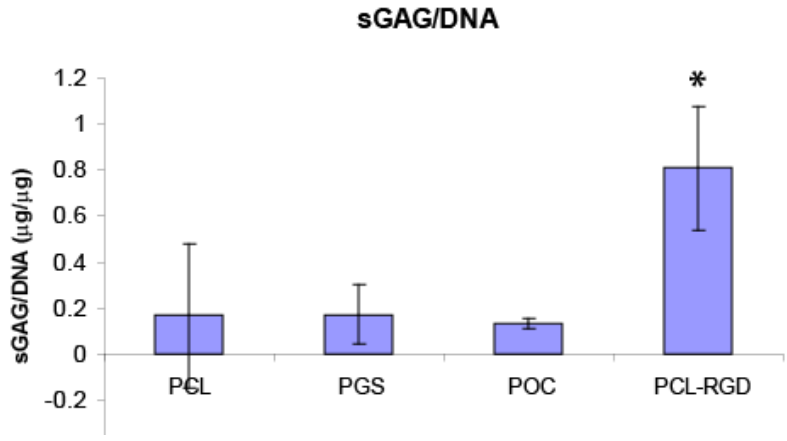

Figure 8.3: The total amount of sGAG per disc was normalized to the total amount of DNA for chondrogenesis (N = 4-5, *p ≤ 0.05).

mRNA gene expressions

The mRNA gene expressions for cartilaginous tissue markers (col2, aggrecan), chondrocytic differentiation marker (col2/col1), de-differentiation marker (col1), terminal differentiation (known as chondrocytic ossification) marker (col10), and degradation proteins (MMP3 & 13) were quantified and compared between materials as illustrated in Figure 8.4. There was no significant difference or pattern in the differentiation index (col2/col1), expressions of col10, MMP13 or MMP3.

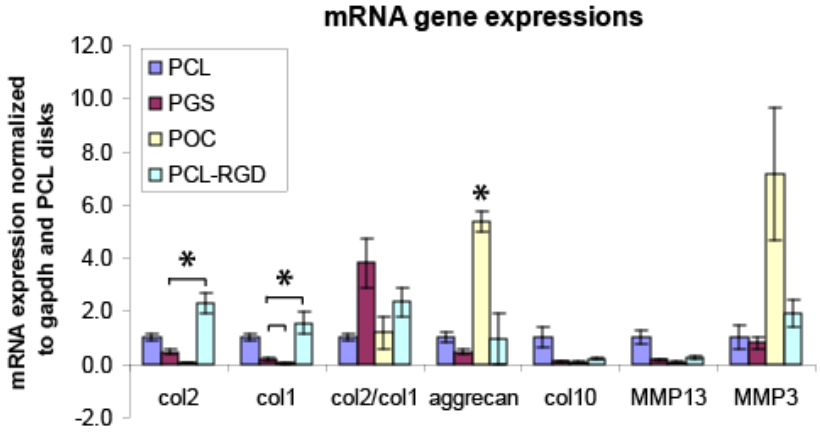

Figure 8.4: The mRNA gene expression levels of chondrocytes seeded on 2D discs of each material were presented as ratios compared to PCL (via first normalization by gapdh and further normalization by PCL for comparison) (N=3-4, *p≤0.05).

8.4 Discussion and Conclusion

We hypothesized that hydrophilicity was one of the major factors driving the difference in chondrocytic response to polymer material. In this case, POC has the greatest hydrophilicity, followed by PGS and RGD-modified PCL. Based on DNA and sGAG quantification data (Figure 8.1 and 8.2), it is clear that POC discs exhibit significantly better cell-material interaction for cell adhesion, cell attachments, proliferation, and formation and maintenance of matrix even in 2D environments. In fact,

POC has the lowest water contact angle and thus the highest degree of hydrophilicity among all four materials, which correlates to the results shown in quantification of the amount of DNA and sGAG. The degree of hydrophilicity indeed seemed to affect chondrocyte proliferation in the direct cell-material interactions as the amount of DNA parallels to the degree of hydrophilicity (Figure 8.1, Table 8.1). However, this does not hold true for sGAG quantification; for instance, PGS should be the next best material for sGAG formation if the degree of hydrophilicity is the main factor in matrix production and maintenance. In fact, PCL-RGD which has slightly higher water contact angle and is thus more hydrophobic than PGS. However, PCL-RGD has shown to form slightly higher amounts of sGAG suggesting that there is some material/chemical factor of PGS material which causes an unfavorable environment for chondrogenesis. Regardless, PCL was shown to be the least favorable material for chondrogenesis. PCL-RGD was shown to be better than PCL for both chondrocyte proliferation and matrix formation, leading to the conclusion that the hydrophobic and non-adhesive surface nature of PCL may be a major hindrance to cartilage formation. For sGAG/DNA normalized data, there were no significant material effects among PCL, PGS, and POC on the tendency of single cell towards chondrogenesis. In contrast, PCL-RGD surface modification tends to help single chondrocytes for chondrogenesis. Not only do the increases in hydrophilicity affect cell attachments and matrix synthesis, but also RGD-induced signal transduction can be involved in chondrogenesis. Some studies[8-10] have reported that an adhesive sequence, RGD, promotes survival of cells and has shown to induce early stages of chondrogenesis, while its persistence can limit complete differentiation. Hwang et al.[10] showed that RGD seemed to cause cartilage-specific gene up-regulation and extracellular matrix production.

However there were some contradictory reports[11,12] demonstrating that integrin-mediated adhesion within a three-dimensional environment inhibits bone marrow stromal cells (BMSC) chondrogenesis through actin cytoskeleton interactions and the effects of RGD-adhesion on mesenchymal differentiation are lineage-specific and depend on the biochemical composition of the cellular microenvironment. This controversy still remains open as to how RGD affects chondrogenesis and there is no report that elucidates how RGD affects chondrocytes in chondrogenesis in terms of signal transductions to date. Hence, it is possible that RGD induces cell signaling events that may drive and promote more matrix formation by chondrocytes, however this is only a speculation at this stage and further investigation needs to be conducted to elucidate the mechanism involved.

The mRNA gene expressions of any proteins do not seem to give any clear conclusions and no significant trends among different materials could be found. For cartilaginous tissue gene expression markers, it was shown that PCL-RGD (col2) and POC (aggrecan) were preferred materials yet PGS was shown to be the best material for differentiation (col2/col1). PCL and PCL-RGD demonstrated a highest tendency towards de-differentiation (col1), terminal differentiation (col10), and matrix degradation (MMP13), which are somewhat contradictory to the results of cartilaginous markers. POC showed the least collagen type II level with the significantly highest level of aggrecan, both of which are considered to be indicators for cartilage differentiation. Based on the mRNA gene expressions, it is hard to make a conclusion of favorable materials and there seems to be no definitive trends among materials for any genes involved in chondrogenesis. This is probably due to several reasons: first, one week of culture time is too short for cells to lay matrix and form cartilaginous tissues. Secondly,

chondrocytes tend to de-differentiate in 2D environments even within a week, thus no matter what materials are used, the 2D environment is not favorable for chondrogenesis.

From this short simplified experiment comparing biomaterials and the effects of hydrophilicity on chondrogenic proliferation and differentiation of chondrocytes, we can conclude that the degree of hydrophilicity does play a role in terms of cell attachments and proliferation. However, the amount of matrix formation is not necessarily dependent on or directly correlated to the degree of hydrophilicity. We did observe, however, that PCL should be somehow modified to increase its hydrophilicity and adhesive surface characteristic to provide more suitable environments for chondrocytes in chondrogenesis. Regardless of its relatively high hydrophilicity, there is some material based disadvantage of PGS which does not enhance chondrocytic based chondrogenesis despite its being hydrophilic. However, in order to elucidate the mechanism behind, the morphology of cell attachment, careful characterizations of surface chemistry and surface morphology, possible impacts imposed by degradation byproducts from POC and PGS etc. need to be further evaluated for future.

Acknowledgements

The authors thank Carolyn Slope for help with discs fabrication, cell harvest, Huina Zhang for help with RGD-modification.

References

1. Zhang, H., and Hollister, S. Comparison of bone marrow stromal cell behaviors on poly(caprolactone) with or without surface modification: studies on cell adhesion, survival and proliferation. Journal of biomaterials science.Polymer edition 20, 1975, 2009.

2. Zhang, H., Lin, C.Y., and Hollister, S.J. The interaction between bone marrow stromal cells and RGD-modified three-dimensional porous polycaprolactone scaffolds. Biomaterials 25, 4063-9, 2009 Sep;30.

3. Hsu, S.H., Chu, W.P., Lin, Y.S., Chiang, Y.L., Chen, D.C., and Tsai, C.L. The effect of an RGD-containing fusion protein CBD-RGD in promoting cellular adhesion. Journal of Biotechnology 111, 143, 2004.

4. Liao, E., Yaszemski, M., Krebsbach, P., and Hollister, S. Tissue-engineered cartilage constructs using composite hyaluronic acid/collagen I hydrogels and designed poly(propylene fumarate) scaffolds. Tissue engineering 13, 537, 2007.

5. Wang, Y., Sheppard, B.J., and Langer, R. Poly(glycerol sebacate) — A Novel Biodegradable Elastomer for Tissue Engineering. Mat Res Soc Symp Proc 724, N11.1.1, 2002.

6. Yang, J., Webb, A.R., Pickerill, S.J., Hageman, G., and Ameer, G.A. Synthesis and evaluation of poly(diol citrate) biodegradable elastomers. Biomaterials 27, 1889, 2006.

7. Schnabel, M., Marlovits, S., Eckhoff, G., Fichtel, I., Gotzen, L., Vecsei, V., and Schlegel, J. Dedifferentiation-associated changes in morphology and gene expression in primary human articular chondrocytes in cell culture. Osteoarthritis and cartilage / OARS, Osteoarthritis Research Society 10, 62, 2002.

8. Salinas, CN., Anseth, KS. The enhancement of chondrogenic differentiation of human mesenchymal stemcells by enzymatically regulated RGD functionalities. Biomaterials, 2008; May 29 (15); 2370-7.

9. Chang JC, Hsu SH, Chen DC. The promotion of chondrogenesis in adipose-derived adult stem cells by an RGD-chimeric protein in 3D alginate culture. Biomaterials. 2009 Oct; 30(31): 6265-75

10. Hwang, NS., Varghese, S.. Zhang, Z., Elisseeff, J. Chondrogenic differentiation of human embryonic stem cell-derived cells in arginine-glycine-aspartate-modified hydrogels. Tissue Eng. 2006; Sep 12(9): 2695-706.

11. Connelly, JT., Garcia, AJ., Levenston, ME. Inhibition of in vitro chondrogenesis in RGD-modified three-dimensional alginate gels. Biomaterials. 2007; Feb 28(6): 1071-83.

12. Connelly, JT., Garcia, AJ., Levenston, ME. Interactions between integrin ligand density and cytoskeletal integrity regulate BMSC chondrogenesis. J Cell Physiol. 2008 Oct; 217(1): 145-54.

CHAPTER 9

CONCLUSIONS AND FUTURE DIRECTIONS

9.1 Conclusions

Poly (1, 8 Octanediol-co-citrate) scaffold for cartilage engineering

The quest for alternative and effective treatments to repair articular cartilage damage and the prevalence of osteoarthritis in a growing population are forcing the advancement of tissue engineering methods. Tissue engineering utilizes synthetic matrices seeded with chondrocytes or chondrogenic precursor cells to attempt to regenerate articular cartilage matrices. This work explores how scaffold architecture and material affect scaffold permeability, mechanics and degradation and in turn how these measures influence chondrogenesis. Solid freeform fabrication (SFF) is used as a method of fabrication for all scaffolds, but especially to examine the feasibility of poly (1, 8 Octanediol-co-citrate) (POC) as a scaffold material for cartilage engineering. SFF allows the fabrication of precisely controlled and reproducible scaffold architectures such that the mechanical, permeability, and degradation properties of 3D designed POC scaffolds could be characterized, and thus how these architectural scaffold properties influence chondrocytes *in vitro* and *in vivo*. Also due to the control and reproducibility in fabrication, POC scaffolds could be compared to poly (ε-caprolactone) (PCL) and poly (glycerol sebacate) (PGS) scaffolds with the identical 3D design to delineate an optimal material for cartilage regeneration.

The first part of this work was devoted to testing the feasibility of fabricating POC scaffolds via SFF and characterizing the architectural, degradation, and mechanical properties of each design. POC scaffolds exhibit controllable biodegradation and nonlinear mechanical properties which are suitable for cartilage. Increasing porosity decreases stiffness and the degree of nonlinear behavior, but increases permeability and degradation rate of POC scaffolds. Thus, when designing scaffolds for soft tissue application, the trade off between effective scaffold mechanical, mass transport and degradation behavior resulting from designed porosity should be taken into account. The characterization of 3D POC scaffolds and the relation between scaffold architectures and mechanical properties provide a basic foundation for determining how scaffold architecture affects tissue regeneration, and thus, how to design cartilage tissue engineering scaffolds.

From the four scaffold designs explored, two designs, S50 (low permeable, spherical pore shape) and C62 (high permeable, cubical pore shape), were chosen to compare and observe the effects of scaffold pore shape and permeability on chondrogenesis in *vitro* and in an *in vivo* sub-cutaneous model. These designs were chosen as they were significantly different in pore shape and resultant permeability while the other mechanical or physical scaffold properties of the other designs were similar. We found that chondrocytes prefer lower permeable scaffolds with a spherical pore shape in terms of matrix production and differentiation both *in vitro* and *in vivo*. However, it was interesting to see how *in vitro* vs. *in vivo* culture environments could change the trends of mRNA expressions as they showed a reverse pattern. The mRNA expressions at 4 weeks

in vitro were reflective of sGAG quantification data *in vitro* in that all cartilaginous tissue indicators (col2, col2/col1, aggrecan) for cartilaginous tissues had higher expression in the *low* permeable design (S50). In contrast, the mRNA expressions at 6 weeks *in vivo* demonstrated the opposite of *in vitro* study such that all cartilaginous tissue indicators (col2, col2/col1, aggrecan) for cartilaginous tissues were expressed higher in the *high* permeable design (C62). In fact, all the gene expressions including the de-differentiation marker (col1), the chondrocytic ossification marker (col10), and the matrix degradation proteins (MMPs) in the *high* permeable design were higher than those in the low permeable design *in vivo*, which explained why the low permeable design contained higher sGAG contents than the high permeable design *in vivo,* just like the *in vitro* case. Overall though, we could still come to a conclusion that the low permeable scaffold design with a spherical pore shape is favored by chondrocytes for chondrogenesis both *in vitro* and *in vivo*.

Scaffold pore shape not only plays a role in determining effective scaffold permeability and degradation kinetics but also it seems to play an additive role ensuring a bounded pore space for enhancing cell aggregation and sGAG retention. The enhanced cartilage matrix production in the POC scaffolds especially for the low permeable design (S50) resulted in superior mechanical properties for the scaffold/tissue construct proving the potential of POC scaffolds as a frame for cartilage regeneration both *in vitro* and *in vivo*.

PCL vs. PGS vs. POC for scaffold material in chondrogenesis

There are numerous synthetic biomaterials developed and used for tissue engineering scaffolds, yet there have been almost no head to head comparisons of these different materials as cartilage scaffolds due to irreproducible scaffold designs and inconsistent random scaffold architectures resulting from traditional fabrication methods. The last part of this work involves a comparison study among different biomaterials with an identical scaffold design, which has never been reported. The study demonstrates that the 3D POC scaffold was more suitable for chondrocytes to form cartilaginous tissues *in vitro* compared to 3D PCL and PGS scaffolds when using the same scaffold design. POC showed the highest DNA and sGAG contents after 4 weeks of *in vitro* cell culture with the highest differentiation index and the lowest hypertrophy and matrix degradation gene expression compared to PCL and PGS. Both PCL and PGS promoted chondrocytes to proliferate and express genes related to cartilage formation, but they promoted gene expression for cartilage destruction and ossification, which were not desired for cartilage regeneration. In order to obtain reasonable explanations why POC is particularly preferred, a simple follow-up study of the direct cell-material interactions for all three materials as forms of two dimensional (2D) disks was performed. It was speculated that the different degrees of hydrophilicity of each material may be the main reason why different materials produced. However, the short study did not show that the degrees of hydrophilicity were directly related to overall material performance in chondrogenesis. However, hydrophilicity still seemed to impact cell-cell interaction, aggregation, and cell-adhesion, attachment to the surface, and proliferation even in the 2D environment. POC was shown to have the greatest capability of supporting chondrocyte attachment and

proliferation along with sGAG matrix production significantly even with the rather unfavorable conditions of a short culture time (1 week *in vitro*) and 2D culture. The mRNA expressions did not confirm any trends among materials in 2D study probably due to a short culture time and 2D culture set-up such that chondrocytes were not stabilized enough to express cartilaginous related genes strongly with a specific trend.

Throughout this work, we verified that POC is a potential and suitable material for cartilage engineering and it can be easily and effectively tailored in terms of architectural and mechanical properties via the SFF fabrication technique. We also proved that the low permeable scaffold design with a spherical pore was preferred by chondrocytes for chondrogenesis. This clearly shows that scaffold pore shape and permeability are important design parameters affecting the overall success of cartilage regeneration both *in vitro* and *in vivo*. Furthermore, our study of 2D and 3D material comparison verifies that POC is the most optimal choice of scaffold material among PCL, PGS, and POC for cartilage scaffold-aided tissue engineering in terms of matrix formation and retention, mRNA expressions, and cell attachments and proliferation. Here, our studies indicate how carefully scaffold architecture and material must be chosen to best enhance cartilage regeneration. These results emphasize the importance of microenvironments provided by scaffolds as a key to the success in cartilage regeneration through scaffold tissue engineering.

9.2 Future Directions

Exploring the effects of other scaffold design parameters

The experiments conducted in this work are an initial step in understanding how scaffold materials and architectures influence cartilage tissue regeneration. Determining if low permeable designs in general versus the specific spherical pore shape are the critical influence on chondrogenesis is important for determining a potential optimal architecture design. Furthermore, exploring methods to further automate manufacture of POC scaffolds using different SFF techniques will be important given the significant advantages of using POC as a cartilage scaffold material. However, as thoroughly reviewed in chapter 3, there are many other scaffold architectural properties such as pore size and porosity, which are yet to be fully characterized in terms of mechanical and mass transport properties and the consequent effects on chondrogenesis. As one of the biggest advantages in SFF fabrication is that scaffold designs can be easily controlled, designed, and fabricated, studies of other design parameters with similar assessments and characterizations performed in this work would complete a full comprehensive review of the effects of scaffold designs on chondrogenesis.

Effects of initial cell seeding density and other cell types

The initial cell seeding density (20-30x10^6cells/ml) used in this work is within the range of the densities that are shown to stimulate chondrogenesis for cartilage tissue engineering.[1-3] In general, higher cell seeding densities will increase the cell aggregation and packing densities per pore yet there will be a ceiling limit on the number of cells that can survive within a limited pore space with limited nutrients and wastes exchange.

Varying the cell densities within the same scaffold design would give a better understanding of how cells recognize pore space and pore architecture.

In addition, the same experimental set-up to examine the effects of scaffold architectures and materials on chondrogenesis can be future explored with other cell types such as adipose derived stem cells (ADSCs) and bone marrow stromal cells (BMSCs) used in cartilage tissue engineering instead of primary chondrocytes. Our previous studies [4,5] have shown that BMSCs prefer higher permeability in PCL scaffolds and the spherical pore shape tends to be favored as it creates pre-condensation of BMSCs in poly(propylene fumarate) (PPF) and PCL scaffolds, which would in turn lead to the chondrocytic differentiation. It would be a great interest to see how different cell types respond to the same microenvironments, which would broaden the use of SFF fabricated scaffolds and material selections. To date, no one has reported the use of ADSCs or BMSCs with POC scaffolds for cartilage regeneration yet, hence further work to explore the effects of scaffold architectures and materials on those cell types would advance the understanding of POC scaffolds for cartilage application.

Evaluation of constructs at an actual defect site in a large animal model

Given the feasibility of SFF fabricated POC scaffolds for cartilage tissue engineering *in vitro* and *in vivo* subcutaneous mice model, the evaluation of those pre-cultured cell/POC constructs implantation at an actual defect or orthotopic site will be the next logical step to further evaluate the cartilage regeneration with our designed pore architectures and with other different scaffold materials. The microenvironments around the actual joint sites will be different from even *in vivo* subcutaneous model such as

mechanical stimuli, nutrient availability, and oxygen tension. Not only this will give more in depth and comprehensive evaluation of our designed scaffolds and scaffold materials to closely relate to future clinical applications but also it may allow us to differentiate the performance of the three biomaterials that were used in this thesis clearly among PCL, PGS, and POC.

References

1. Iwasa, J., Ochi, M., Uchio, Y., Katsube, K., Adachi, N., and Kawasaki, K. Effects of cell density on proliferation and matrix synthesis of chondrocytes embedded in atelocollagen gel. Artificial Organs **27**, 249, 2003.

2. Elisseeff, J.H., Lee, A., Kleinman, H.K., and Yamada, Y. Biological response of chondrocytes to hydrogels. Annals of the New York Academy of Sciences **961**, 118, 2002.

3. Hutmacher, D.W., Ng, K.W., Kaps, C., Sittinger, M., and Klaring, S. Elastic cartilage engineering using novel scaffold architectures in combination with a biomimetic cell carrier. Biomaterials **24**, 4445, 2003.

4. Kemppainen, J.M., and Hollister, S.J. Differential effects of designed scaffold permeability on chondrogenesis by chondrocytes and bone marrow stromal cells. Biomaterials **31**, 279, 2010.

5. Liao, E., Yaszemski, M., Krebsbach, P., and Hollister, S. Tissue-engineered cartilage constructs using composite hyaluronic acid/collagen I hydrogels and designed poly(propylene fumarate) scaffolds. Tissue engineering **13**, 537, 2007.

APPENDICES

APPENDIX A: poly (1, 8 Octanediol-co-citrate) (POC) scaffold fabrications

---

Name of Procedure: Synthesis of pre-polymer (pPOC) and 3D POC scaffolds
Prepared by: Claire Jeong
Location: This procedure is performed in LBME 2420
Hazards: none
Protective equipment: Use latex gloves when working with RDO, or to keep your hands protected from hot pPOC.
Waste disposal: contaminated bin or waste bottle

Synthesis of pre-polymer (pPOC) for 1:1 molar ratio & scaffold fabricaiton

Materials/equipments: citric acid anhydrous (Fisher Chemical: #A940-500), 1,8 octanediol (sigma aldrich: #3303)

Synthesis of pre-polymer

1. For POC synthesis, equimolar amounts of citric acid and 1,8-octanediol (i.e. 19.21g (CA) + 14.62g (OD) were added to a 250 ml or 500ml (for 2x amount) three-neck round-bottom flask fitted with an inlet and outlet adapter. Use high temperature silicone oil bath and its temperature controllers. One neck should be connected to nitrogen flow in, the middle is clogged by a stopper, and the third neck should be connected to a tube coming out. (It would be good if you connect the bubbler to check the constant flow of the nitrogen in and out.)
2. The mixture was melted at 160–165 °C for 15 min under a flow of nitrogen gas while stirring. The temperature of the system was subsequently lowered to 140 °C for 30 min - 45 min under stirring to create a pre-polymer. Nitrogen should be constantly flowing through.
3. You can keep this in -20C freezer with desiccators after cool down OR used as is for further post-polymerizing or cross linking.

POC Scaffold fabrication

1. The pre-polymer was cured at 100°C for 1 day without vacuum and continued curing at 100°C for 3 days with vacuum (-30 in.Hg.) with HA scaffolds. (You can cure at 60 - 120 °C under vacuum or no vacuum for times ranging from 1 day (120°C) to 2 weeks (60°C) to create POC with various degrees of cross-linking). Heat up the already assembled Teflon mold upto the temperature that you are going to cure. Also, Heat up pre-polymer upto 110-120°C for 5-10 mins to decrease the viscosity and pore it into the well of Teflon mold then push HA scaffolds into the well slowly.
2. After post-polymerization completes, clean up the extra layers of POC around HA scaffolds (let all the sides of HA expose to RDO).
3. Dissolve HA out of RDO for 6-12 hours. (Try to reduce this RDO immersion time by putting less scaffolds per RDO volume or change RDO frequently (i.e. every 4 hours)).
4. Neutralize POC scaffolds in mili-Q water for 2-3 days until it reaches pH7.0-7.5. Sterilize with 70% ethanol for 30min-1hr or dry them then autoclave.

APPENDIX B: PROTOCOL FOR MEASURING DNA CONTENT

Name of Procedure: Hoechst 33258 protocol for measuring DNA content
Prepared by: Claire Jeong (modified from Huina Zhang)
Location: This procedure is performed in LBME 2420
Hazards: Hoechst 33258 is toxic. Please read MSDS carefully before use.
Engineering Controls: none
Protective equipment: safety glasses, gloves
Waste disposal: Hoechst waste bottle

Scaffold Preparation before DNA content measurements and Papain digestion

1. Prepare papain solution: (papain #p4762, Sigma Aldrich, 10u/mg protein) Dissolve 50mg of papain in 50ml 1x PBS (papain needs to be 10u/ml for digestion) with 43.9mg Cystein (5mM) and 0.5ml EDTA. Check the pH and make it to be 6.0 by either adding 1x PBS or EDTA. Filter the papain solution to make it sterile.
2. Label 1.5ml microcentrifuge tubes (sterile) and aliquot 1ml of papain solution (#1).
3. Rinse all the scaffolds briefly with PBS. Cut scaffolds into smaller pieces (1-1.5mm^3) with scalpel blade (for each scaffold, sterilize the blade with 70% Ethanol).
4. As soon as you cut them into smaller pieces, place them into the papain solution (#1) aliquoted in the tube. Also, make sure you have a control papain which does not have any scaffolds in.
5. Set the degradation oven at 60°C and place all the sample containing tubes on a vortex shaker placed inside the degradation oven. Incubate and shake (1000rpm) the samples for 16-24 hours inside the degradation oven at 60°C. Store at -20--80C for DNA content and sGAG content measurements later. Otherwise, go to the next step.

DNA Quantification

Prep: DNA quantitation kit, Fluorescence assay (#DNA-QF, sigma), ultra-purified water, 96 multiwell plates, fluorometer (excited at 360nm, emission at 460nm), ice.

1. Place all the samples in ice. Make all the solutions according to kit protocols.
2. Put STD DNA (100 and 10ug/ml) inside the degradation oven at 50C for 30 mins (no longer than 30 mins!). Vortex well. Put them back into ice.
3. Make standard DNA solutions according to kit protocols (blank, 50, 100, 200, 500, 1000, 2000 ng).
4. Mix H33258 (1mg.ml) 40ul + 2ml of 10x assay buffer + 18ml ultra-pure water in 50ml tube (for 1 plate of 96 well plate reading) and aliquot 200ul per well and 10ul of each sample. For standards, do replicates and for samples, do triplicates for accuracy.
5. Read: excitation: 355nm, emission: 460nm (Fluoroskan Ascent FL, Thermo, Waltham, MA).

APPENDIX C: PROTEOGLYCAN PRODUCTION ASSAY PROTOCOL (DMMB)

Name of Procedure: Dimethylmethylene Blue (DMMB) Assay for measuring s-GAG content
Prepared by: Claire Jeong (modified from protocols by Huina Zhang and Jessica Kemppainen)
Location: This procedure is performed in LBME 2420
Hazards: none.
Engineering Controls: none
Protective equipment: gloves
Waste disposal: DMMB waste bottle

1. Make DMMB reagent:
Dissolve 8 mg 1,9 dimethyl-methylene blue dye (Sigma, # 341088)
1.52 g Glycine
1.185 g NaCl
47.5 ml 0.1M HCl in 500ml of ultra-pure or distilled H2O and check pH to be 3.0

2. Make standards from shark chondroitan-6-sulfate (CS) (Sigma, # C4384) (a stock concentration of 5mg/ml). Mix 390ul 1x PBS with 10ul 5mg/ml CS solution to make a 400ul of STD1 = 0.125mg/ml = 2.5ug; STD2 = 0.0625mg/ml = 1.25ug etc.), then do a serial dilution (i.e STD2 = 200ul STD1 + 200ul 1xPBS, STD3 = 200ul STD2 + 200ul 1xPBS and so on.) upto STD7. Here, you have 7 standards plus a blank for a standard curve.

3. Aliquot 200ul of DMMB reagent into each 96 well of the plate using multi-channel pipettor.

4. Measure sGAG content of samples and standards: Test your sample concentration to determine how much volume you need to add by comparing color changes. Add 20 ul of standards OR 2, 5, or 10ul sample (well-mixed, centrifuged at 14,000, 10 min, 4°C if you need to remove polymer residue) into the DMMB reagent. (Note: DMMB is extremely light sensitive.) Read immediately on a plate reader (MultiSkan Spectrum, Thermo, Waltham, MA) at 525 nm.

APPENDIX D: PRIMER SEQUENCES FOR qtPCR

Type II Collagen:
Forward: TYIICOLL-ANYF TCCTGGCCTCGTGGGT
Reverse: TYIICOLL-ANYR GGGATCCGGGAGAGCCA

Type I Collagen:
Forward: TYPEICOLLA-ANYF CCGTGCCCTGCCAGATC
Reverse: TYPEICOLLA-ANYR CAGTTCTTGATTTCGTCGCAGATC

Type X Collagen:
Forward: TYPEXCOLLA-ANYF GGCACCCAGGTCCATCTG
Reverse: TYPEXCOLLA-ANYR CAGCCCTGGCTGTCCTT

Aggrecan:
Forward: AGGRECAN-A1BF CGAGGCACCGTGATCCT
Reverse: AGGRECAN-A1BR GGCAGTGGCCCCTGT

MMP3:
Forward: MMP3_F ACTGGATTTGCCAAGAAGTGTTATTGA
Reverse: MMP3_R GAATGTAAGCGGAGTCACTTCCT

MMP13:
Forward: MMP13_F AGTTTGGCCATTCCTTAGGTCTTG
Reverse: MMP13_R GGCTTTTGCCAGTGTAGGTATAGAT

GAPDH:
Forward: GAPDH-1A2F CCATCTTCCAGGAGCGAGATC
Reverse: GAPDH-1A2R AGTGGACTCCACGACATACTCA